Inverter based generation for large industrial plants

Using PV and batteries to reduce emissions and cost of a LNG plant

BSc. N.K.R. De Winter

Inverter based generation for large industrial plants

Using PV and batteries to reduce emissions and cost of a LNG plant

by

BSc. N.K.R. De Winter

to obtain the degree of Master of Science in Electrical Engineering.
Track: Electrical Power Engineering
at the Delft University of Technology,
to be defended publicly on Thursday 7 November 2019 at 09:30 AM.

Student number:	4325052	
Project duration:	February 14, 2019 – November 7, 2019	
Thesis committee:	Prof. Dr. P. Palensky	TU Delft
	Dr. Ir. J. Rueda Torres	TU Delft, supervisor
	J. Dong	TU Delft

TU Delft

Abstract

Reducing the cost and CO_2 emission for the power generation for a liquefied natural gas (LNG) production plant by using inverter based generation is the main challenge posed in this thesis. Both factors can be decreased by using inverter based generation instead of the conventional gas powered power plant for generating the power for a islanded LNG plant.

The overall objective is to develop and investigate the dynamic performance of these inverter based generation for usage in an industrial islanded plant. Within existing literature there are no examples of large scale (230 MW) inverter based generation in islanded mode. This thesis provides insight on the economical cost and the impact during different operational scenarios of using the inverter based generation in large industrial islanded plants.

The general methodological approach consist of 5 steps. Firstly the conventional generation is analysed, then the financial analysis is conducted. Two proposals for inverter based generation are introduced and financially analysed. The fourth step is to develop a Powerfactory model for the inverter based generation and finally several disturbances where applied to the new system to evaluate the performance during operational scenarios.

The first step was to develop a model for the LNG plant and the power generation. I made a Powerfactory model with topology and parameters based on a recent study by Shell. The model was adjusted to resemble a real case study of a LNG plan located in Tanzania and generic controls from existing literature where implemented.

The second step was a financial analysis of the conventional power plant. This lead to two proposals for implementing inverter based generation in a LNG plant. These where to replace the spinning reserve for a lithium ion battery and to replace a gas turbine by a combination of solar PV and a VRF battery. Both options where financially analysed.

Replacing the spinning reserve with a lithium ion battery leads to a reduction of capital expenditure by 34 M$ at expense of increasing the risk of load shedding. This can be mitigated by implementing a lithium ion battery as spinning reserve. The capital expenditure of the battery is 50 M$. The maintenance of the gas powered power plant is reduced by 0.94 M$ resulting in a return of investment within 16.6 years.

The replacement of a gas turbine by a combination of solar PV and a VRF battery increases the capital expenditure by 222 M$ but reduces the operational expenditure by 15 M$/year/turbine making for a return of investment within 13.1 years.

The third step was to develop models for the two proposals. This was done using Powerfactory 2019. The lithium ion battery Powerfactory model is adapted for the operation in islanded mode. For the second proposal a technical model is developed. This model was implemented in the Powerfactory software.

The fourth step was the case study of the system including the new proposal. Three studies where conducted: generation loss, 3 phase short circuit and load rejection. All of theses studies are compared to the conventional generation model.

For the lithium ion battery the result was an improved reaction in the generation loss scenario. Because the ramp rate of the battery is much larger than the generator it is replacing. The control is able to detect a variation in frequency and starts to provide active power. In both the load rejection and the short circuit the contribution of the inverter is limited. The battery is unable to be absorb the excess energy since the battery is already full in the load rejection scenario. In the short circuit study case the maximum output current of the inverter is 20x lower than that of the generator it is replacing.

For the solar PV and the VRF battery the load rejection study case shows improved reaction. The reaction is faster than that of the turbine it is replacing since the extra energy can be converted instantly so the result is less frequency deviation. In the generation loss study case and the short circuit the reaction of the inverter is limited. In the generation loss scenario the inverter is providing maximum output power to decrease the gas consumption of the remaining turbines and is unable to provide more. The inverter is also limited in the short circuit current during the short circuit study case. It is unable to provide more 1 pu current.

Overall, the combination of implementing inverter based generation in to an islanded LNG plant a good solution to reduce the cost and emission of the power generation. Both solutions have a return of investment

within 20 years and have positive effects in the study cases. A combination of the two proposals can mitigate the limited reaction of each of the individual proposals. For the short circuit scenario conventional protection will not be triggered.

Acknowledgement

This thesis research was done in collaboration with Royal Dutch Shell in Pernis, The Netherlands. I give my sincere gratitude to my colleagues and in particular the Shell Pernis Electrical Engineering Team and Paul Donnellan for supporting and educating me during my time at Shell. I would also like to thank my supervisor at TU Delft, Jose Rueda Torres for his feedback during the thesis project. Finally, I want to show my gratitude to my girlfriend, for her reviews and continued support during the project, my father, for his critical reviewing and fellow students for their continued support and encouragement during the course of this thesis.

BSc. N.K.R. De Winter
Delft, October 2019

Abbrevations

NG	Natural Gas
LNG	Liquid Natural Gas
PMR	Pre cooling Mixed Refrigerant
MR	Mixed Refrigerant
SOC	State of Charge
GT	Gas Turbine
ST	Steam Turbine
OCGT	Open Cycle Gas Turbine
CCGT	Closed Cycle Gas Turbine
PV	Photovoltaic - also called solar panel
IC	Internal Combustion
CapEx	Capital Expenditure
OpEx	Operational Expenditure
VSD	Variable Speed Drive
TSO	Transmission System Operator
ROI	Return Of Investment
DEP	Design Engineering Practices
VRF	Vanadium Redox Flow
PWM	Pulse Width Modulation
PI controller	Proportional and integral controller
ROCOF	Rate Of Change Of Frequency

Contents

1
Introduction

1.1 Background information

The need for electric energy is constantly increasing. The Shell Energy Report expects this growth to be 57 % in the next 50 years [35]. While the demand is rising, society expects this energy to be delivered in a less polluting way. The Paris Climate agreement is a commitment from most nations to reduce their impact on the amount of CO_2 produced [39].

Currently most electrical energy is produced by converting chemical energy. This process is done by burning products such as coal, gas and other fossil fuels. Burning these fossil fuels createsCO_2. The amount of CO_2 a country can emit is limited by the Paris Climate agreement [39]. Per unit of energy the amount of CO_2 emitted by burning natural gas (NG) is around 50 % to 60 % less when compared with coal according to National Energy Technology Laboratory [26].

Increased demand of natural gas

This means that the demand for natural gas will increase in the following years by 4 % per year. In 2060 60 % of the energy (produced by fossil fuels) will be produced by burning natural gas according to the Shell Energy Report [35].

NG is a gas trapped in the ground. These NG fields can be extracted by drilling into them en letting the gas flow out. The gas can then be sold. In most countries the production of this gas is higher then the local demand. This means that much of the NG is exported. To transport NG it is beneficial to reduce its size, this is done by liquefaction. Liquefaction is the cooling of a substance to the temperature at which it becomes a fluid. This fluid is 600 times more dense than its gas equivalent.

The liquefaction is done in a LNG plant. The plant explained in the following paragraphs is a typical design for a LNG plant. This liquefaction is done by compressing a refrigerant and letting it expand, this cools the refrigerant. The cooled refrigerant is blown over the NG and absorbs the heat. Thus cooling the NG to liquefied natural gas (LNG). A simplified model of the liquefaction process can be seen in Figure 1.1.

Electrical demand of an LNG plant

The compression of these refrigerants is done using large motors. These motors consume 99 MW when compressing the refrigerant. The two main stages precooling and liquefaction require each 33 MW and 66 MW. Each LNG facility has two of these cooling strings, totalling to a load of 236 MW (2 MW × 99 MW for cooling and 38 MW for auxiliary)

To summarise this means that the demand for NG will increase. To enable shipping the NG is cooled to LNG. This requires 236 MW of electric power.

1.2 Research theme

In order to ship LNG around the globe the NG should be cooled to $-163°C$. The LNG plant requires a continues supply of electrical energy in order to keep the system cool. Maintaining a low temperature in the system is necessary to keep the system running efficiently and economically viable. This requires that the power source is stable and reliable.

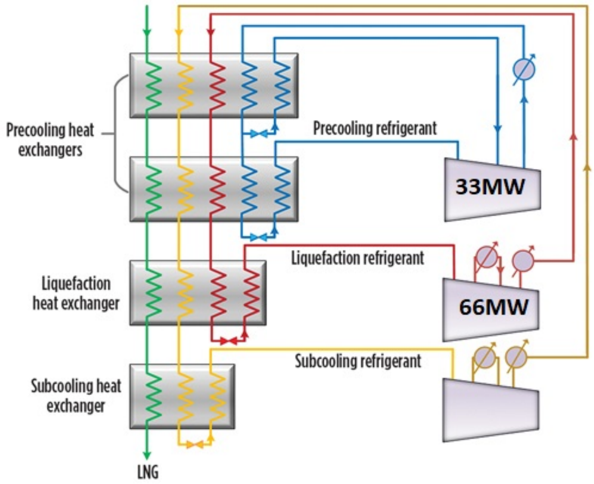

Figure 1.1: A simplified mechanic of cooling NG by exchanging heat with different refrigerant. Each step decreasing the temperature of the NG towards the $-163\circ$ C which is required to liquefy the NG.

Conventionally gas turbines are used to provide this power. These gas turbines are installed in a N+1 configuration, this means that N turbines are needed to power the site. The +1 is added to provide power if any of the other gas turbines fail. By using a N+1 configuration the system is able to react to changes (since it has overcapacity) and is reliable (the failure of one turbine does not lead to a system failure) .

The frequency and voltage in a power system are important figures and a variation in them can lead to load shedding, damage to connected machine, system instability and sometimes even a blackout can occur [13]. In conventional power generation the frequency and voltage are controlled by the ancillary services that each of the gas turbines can provide. The frequency and voltage are controlled via the amount of active and reactive power in the system. These conventional gas turbines have high inertia's and thus will react slowly to changes in the system.

Inverter based generation does not have this inertial response [18]. Having large numbers of inverter based generation in the system decreases the inertia, thus increasing the impact on the system once a variation occurs. In order to prevent these situations the inverter based generation should be able to provide these ancillary services. In a grid connected system the ancillary demands are regulated by the transmission service operator (TSO), but the LNG plant will not be connected to the grid. Since the location is located in a remote place in Tanzania. This requires that the inverter based generation is capable of providing these ancillary services, thus requiring active controls.

The main challenge of this research is decrease the cost and CO_2 emissions by integrating large amounts of inverter based power generation while keeping the system operating as it would do in conventional setup. This requires the inverter based generation to be able to react to changes in the system.

1.3 State of art and scientific gap

The main problem is keeping an industrial islanded grid stable in terms of frequency and voltage with the increasing number of inverter based generating units. To identify possible solutions a literature review has been conducted. This showed the lack of control for large inverter based controlled generation in islanded grids for industrial purposes.

Controlling islanded solar PV is commonly done by enabling P-Q control [42]. This means that the active and reactive power output are constant. Any frequency deviation in the micro grid will not lead to a change in output power. This control strategy is used to enable maximum use of the PV in all situations. This control type is found in small micro grid conditions [42]. The maximum usage of solar PV will decrease the emissions caused by the remaining gas turbines. It is unknown if this is scalable for a large industrial plant.

A method used for larger grid connected plant is the use of a virtual synchronous generator control (VSG). This model models the rotational inertia of a synchronous generator and adjusts the Solar PV output accordingly [23]. If the limit of the solar PV is reached an additional energy storage system is used. This system is able to control and provide reliable power to the system but does not use the solar PV to its maximum.

The combination of these two control methods would enable a solar PV plant to provide reliable maximum output power while being able to adjust to changes to prevent over generation.

The stability of large scale grid connected solar PV using VSG-control and small scale islanded solar PV using P-Q-control are both studied extensively. A combination, a large scale (230 MW islanded solar PV, is not yet developed and will be the scientific gap to fill in this research.

Using VSG-control on a battery to replace the spinning reserve within a system could reduce the cost of maintenance. Providing energy for a prolonged support (2 hrs) on a large scale (100 MWh) in a islanded grid has not been researched. This scientific gap will be filled with this report.

1.4 Research scope and research question

This research is done in cooperation with Shell. Shell defined the challenge as follows: *" Power system studies will be carried out to first determine and then examine the dynamic response of the system during such events including but not limited to process facility and conventional power generation disconnection (trip), power generation ramp up and down, PV system faults including clouds and other similar dynamic events."*.

Research question

To define the scientific research a main question was devised: *What are the implications of replacing gas turbine driven synchronous generators with a combination of solar PV and batteries on dynamic performance and cost within a islanded LNG plant with a load of* 230 MW*?* In order to compare the return of investment (ROI) times of the different implementations of inverter based generation a conventional system will be financially investigated. This will lead to recommendation on where inverter based generation can improve to reduce emissions and cost. If these inverter based generation options are financial viable, which is defined as a return of investment within 20 years within Shell, the operational impact will be analysed.

Thus sub questions arising are:

- What are the cost drivers within conventional power generation of a islanded LNG plant?
- Which inverter based generation can be used to reduce the emissions and/or costs of the power generation for a islanded LNG plant?
- What is the operational impact of integrating these inverter based generation into the LNG plant model?

1.5 Approach

In order to fully answer the main question the research is divided into 5 steps. These steps are visible in Figure 1.2.

1.5.1 LNG plant model

First it is important to define the base case for the LNG plant. The LNG plant is located in Tanzania, a NG rich country on the continent of Africa. The site is located near the ocean as can be seen in appendix A.1, this means that there are only small changes in temperature [38].

Due to this constant temperature the LNG process can be optimised. The optimisation means that the most efficient LNG plant model can be used. This model has 2 compressor strings, each with 2 variable speed drive (VSD) driven compressors. These model are based on the work done in 0.15 T CO2/T LNG, [32]. By having VSD between the compressor and the transformer the powerfactor is 1 [19]. The precooling compressor requires 66 MW and the liquefaction compressor requires 33 MW of power. Other loads in the system (such as pre processing) add up to 38 MW [32].

Baseload

The base load of the system is:

P	=	229 MW
Q	=	23.2 MVar
S	=	230.86 MVA

Generation

Conventional generation is done in an N+1 configuration. This means that 6 generators (50 MW) are used to generate the electric power needed to power the site while only 5 are required to run the site. The details of this configuration will be in detail discussed in Chapter 3.

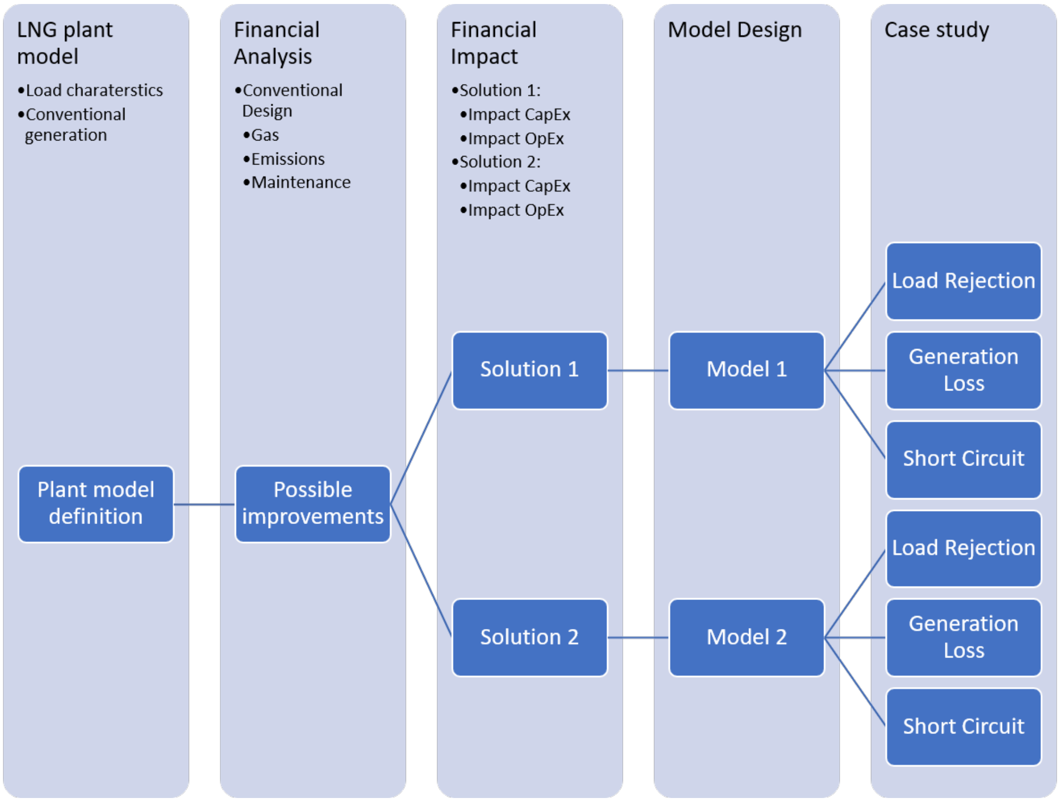

Figure 1.2: Steps required to answer the main research question.

1.5.2 Financial analysis

The second part of the study focuses on the cost a LNG plant. What are the main cost associated with the construction (capital expenditure) and the operational (operational expenditure) of the conventional power plant. The cost are estimated using publicly available sources. The estimates are made using the most efficient models available. The financial analysis will lead to several solutions to reduce the capital expenditure (CapEx) and/or the operational expenditure (OpEx).

1.5.3 Financial impact

By estimating the financial impact of these changes the second sub question can be answered. It is expected that the CapEx of the solutions will increase but the OpEx will decrease. The return of investment period can be determined using Equation (1.1). A typical innovative project needs to have a ROI of less than 20 years.

$$N = \frac{\Delta CapEx}{\Delta OpEx} \tag{1.1}$$

1.5.4 Model design

If the project ROI is deemed viable, the third sub question can be answered. The third sub question investigates the potential impact of these solutions on the LNG plant.

Firstly a model for the inverter based generation is developed. This is done using the Powerfactory software. The models used will be explained in detail.

1.5.5 Case study

To determine the impact of the inverter based controlled generation three case studies will be conducted. These will be conducted in Powerfactory. Powerfactory is chosen since it is a powerful tool and has good support. It is also one of the few software packages that has a thesis license unlike ETAP and thus is available for this research. Prior knowledge is already present at university and with the writer.

The three study cases are:

- Load Rejection scenario;
- Generation Loss scenario;
- Short Circuit.

For these the following tools in the Powerfactory software where used:

- RMS/EMT Simulations
  This simulation is used for all transient behaviour analysis. These are the
  - Load Rejection scenario
  - Generation Loss scenario
- Short Circuit
  The short circuit tool is able to provide accurate data on short circuit contributions.

1.6 Boundaries

To limit the scope of the project several aspects will not be included in the research. These boundaries are:

- The development of secondary and tertiary control for all types of generation.
- Research in other inverter based generation types excluding solar PV and batteries.
- Investigate changes on the load side of the conventional case.
- Develop protection for low inertia systems.
- The site to be able to purchase and use the land needed for the PV without extra cost and/or obstructions.
- The study is limited to the usage of inverter based generation in an islanded grid since there is not much research in this field.

1.7 Stakeholders

Major Petrochemical companies
Many large scale Petrochemical plants are located near the resource they refine. This requires many of them to operate in remote areas. With the knowledge gained by this study it is possible for the to reduce costs and emissions of such plants. This research gives a estimate the total cost of changing the power generation to a more inverter based and gives an insight in potential operational hazards.

Transmission system operators
This research will give a clear insight on the impact of inverter based generation within grid. Small TSO's (up to 500 MW) can use the results in this research to estimate the impact of inverter based storage and generation on the stability within the grid.

1.8 Thesis outline

Chapter 1: Introduction
This chapter introduces the project, describes the research defines the lack of scientific knowledge and highlights the approach. The main boundaries are expressed and the outline is given.

Chapter 2: Financial impact
In this chapter the financial analysis of the conventional system is done. Based on that outcome proposals are formed. The financial impact of these proposal is analysed.

Chapter 3: Conventional generation
To compare the different solutions in their dynamic behaviour a conventional case is created and evaluated.

Chapter 4: Model design solution 1
The model for the first solution is made. Based on a Powerfactory tutorial which is adapted to meet the Shell design engineering practices (DEP).

Chapter 5: Case study solution 1
A case study of the different behaviours in the three scenarios. These are the load rejection scenario, generation loss scenario and short circuit. In all three scenarios the response is compared to the conventional system.

Chapter 6: Model design Solution 2
The second model is designed and adapted.

Chapter 7: Case study solution 2
The second model is tested against the three scenarios.

Chapter 8: Conclusion and recommendation
A conclusion on the viability of implementing inverter based generation in a LNG plant and a recommendation on what Shell and the TU Delft should research next.

2

Financial analysis of the conventional generation and the financial impact of using inverter based generation in an islanded LNG plant

The goal of this thesis is to identify where inverter based generation can assist a LNG plant to reduce its emissions and/or cost. This chapter will first analyse the conventional power generation and then financially analyse two proposed improvements using inverter based generation. This will be done following the sub questions earlier proposed:

- What are the cost drivers within conventional power generation of a islanded LNG plant?
- Which inverter based generation can be used to reduce the emissions and/or costs of the power generation for a islanded LNG plant?

The cost of a plant can be divided into two distinct parts. The total cost of construction is called capital expenditure (CapEx), the yearly cost for the site is called operational expenditure (OpEx). In this chapter both of these cost will be analysed to indicate potential improvements using solar PV and batteries.

2.1 Capital expenditure for the conventional generation of a LNG plant.

In order to determine the cost of the power plant the size of the power plant must be determined. This is done using Formula 2.1.

$$\text{maximum operating electrical load} \leq \frac{(OGC \cdot A) - LUO}{D} \tag{2.1}$$

Where:

OGC	=	Max. Operating Generation Capacity (Prime mover and generator), in MW
LUO	=	Largest unit operating that could trip, in MW.
A	=	Availability Factor: Fraction of the maximum generation capacity that is available to quickly ramp up in case of a trip of a generator. Normally 1.00, but can be constrained by limit on prime mover by process.
D	=	Dynamic Response Margin: e.g. 1.1 to 1.2 for gas turbines. This value can be reduced if confirmed by electrical transient stability studies, but note some smaller gas turbines with dry low-NOx

The maximum operating electrical load is 230 MVA, the largest operating unit is 65 MVA, the availability is 1 and the dynamic response margin is taken to be 1.2. This gives a minimum operating generation capacity of 324.8 MVA. This requires 5.24 generation units of 65 MVA, thus requiring 6 generating units. This means

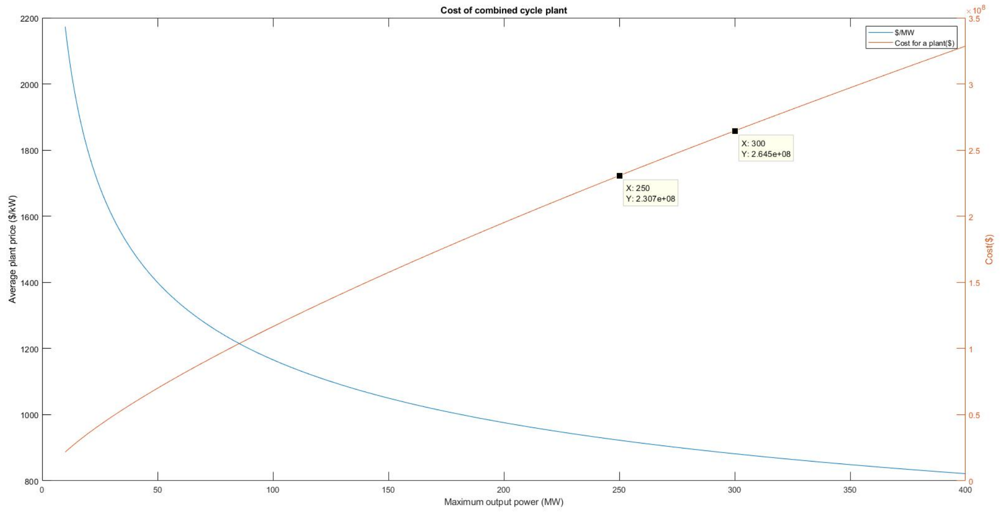

Figure 2.1: Cost for construction of a power plant based on the cost per kW. Source: [41]

that one unit can be out of service while still maintaining spinning reserve. This fulfils the requirement set by the the Shell DEP: *"the stand-by capacity (spinning reserve) shall be incorporated to fulfil the requirement of the peak load with the largest generating set out of service."*.

Using the formula given by Equation (2.2) which is based on a figure given in Zhao Dongmei et al [41], the total price of the 300 MW power plant is 264 M$.

$$\text{Cost of power plant} = (P) \cdot (3.2 * 10^4 \cdot (\frac{P}{1000})^{-0.3} + 154) \quad (2.2)$$

2.2 Operational expenditure for the conventional generation of a LNG plant

There are 3 large costs associated with operating a power plant for a LNG plant[5]:

- Fuel costs
- Emission costs
- Maintenance

2.2.1 Fuel costs of operating a 300 MW power plant

The LNG plant has a power demand of 229 MW of electric power. To produce this electric power the chemical power of gas must be converted. The most efficient combined cycle gas turbine is capable of converting 65 % of the chemical energy to electrical energy [27]. The total chemical energy required to run the plant using this efficiency is 31469 Milion British Thermal Units (mmBTU). This costs 25 M$ per year of not sold gas, at 2.18 $/mmbtu (18/9/2019). See Table 2.1 for the full calculation.

2.2.2 Emission cost of operating a 300 MW power plant

Several countries in Europe are currently developing an additional tax on the amount of CO_2 a user produces. It is expected that almost all countries will embrace these new guidelines [20]. The cost per tonne of CO_2 is 40$ and per mmBTU of natural gas, 53.07 Kg of CO_2 is produced. This totals to 24 M$ per year. See Table 2.1 for the calculation and Table 2.2 for the decreasing cost per removed generator.

2.2.3 Maintenance of a 300 MW power plant

The third cost that is significant in the operational expenditure of a gas turbine is the maintenance. The maintenance is composed of two elements, one based on the rating, the second based on the amount of

Table 2.1: Cost of burning 230 MW of coal using a 65 % efficiency of the combined cycle gas turbine. Expressed in $/year.

P_e	250 MW
η	0.65
P_c	352 MW
E_c	352 MJ
MJ=>mmBTU	0.000947
P_c	0.364 mmBTU
E_c	31469 mmBTU/day
Cost	2.18 $/mmBTU
Cost per day	66602 $
Cost per year	25 M$

Table 2.2: Table indicating the residual cost of decrease conventional generation and its impact on the operational expenditure.

Generators Remaining	Construction Cost (M$)	Gas Cost (M$/year)	Emission Cost (M$/year)	Maintenance Cost (M$)/year	Total (M$)
6	264.87	25.03	24.38	27.4	76.81
5	230.67	25.03	24.38	26.5	75.83
4	195.18	20.03	19.50	21.2	60.73
3	157.50	15.02	14.62	15.9	45.54
2	116.59	10.01	9.73	10.6	30.34
1	69.99	5.00	4.87	5.3	15.17
0	0	0	0	0	0

production hours [40]. This leads to Formula 2.3. This results of a total of 25.6 M$/year for the 300 MW power plant running at 229 MW continues.

$$\text{Cost of maintenance} = \alpha \cdot \text{ Rated Power} + \beta \cdot \text{total amount of energy produced} \tag{2.3}$$

Where:
α = 18400/MW$/year [40]
β = 10/MWh$/year [40]

2.2.4 Summary of the total cost of a gas fired power plant

The capital expenditure of a gas power plant is 284 M$. The price per turbine decreases with every additional installed. The power plant has a spinning reserve of 50 MW.
The operational expenditure is 15 M$/year/turbine. Divided in three equal parts: Fuel (5 M$), CO2 tax (4.87 M$) and maintenance (5.3 M$).

2.3 Solutions of reducing cost by implementing inverter based generation

There are two possible improvements where the total expenditure for a plant can be reduced. These are:

- Removing the spinning reserve and replacing this with a Lithium Ion battery
  A smaller power plant, 250 MW, requires less capital expenditure and requires less maintenance. But if a generator trips load shedding is required to keep a balance between generation and load. This is an unwanted scenario since load shedding will lead to less production. That is an unacceptable scenario. A battery could be implemented to replace the role of the tripping generator. Thus load shedding is then not needed to maintain the balance.

- Replacing a gas turbine with Solar PV and a VRF Battery
  Removing a gas turbine reduces the gas consumption thus reducing the amount of emissions. The maintenance of the gas turbines is reduced by 5.3 M$. But the system is unable to operate with less power generated. Thus an alternative source has to be used. The combination of solar PV for the day and battery storage during the night is needed.

2.4 Financial impact of removing spinning reserve using lithium ion battery

Islanded sites have a spare gas turbine on cold standby, this machine is not active in normal operations but can be activated within 2 hrs. Starting a turbine fast as possible but will reduce the lifetime [8]. In a conventional setup the cold standby machine is sped up during a trip of any of the other generators.

With the spinning reserve replaced by a lithium ion battery the system should still continue to run for 2hrs when a generator is disconnected. This requires the battery to be 100 MWh (50 MW · 2 hrs). A recently installed 50 MW/100 MWh battery had a capital expenditure of 50 M$ [31][9].

With the reduced size of the power plant to 250 MW, the cost changes according to Formula 2.2 as can be seen in Table 2.2. The power plant excluding the battery would cost 230 M$. The total capital expenditure will thus be 280 M$.

Change in operational expenditure by removing spinning reserve and replace by battery

The lithium ion battery examined in [31] and [9] does not require preventive maintenance. The maintenance cost of the GT's is reduced by 0.96 M$, since the amount of MWh does not change and only the MW is reduced (see 2.3). This will result using formula 2.4, to a return of investment (ROI) period of 16.66 years.

$$N = \frac{CapEx_{New} - CapEx_{conventional}}{OpEx_{New} - OpEx_{Conventional}} \tag{2.4}$$

2.5 Replacing a gas turbine with solar PV and a VRF battery

Reducing the amount of natural gas used by the turbines will increase the amount which can be sold and reduce the tonnage of CO_2 produced by the power plant. This requires that solar PV is capable of generating the 1200 MWh (24 Hrs · 50 MW) required to replace a single gas turbine energy production.

Location based panel requirements

The LNG plant is located in Tanzania. Tanzania is identified as a high solar PV potential country [2]. This means that kWh/kWp ratio is very high as can be seen in appendix A.1. The ratio for tilting panels is 6.5 kWh/kWp and for non tilting panels the ratio is 4.3 kWh/kWp [17].

Capital expenditure for the solar PV

With the kWh/kWp ratios known the total number of panels can be calculated using Formula 2.5.Resulting in 520043 (tilting) and 786112 (non tilting) panels. With a solar PV cost of 0.324 $/Wp and that the panel is 50 % of the total cost [15].

The tilting panels are 30 % more expensive than per panel according to Mario; Eichhammer et al [15] The total price for the non tilting panels is 180 M$ and 155 M$ for the tilting panels.

2.5.1 Size allocation for solar PV

The panels are 2 meters long and are titled according at 9° according to [17]. This requires 1.97 meters per panel. If placed on rows of 1km long (1000 panels) 800 rows are necessary. The total requirement is thus 1.6 km^2 per turbine replaced with the non tilting option. For the tilting option the sizing would only require 1 km^2

$$N = \frac{P_{required} \cdot t}{P_{Panel} \cdot R} \tag{2.5}$$

Where:

N	=	Number of panels needed
$P_{required}$	=	Power the PV needs to replace
t	=	Time the PV panels need to replace the GT in hours
P_{panel}	=	Maximum power point of the panel
R	=	Ratio of Wh/Wp

2.5.2 Nighttime storage

Since solar PV only produces energy during the day a storage medium is needed to provide energy during the night. A vanadium redox flow (VRF) battery storage is chosen to store the power for the night period. VRF battery technology is able to have a large cycle life (exceeding 20 years). Tanzania is located near the equator, meaning the average solar day is 12 hrs, this requires 600 MWh of storage.

Table 2.3: Overview of cost for the part for replacing a gas turbine.

	Amount	Max Power(Wp)	Cost per unit	Total cost(M$)
Non Tilting panels	792117	355	0.648/Wp	180
Tilting panels	524015	355	0.842/Wp	155
VRF battery	600 MWh	50×10^6	108/kWh	64
Additional storage	14.16 MWh	50×10^6	108/kWh	1.59

Winter period storage

During winter period the solar time is reduced to 11:43 hrs. It is possible to generate these 17 minutes of energy during the summer. This requires (on average 11 minutes for 186 days per year totalling 34 hrs, see Appendix A.2) 34 hrs of total extra capacity. This would total to 50 MW · 34 hrs = 1705 MWh of additional storage required.

Alternative approach to compensate for the shortest day

An alternative solution is to increase the generation and storage to accommodate for the shortest day. During this day 17 minutes of extra storage will need to be charged. This requires an additional 14.16 MWh battery and thus using Formula 2.5, 6005 non tilting panels or 3972 tilting panels are required.

Capital expenditure for night time storage

VRF batteries are the only technology currently market ready (see B.1) for large scale high cycle operations. The battery has no degradation and can be scaled with relative ease. The cost for large scale VRF batteries is 1130 $/kWh (2011, [16]) and is estimated to fall to 108 $/kWh to 350 $/kWh [16]. Installing the previously mentioned 1705 MWh battery would cost 184 M$. The 6005 and 3972 panel would cost 1.4 M$ and 0.94 M$, the additional 14.16 MWh battery will cost 1.59 M$.

2.5.3 Conclusion on the capital expenditure for replacing a gas turbine

Installing the extra panels and the additional small battery is cheaper and thus the total number of panels will be, 792117 non tilting or 524015 tilting panels. Combined with the 614.16 MWh battery the total cost will be 247.79 M$ or 222.33 M$.

With the additional solar PV and battery combination the size of the power plant is reduced. In Table 2.2 the remaining cost for the gas operated power plant can be seen.

2.5.4 Reduced operating cost by implementing solar PV and batteries

As mentioned in Section 2.2, all three operational cost impacted by the reduced need for gas turbines. The gas consumption and CO_2 emissions are reduced by 1/5th per additional gas turbine removed this means that 5 M$ of additional natural gas can be sold and that 4.87 M$ of CO_2 emission is not emitted. An additional 5.3 M$ is not spend on maintenance since the size of power plant is reduced and the amount of energy generated is reduced. Totalling the saving on OpEx to be 15.18 M$.

The solar PV is not maintenance free. The cost of maintaining the non tilting solar park is 1.01 M$ and for the tilting park the 0.68 M$. These figures are the replacement cost based on [15].

2.5.5 Return of investment

Using Formula 2.4, Table 2.4 can be constructed. The ROI for the first PV park is highest because the cost of this turbine is only 34 M$, the removal of each extra unit can be seen in Table 2.5

2.5.6 Impact of changing conditions on the ROI

The demand for NG is expected to grow [35], this will lead to an increase in price. This increase in price has a positive reaction on the ROI period. In Figure 2.2 this trend can be observed. Another variable which has large impact on the ROI period is the price per tonnage of CO_2 emitted. This price is currently at 40 $/T but is expected to grow according to demand. Since the total amount of tonnage emitted is decreased in the coming years by the EU [15], the price is expected to rise. The impact of an increase emission price can be seen in Figure 2.3.

Table 2.4: ROI change with increasing inverter based generation.

Generators remaining	PV parks installed	ROI Non Tilting	ROI Tilting
5	1	15.27	13.14
4	2	15.15	13.03
3	3	15.07	12.95
2	4	14.97	12.85
1	5	14.82	12.70
0	5	14.39	12.28

Table 2.5: Cost per GT.

Generators replaced	Not spend M$
First	35.49
Second	37.68
Third	40.91
Fourth	46.60
Fifth	69.99

2.5.7 Conclusion

For implementing inverter based generation in a LNG plant within a high solar potential country two options have been financially analysed. The first option is to replace the spinning reserve with a lithium ion battery. The capital expenditure is slightly increased (16 M$ on 264 M$ conventional setup) and the operational expenditure is reduced by 0.94 M$. This means that the ROI period of this investment is 16.66 years. This makes the business case viable and worth investigating the dynamic performance.

The second implementations is the replacement of a gas turbine by solar PV and a VRF battery storage. The cost of replacing a single gas turbine is 222 M$, the reduced cost of installing a single gas turbine less can be seen in Table 2.5. The total gas cost, emissions cost and maintenance is reduced by 1/5th (per additional gas turbine) totalling 15 M$ per year. The ROI period for this investment is thus 13.1 years for the first turbine. This makes the business case viable and worth investigating the dynamic performance.

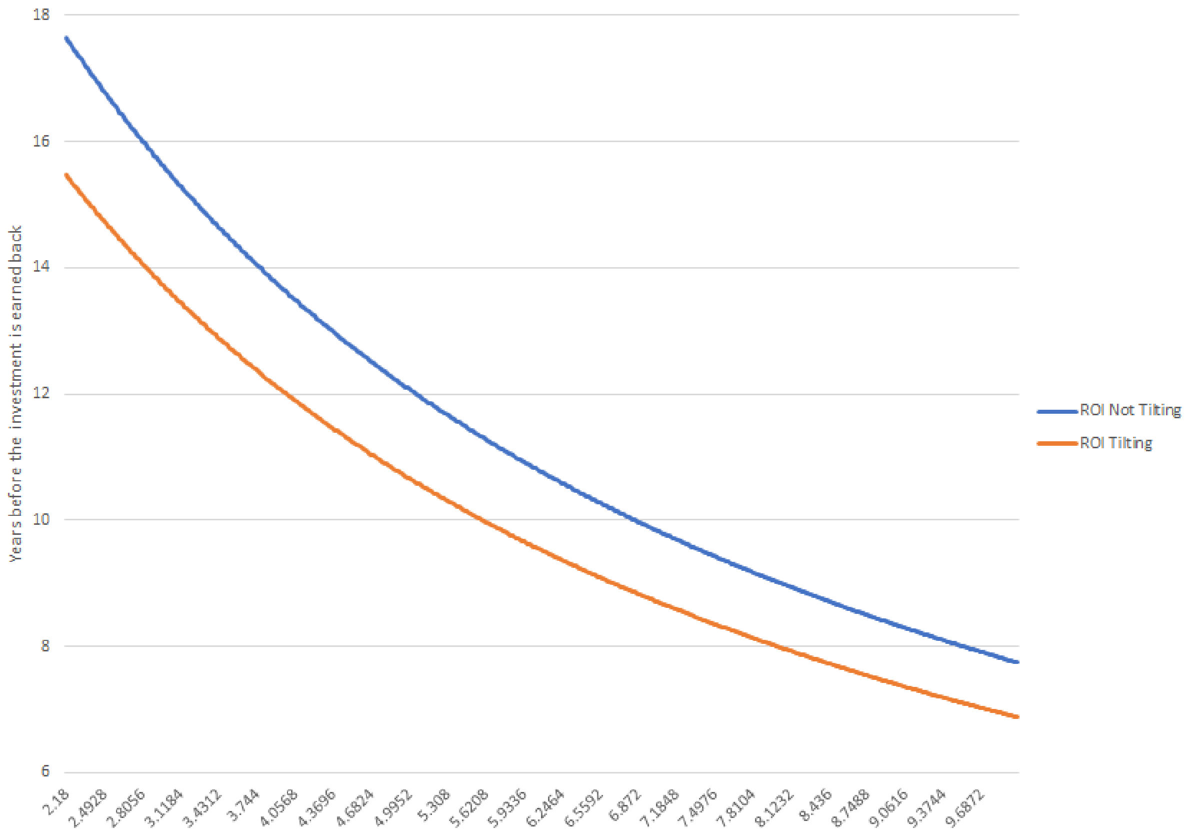

Figure 2.2: Influence of gas price on the ROI.

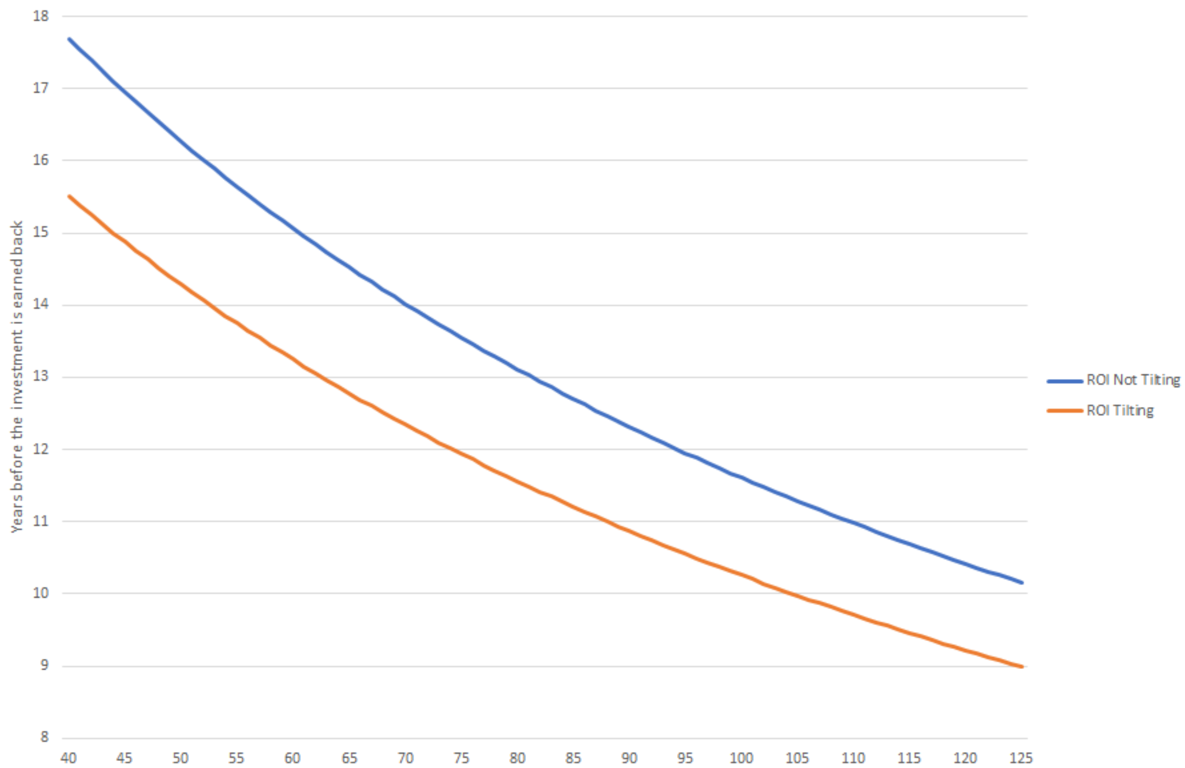

Figure 2.3: Influence of emission prices on the ROI.

3

Load and conventional generation description

Comparing inverter based generation to a conventional system requires that the conventional system is stable in all circumstances. Stability is defined as the ability to maintain a state of equilibrium under normal operating conditions, as well as its ability to regain an acceptable state of equilibrium following a disturbance [22]. These disturbances can be derived from the physical process of the LNG plant.

Requirement by the Shell DEP

The LNG plant can be separated into three distinct parts. Generation, distribution and load (see Figure 3.1. In each of these parts disturbances can occur. Failure of a generator, short circuit and load rejection. A conventional power system should be able to remain stable. The requirements for this stability are given in the Shell Design and Engineering Practice (DEP). These are:

- During normal system operation and under steady-state conditions(article 3.3.2 from the shell DEP):
  - a. The voltage at generator and consumer terminals shall not deviate from the rated equipment voltage by more than 5 %
  - b. The system frequency shall not deviate from the rated frequency by more than 2 %.
- Stand-by capacity (spinning reserve) shall be incorporated to fulfil the requirement of the peak load with the largest generating set out of service (article 3.5.3.1 from the shell DEP).

3.1 Dynamic response tests to verify the power generations auxiliary function

These requirements lead to transient test for the response to dynamic disturbances, the load rejection scenario and the generation loss scenario.

3.1.1 Load rejection scenario

Processing NG to LNG requires several steps in pre processing the NG. Water and other acids will be removed in this pre processing. This requires 38 MW of electric power. This total load is divided into several smaller parts. For our Load rejection scenario these are minor since the strings(with the compressors) require much more energy. To compress the refrigerant (as seen in Figure 1.1) large motors are needed. For the pre cooling refrigerant 33 MW of power is required, for the liquefaction refrigerant compressor 66 MW of power is required. Totalling to 99 MW per string. If a disturbance occurs in one compressor the other compressor shutdown after 10 seconds. A single compressor cannot deliver enough energy to cool the LNG and thus the string is stopped.

The halting of operations of the largest compressor followed by the second compressor is a viable scenario and should be handled by the generation within the limits set. This is the scenario which will be used to evaluate the integration of inverter based generation.

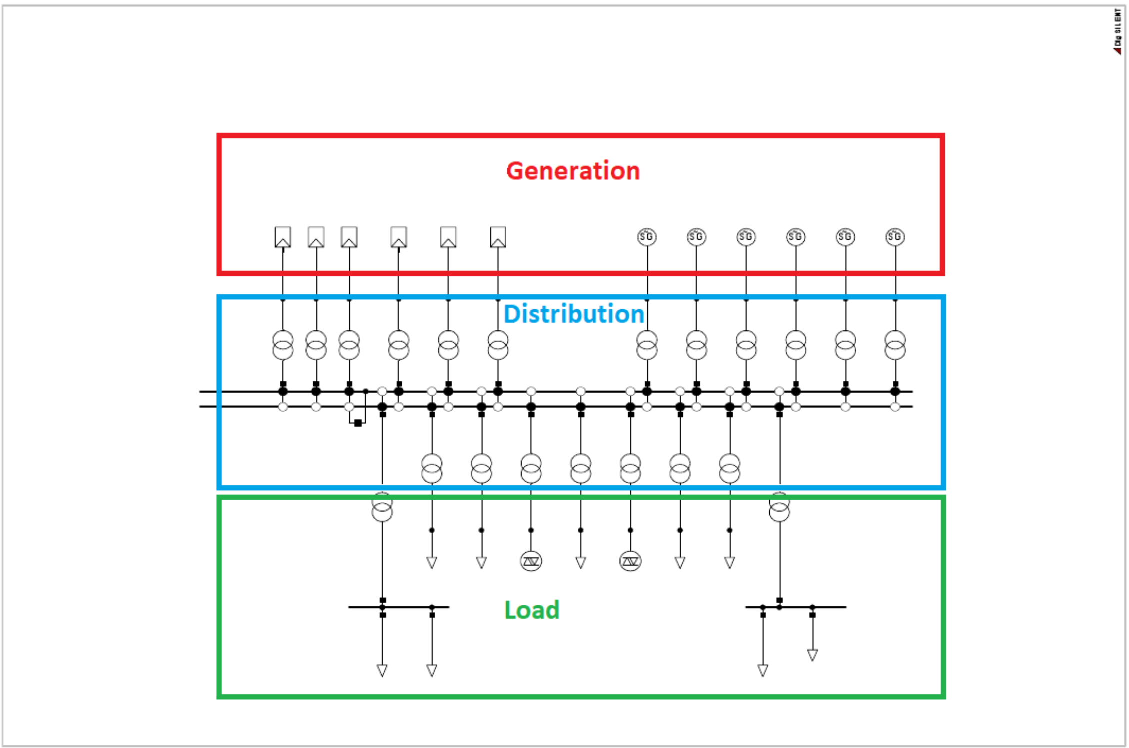

Figure 3.1: Separation of the power system of an LNG plant into 3 distinct sections, Generation, distribution and load. With indication of the two major power consumers String 1 and 2, totalling 198 MW of the total 236 MW.

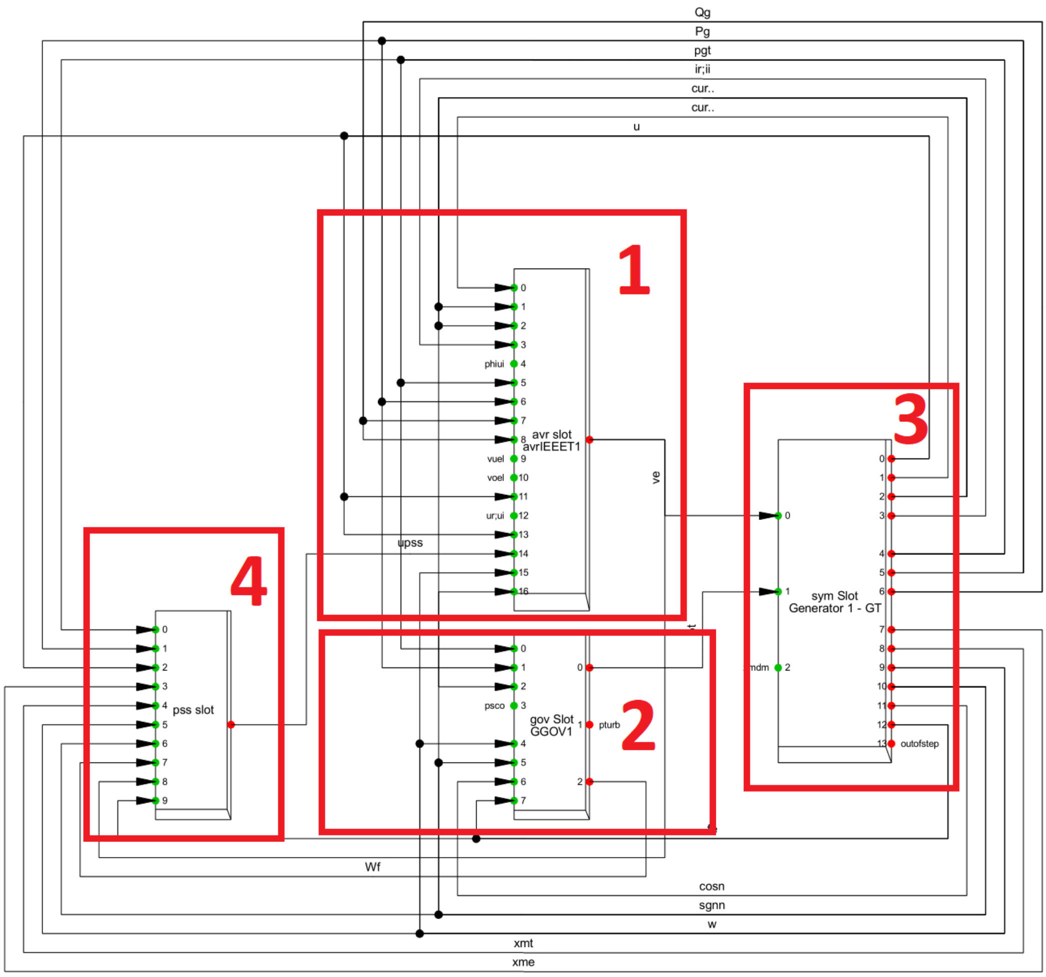

Figure 3.2: Block diagram indicating the control flows of the synchronous generator. Explained in Table 3.1

3.1.2 Generation loss scenario

The Shell DEP states that there is standby capacity for the peak load and the largest generating set out of service. The generation set chosen for this project is a combination of steam turbines and gas turbines. Each of them is capable of producing 50 MW of power. With the largest generating set out of service the total capacity is (N) 250 MW with a peak load of 236 MW this requirement is fulfilled. The trip of a generating set should remain within the limits earlier set.

3.2 Dynamic model of conventional generation

To verify that the conventional generation remains within the limits a dynamic model was chosen. This is visualised in Figure 3.2. This is a conventional description for the control of a turbine.

Table 3.1: Explaination of the different items in the model for the synchronous generator. Source and details: [30]

#	Item	Element
1	AVR	ElmAvr*,ElmVco*
2	Govenor	ElmGov*,ElmPcu*
3	Synchronous generator	ElmSym*,IntRef*
4	PSS	ElmPss*

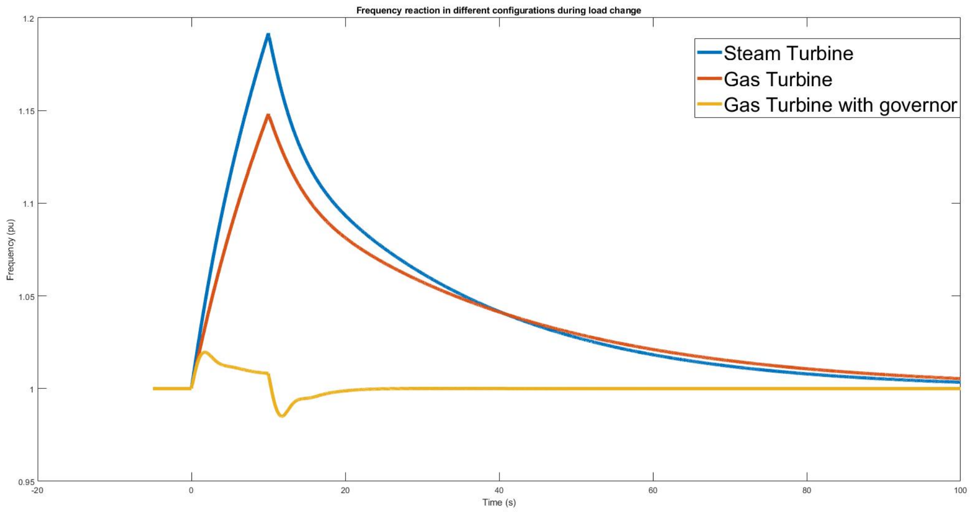

Figure 3.3: The orange and blue line indicate the response of a gas turbine generator and a steam turbine generator to a load change of 50%. Both system are uncontrolled and start to increase their frequency based on Equation 3.1. The yellow line is the reaction of a gas turbine generator with the governor control implemented. The governor stabilises the system, both during the disconnection and the connection of the load. Thus keeping the system stable.

3.2.1 Choice of generator and the inertial response

For the dynamic model of the the synchronous generator an adaptation of the GE 6.03B[1] was used. The rating of the original machine was 46 MVA and for this purpose it has been increased to 62.5 MVA. This larger rating increase the rated active power output to 50 MW. The inertia is kept the same. Having a relatively smaller inertia in the system will result is larger frequency variation, following Equation (3.1). The generator has an inertia constant H = 4s.

A 50 MW steam turbine is available in the Powerfactory library. The moment of inertia of the steam turbine is 8.7s. The lower inertia will create a large frequency swing as shown by Equation (3.1). This change can be observed in Figure 3.3.

$$\delta\omega = \sqrt{\frac{P_g - P_l}{2H_{system}}} \tag{3.1}$$

Where:

$\delta\omega$	=	Rotor acceleration (rads/s)
H	=	Inertia of the system (s)
P_g	=	Generated power (W)
P_l	=	Consumed power (W)

3.2.2 Primary frequency control

In every synchronous generator a speed control is present, called a Governor. This governor is able adjust the prime mover to adjust for speed variations. The goal of the governor is to stabilise the system. In Figure 3.3 the influence of this governor can clearly be seen. After stabilisation the secondary control should restore the frequency back to 1 pu (the frequency normalised such that 1 pu = 50 Hz). The governor used for this project is the GGOV1 governor. This model is recommended by the NERC [7]. The data provided by the NERC [7] is used to adjust the response of the gas turbine. An overview of the GGOV1 model can be seen in Appendix A.3.

3.2.3 Choice of AVR

Maintaining the correct voltage level within a power system is a key attribute to the security of supply. By adjusting the reactive power output of a synchronous generator the voltage level in the system can be controlled. The Automatic Voltage Regulator (AVR) is responsible for adjusting the field voltage in the generator

[1] `https://www.ge.com/power/gas/gas-turbines/6b-03`

[22]. Since AVR controls the excitation of the generator the reaction is instant compared to the gas flow reaction of the governor. The IEEET1 model for the AVR can be seen in Appendix A.4.

3.3 Case studies into the dynamic response of conventional generation

To compare the impact of the inverter based generation a base case is developed for the conventional generation. In three scenarios (load rejection, generation loss and short circuit) the system will be tested. In the two dynamic scenario's the test will be executed at $t = 0$. The start time of the simulation is set $t = -5$ seconds earlier to show the pre change condition. The time frame of the total system is 25 seconds. The system needs to be stable with in the 20second timeframe. After this preiod the secondary controller starts to react to the system.

3.3.1 Load rejection scenario

The cascading loss of two compressors is a scenario which can occur, 43 % off the load is rejected in this scenario. The frequency change is 1.025 pu, this violates rule 3.3.2b. But this rule can be discarded for this scenario as the system is no longer in normal operations.

3.3.2 Generation loss scenario

When a generating unit is lost the other generators will increase their output to meet the demand from the load.

For this test Generator 2 is disconnected at t=0, resulting in 38.3 MW (230 MW/6Turbines) of generation being lost.

The four gas turbines increase their output by 21 % to 47 MW, combined with the output of 40 MW by the steam turbine restores the power balance. After the initial dip of 2.3 % frequency the generator settles at 0.993 pu. This is in accordance with the droop line given by Equation (3.2).
$K_{pf} = 4\%, f_0 = 50 Hz. \Delta P = -38$ MW,
gives a frequency of 49.66 Hz (or 0.993 pu, −0.7 %).

$$f = f_0 + K_{pf} \Delta P(Hz)) \quad (3.2)$$

Where:

$$K_{pf} = \frac{\Delta f}{P_{max}} \quad (3.3)$$

Where:

P_{max}	=	Maximum power (W)
K_{pf}	=	Drooprate
Δf	=	Frequency change (Hz)
f_0	=	50Hz

3.3.3 Short circuit

During a short circuit the voltage in the system decreases. Because the amount of power generated by the generators is still the same due to inertia, the current increases as can be seen in Equation (3.4).

$$P = UI \quad (3.4)$$

These currents follow distinct characteristics based on the reactance and the time constants associated. These are the:

- DC current contribution = $\frac{E\sqrt{2}}{X_d^{"}} e^{-t/T_a}$
- Subtransient current contribution = $E\sqrt{2}(\frac{1}{X_d^{"}} - \frac{1}{X_d^{'}}) e^{-t/T_d^{"}} sin(\omega t)$
- Transient current contribution = $E\sqrt{2}(\frac{1}{X_d^{'}} - \frac{1}{X_d}) e^{-t/T_d^{'}} sin(\omega t)$
- Steady state current contribution = $E\sqrt{2}\frac{1}{X_d^{"}} sin(\omega t)$

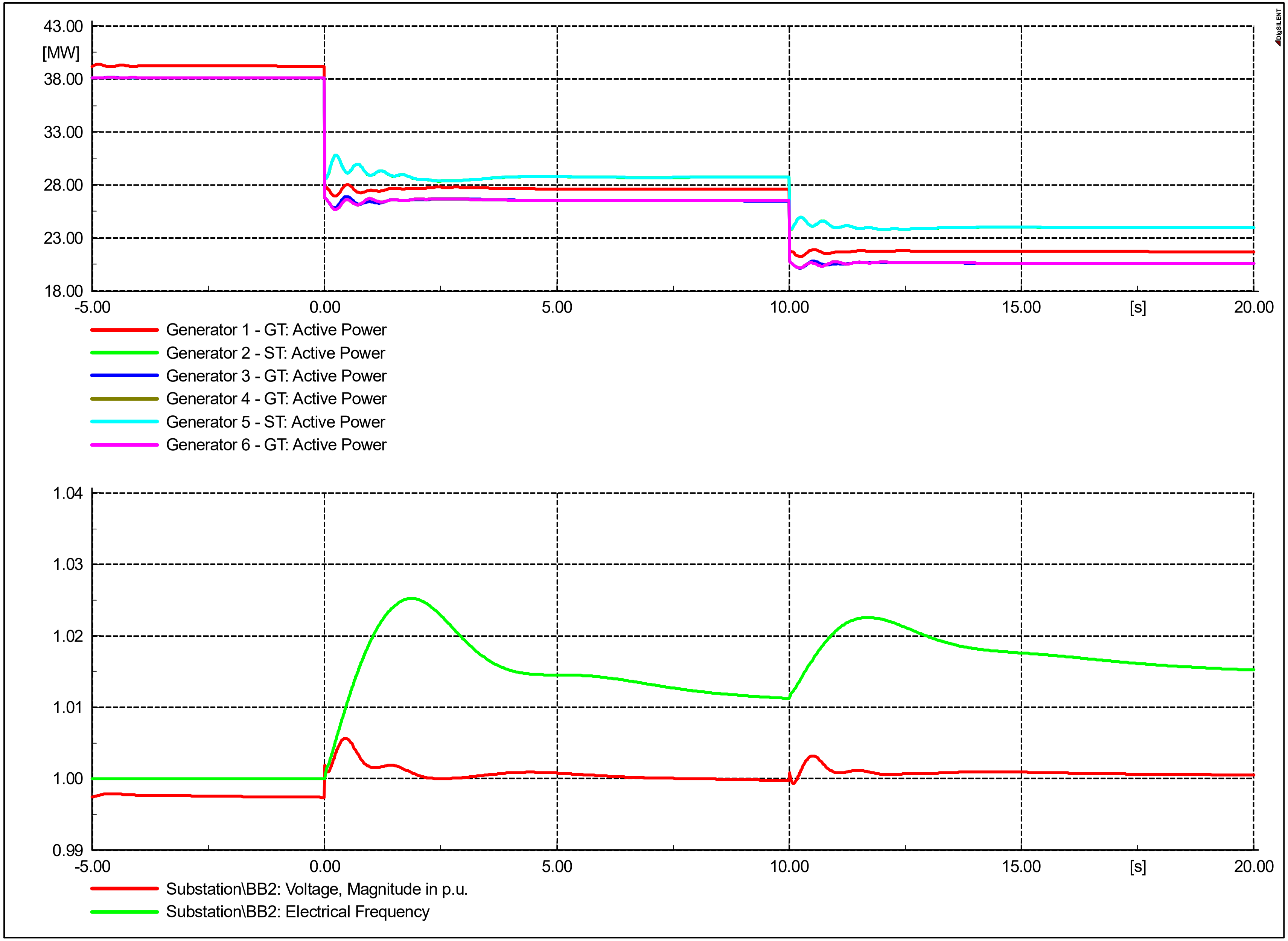

Figure 3.4: The load rejection scenario shows a cascading failure of two compressors. This results in a load loss of 43 %. The control reacts by lowering the output of all generators as can be seen in the top figure. The resulting frequency change is observed in the bottom part. The rejection of the first 66 MW results in a violation of the DEP 3.3.2b (see Chapter 3) but the loss of more than 20 % is not considered normal operations. At t=1.875, The frequency reaches 1.025, and at t=11.7 another maximum over frequency of 1.023 pu is reached. It is observed that there are oscillations up to that point between the various gas turbines.

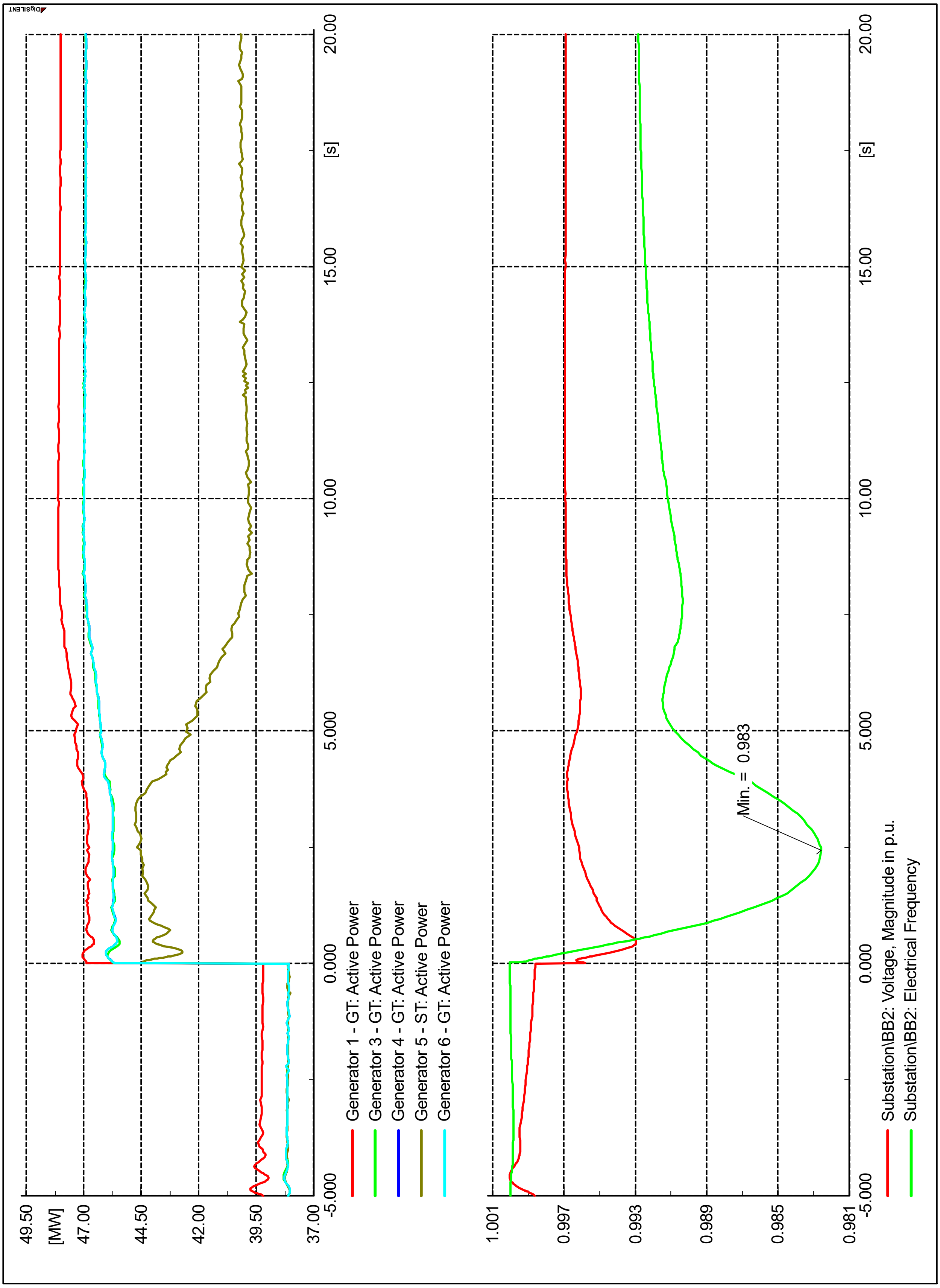

Figure 3.5: In this scenario Generator 2 is lost at T=0s. In the top figure the increase of individual loading is observed. The gas turbines (1,3,4,6) increase their output 21 %. The Steam turbine increases its output to 44 MW and then settles at its rated output of 40 MW.

Table 3.2: Short Circuit impedance's and time constants of a gas turbine.

X"d	0.169 (pu)
X'd	0.219 (pu)
Xd	2.39 (pu)
T"d	0.022 s
T'd	0.64 s
Td	2.89 s

The total current thus follows the curve:

$$i(t) = E\sqrt{2}((\frac{1}{X_d^"} - \frac{1}{X_d^{'}})e^{-t/T_d^"} + \frac{1}{X_d^{'}} - \frac{1}{X_d})e^{-t/T_d^{'}} + \frac{1}{X_d})sin(\omega t) + \frac{E\sqrt{2}}{X_d^"}e^{-t/T_a} \tag{3.5}$$

Where:

E	=	Phase-to-neutral rms voltage across the generator terminals (V)
$X"d$	=	Subtransient reactance (Ω)
$X'd$	=	Transient reactance (Ω)
Xd	=	Synchronous (steady-state) reactance (Ω)
T"d	=	Subtransient time constant (s)
T'd	=	Transient time constant (s)
Ta	=	Aperiodic time constant (s)

In Table 3.2 the exact numbers for the gas turbine can be seen.

Analysis of Short Circuit data provided by Powerfactory

The Short Circuit calculation in the Powerfactory software exports a table with the individual contributions of the different machines. This table can be found in Appendix A.5. The following short circuit parameters are calculated, in accordance with IEC60909 [3]:

- Subtransient current contribution = $Ik"$
- Transient current contribution = Ik'
- Steady state current contribution = Ib
- Peak short-circuit current = I_p
- Peak short-circuit breaking current = i_b
- Thermal equivalent short circuit = I_{th}

Fault location and result

The short circuit used for this test is a 3 phase to ground fault on the 132 kV central busbar. During a fault at the 132 kV busbar in the distribution grid this would lead to 23.3 kA of current feeding the fault as can been in Appendix A.5).

During normal operations the maximum current delivered to the 132 kV busbar is 1.013 kA. During a short circuit the current flow is increased by a factor of 23. Normal protection devices are capable of distinguishing the difference. Conventional protection should easily see the difference between normal operations and a short circuit [34].

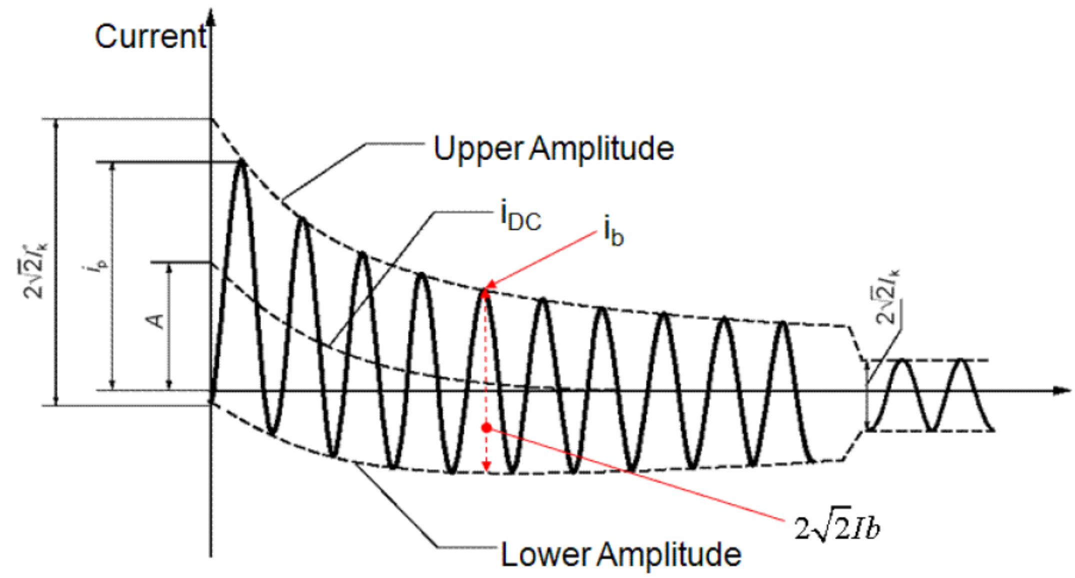

Figure 3.6: Visual representation of the short circuit currents calculated by the Powerfactory software. (Source: [30])

4

Control design for replacing spinning reserve with a lithium ion battery

The replacement of spinning reserve with a lithium ion battery is one of the solution to the sub question: *"Which inverter based generation can be used to reduce the emissions or costs of the power generation for a LNG plant?"*. In this Chapter the dynamic performance model of such a battery is constructed followed by the test (see Chapter 5). In Chapter 5 the relevant sub questions are answered, in this chapter the model design is constructed.

With an estimate of 16.66 years until the investment is earned back the the lithium ion battery replacing the spinning reserve seems viable. In this chapter the electrical model of such a battery will be analysed to determine if such a battery system is able to comply with the Shell DEP.

Requirements of the spinning reserve replacing Lithium Ion battery
The Shell DEP specifies that the system complies with the following requirements when in steady state condition.

- (3.3.2) During normal system operation and under steady-state conditions:
  - a. The voltage at generator and consumer terminals shall not deviate from the rated equipment voltage by more than 5 % and
  - b. The system frequency shall not deviate from the rated frequency by more than 2%.

Other specification that are specific to the LNG plant are:

- Be able to provide 2 hrs of power to replace a single gas turbine.
- The battery should only provide power once a change of frequency greater than 200 mHz is observed. This to reduce the amount of loading cycles of the battery.

4.1 Control design for a spinning reserve lithium ion battery

In Chapter 3 three main parts of the electrical system and its failures where determined. The lithium ion battery should be able to respond to each of these scenario's. These scenario's and the response by the battery are visible in Figure 4.1.

The control must be able respond to changes in the system accordingly. In Figure 4.2 the control structure can be seen. This control is an adaptation of the "BESS with PWM converter" tutorial [28].

4.1.1 PQ controller

The PQ controller is the main controller of the inverter. Responding to changes in voltage and frequency within the AC grid. The voltage is measured at the AC terminal of the inverter. See Figure 4.3 for the location and direction of the measurements.

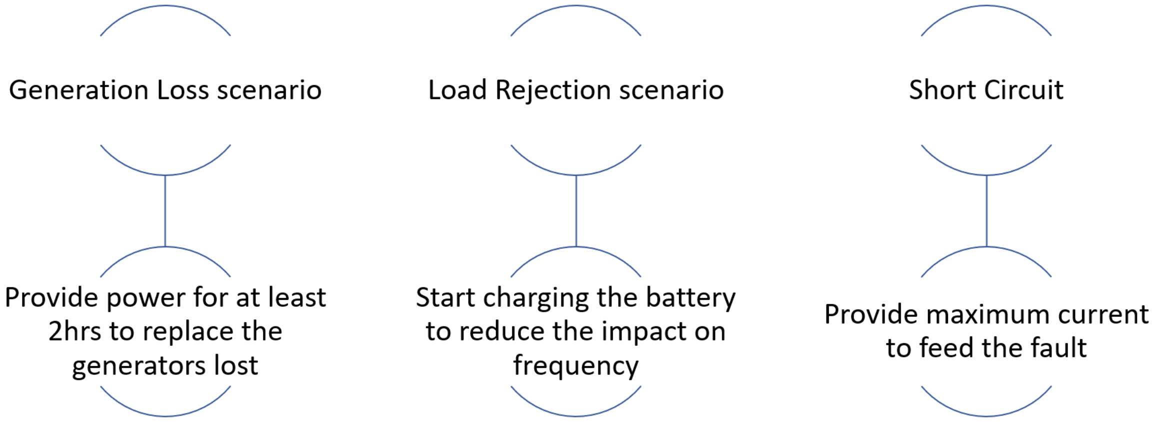

Figure 4.1: The goal of each of the three test scenarios visualised.

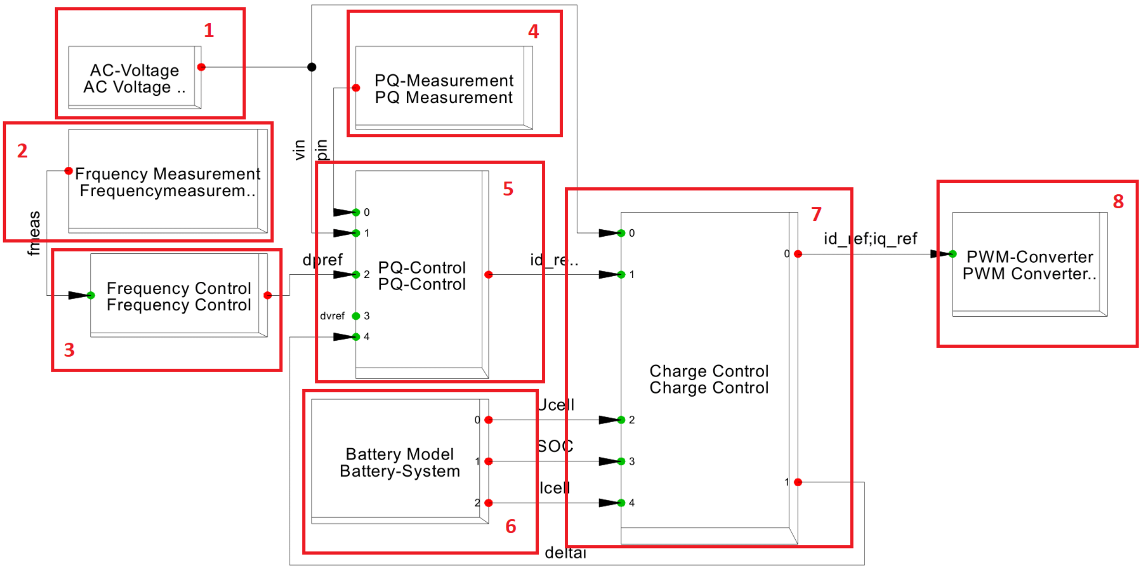

Figure 4.2: Control structure of the Lithium ion battery indicating the several input/control parts.

Frequency input and power demand calculation based on frequency

The frequency is measured at the same terminal but is compared to a deadband (200 mHz, or a change of 5MW translated via Formula 3.2). The deadband is implemented to make maximum use of the gas turbines during normal operations and not have the lithium ion battery charge and discharge at every change of load. Lithium ion batteries degrade based on the number of (dis)charges [25]. If the deadband is exceeded the control receives a requested output power translated via the drooprate (see Equation (3.2)).

Current output power measurement

A third measurement is done at the terminals of the AC side of the inverter to determine the current output power. The PQ controller needs to control the active and reactive power produced by the PWM converter. Active power is tied to the frequency, thus the power measurement and the required change by the frequency control module is used to calculate the controls for the PWM converter. The voltage measured is compared to the reference voltage of 1 pu in order to determine the amount of reactive energy required to change the voltage.

Table 4.1: Element definition of Figure 4.2.

#	Item	Element	Details
1	AC-Voltage	StaVmea	
2	Frequency Measurement	ElmPhi	
3	Frequency Control	ElmDsl	
4	PQ-Measurement	StaPqmea	
5	PQ-Control	ElmDsl	
6	Battery Model	ElmDsl	
7	Charge Control	ElmDsl	
8	PWM-Converter	ElmVsc	Sinusoidal Two level PWM

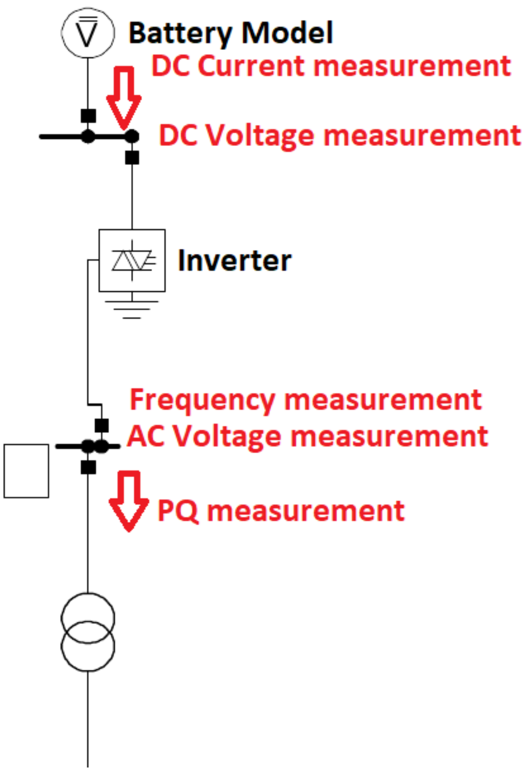

Figure 4.3: Powerfactory implementation of inverter with the measurement location and direction indicated.

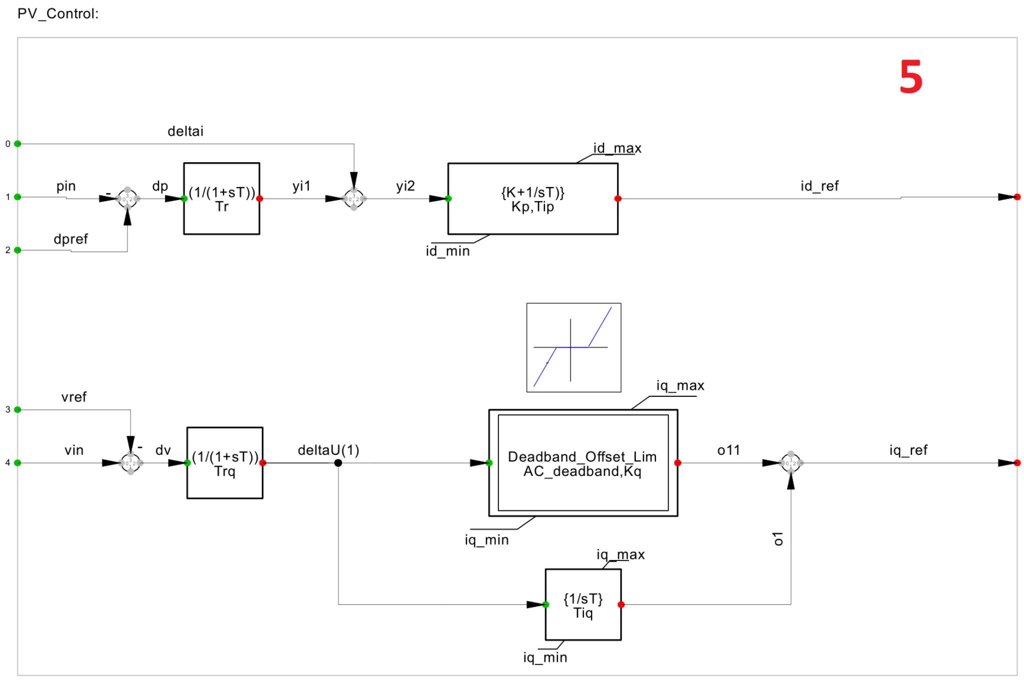

Figure 4.4: Inside overview of the PQ controller.

4.1.2 PI controller

Both signals are given to their own PI controller as can be seen in Figure 4.4. These control the response and damp rapid changes in the output.

Active power - current calculation

The current power output measured by the PQ Measurement (element 4 in Figure 4.2) is deducted from the output of the frequency (element 3 in Figure 4.2). This result is integrated and added to the difference in previously calculated output current and the real output current (see Figure 4.5, for the calculation of *deltai*). This number is then amplified and integrated with maximum. All these numbers can be found in Appendix A.7.

Reactive power - current calculation

To calculate the required voltage output the current voltage is removed from the reference. This is integrated twice with a deadband and limits to determine the reactive current required to change the voltage on the AC side.

Charge control

Lithium ion batteries have maximum of stored energy, when the battery is fully charged the control will have to stop charging. When the battery is empty the control should stop providing power. This is done by the charge control. The state of charge (SOC) is based on the voltage of the battery (which changes with the amount of stored energy). If the SOC is 0 or 1 the dis/charging stops in all other cases the output of the PQ controller is given to the PWM converter.

This is done by determining if the battery will be charged or discharged based on the direction of id_{ref_in} and comparing this to the maximum and minimum charge levels of the battery. If the SOC is within the limits

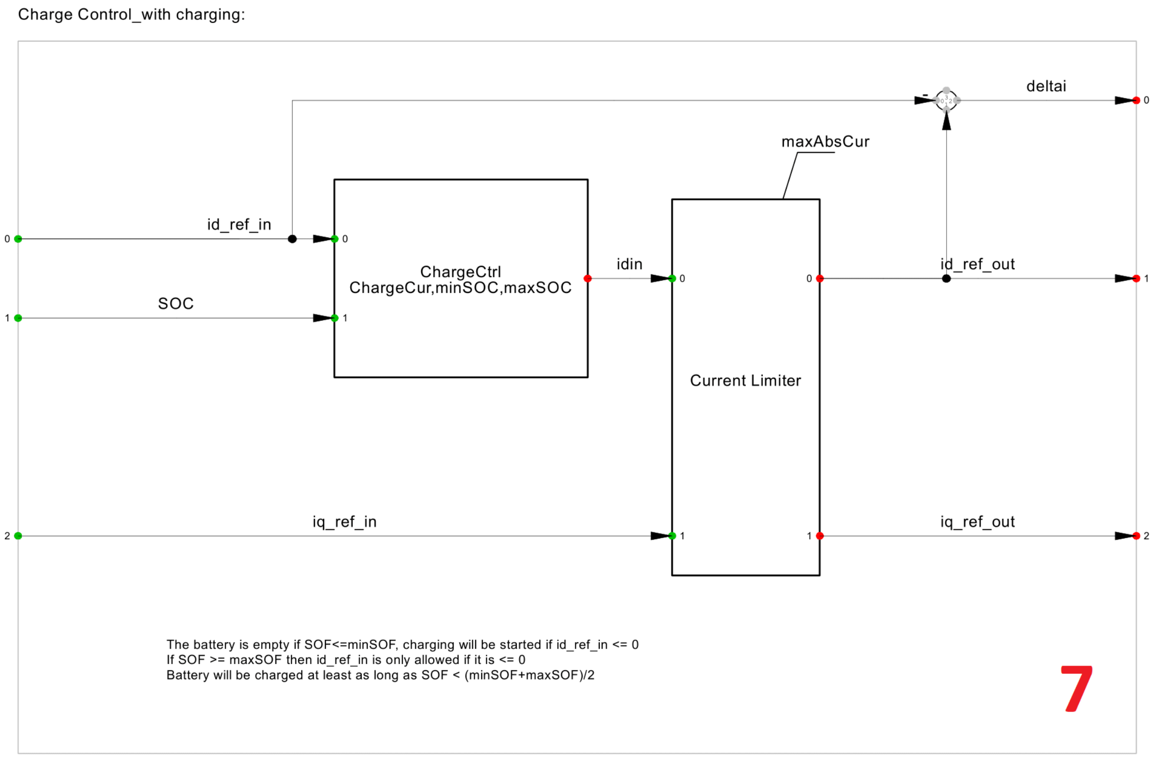

Figure 4.5: Block diagram of the charge control block. Limiting the power output based on the SOC.

of charge the PI controllers output signal is fed to the current limiter. This limits the maximum current output current such that inverter is not damaged. See Figure 4.5.

5
Case studies and result for the lithium ion battery

Integrating inverter based generation into the islanded grid is financially interesting. But for a company the reliability of this innovative technology is also important. The impact a lithium ion battery can have is examined by answering the sub question: *"What is the operational impact of integrating these inverter based generation into the LNG plant model?"*.

In Figure 4.1 the required response of the battery can be observed. In this chapter these scenarios will be checked to see if the lithium ion battery is capable of replacing spinning reserve.

5.1 Load rejection scenario

The 100 MWh battery is designed to replace a failure of a generator. This happens 3 to 4 times per generator per year [24][36]. This means that the battery pack will be used on average 20 times per year. If SOC is not 100 % the battery can be used to absorb load, rejected by the system. The charging rate of large scale lithium ion batteries is equal to the discharge rate [10].

5.1.1 Description of the dynamic behaviour

In Figure 5.1 the load rejection scenario can be seen. The battery starts to charge with a rate of 50 MW and within t= 0.5 s. This results in less over generation by the generators. And thus less frequency change. In the conventional scenario (see Figure 3.4) the frequency exceeded the 2 % requirement set by the Shell DEP. Due to the lithium ion battery charging this is not the case.

5.1.2 Fully charged battery response

The lithium ion battery will mostly be full and ready to discharge since that is the main function. When the battery is full it is unable to react to any load rejections. Since the inertia of the system is reduced by having 5 instead of 6 generators, the impact of the halting of the compressors is larger. As can be seen in Figure 5.2.

5.2 Generation loss scenario

The main goal of the battery is to replace the power generated by a tripped generator. In this scenario the generator is disconnected and there is not enough spinning reserve to replace this turbine. The battery will fill this void as can be seen in Figure 5.4. Since the ramp rate of lithium ion batteries is 91 MW/s the battery is almost instantly providing the lost generating unit. This results in only a 0.5 % frequency change. The battery is only providing 32 MW of continues power since the other turbines also reacted to the changing condition and increased their output. The battery is now able to last longer than the required 2 hrs, the size of the battery cannot be reduced since it is the only unit with capacity left to react to changes in the system. A sudden increase of required power by the system (energisation of a transformer, etc) will require the battery to deliver more energy to the system. The comparison between the conventional generation and the lithium ion battery can be seen in Figure 5.3.

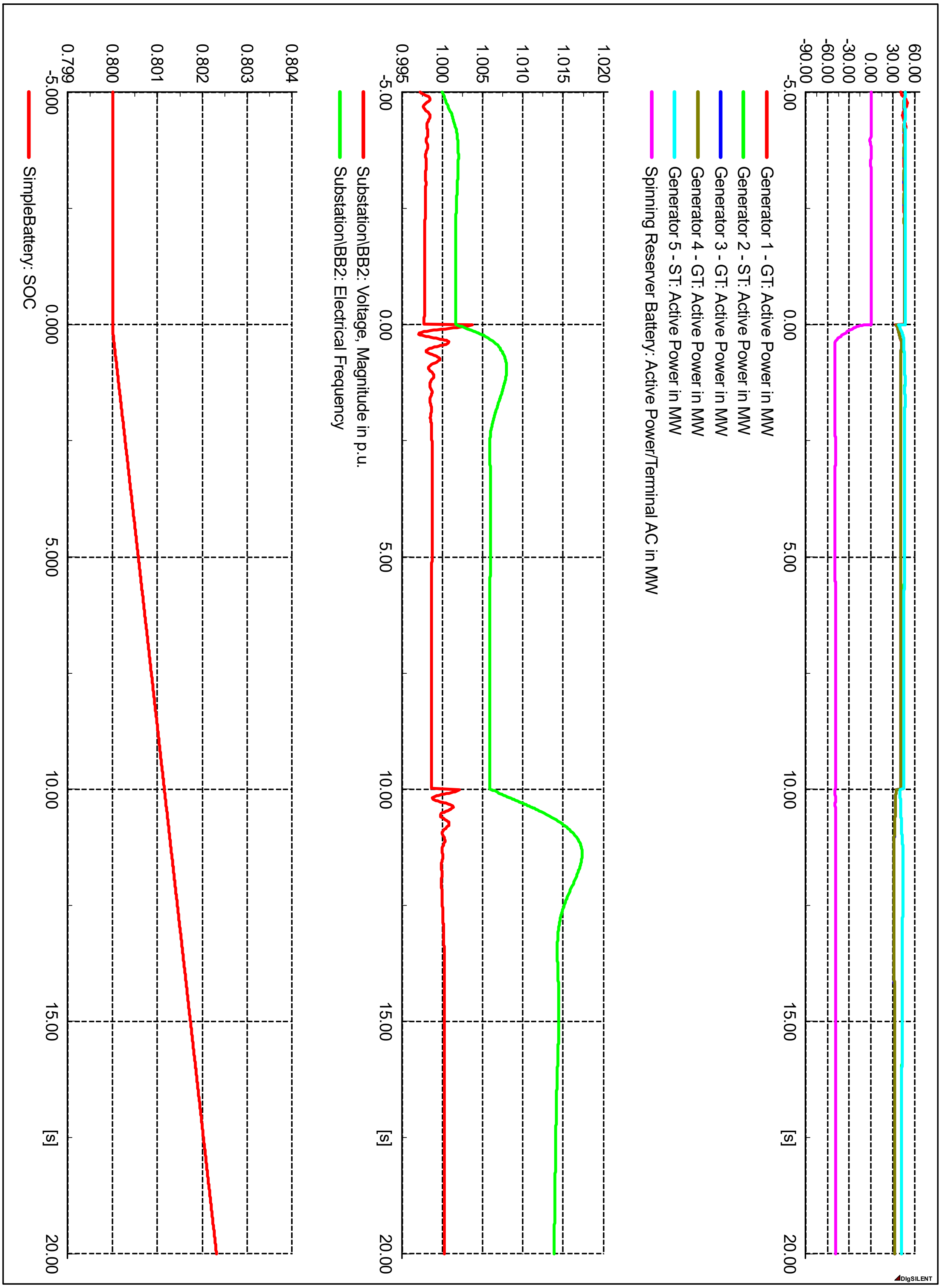

Figure 5.1: At $t = 0$s, 66MW of load is rejected due to the stopping of a compressor. The battery starts to charge at maximum capacity to reduce the impact of this change on the frequency. The second compressor stopping at $t = 10$s does not lead to a violation of rule 3.3.2b of the Shell DEP, a positive change compared to the conventional scenario.

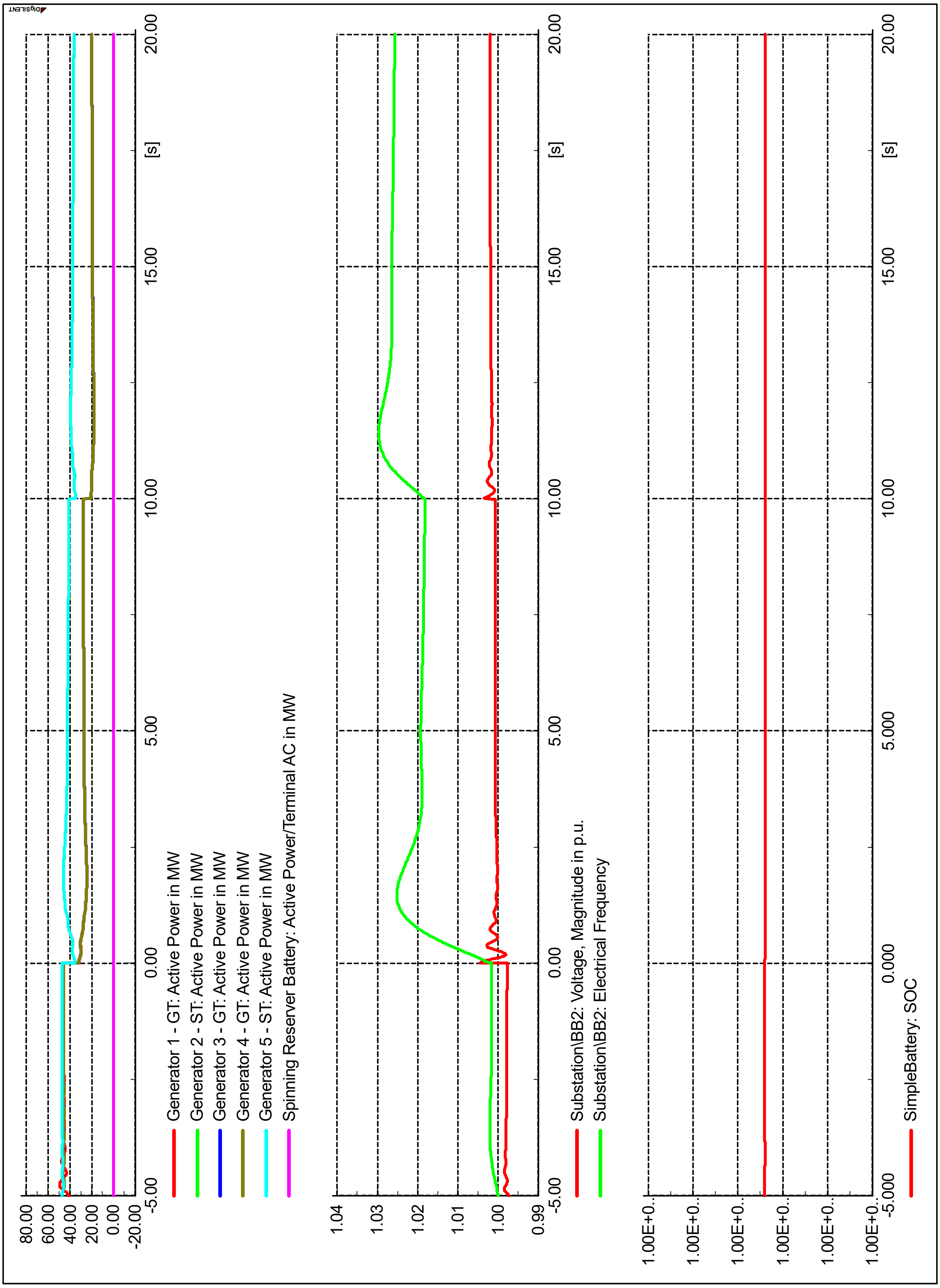

Figure 5.2: With a SOC of 100% the battery is unable to absorb more load and since the inertia is reduced by the removal of the spinning reserve battery the frequency change is larger than previously observed.

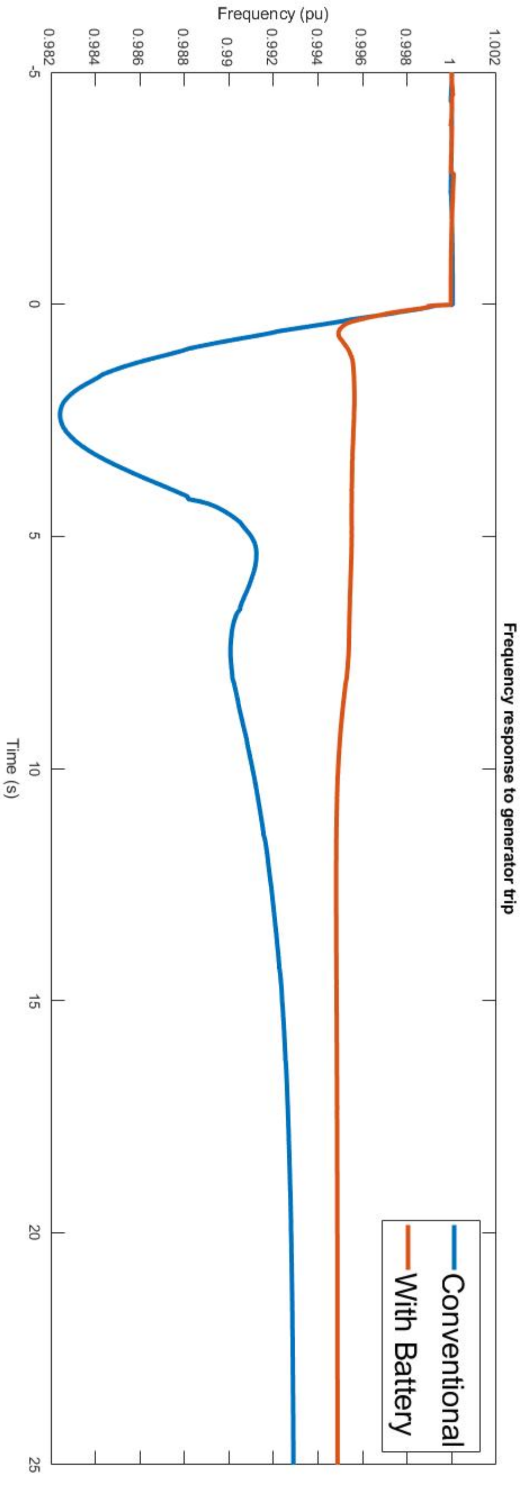

Figure 5.3: Comparison between the frequency change in the generation loss scenario between conventional and lithium ion assisted generation.

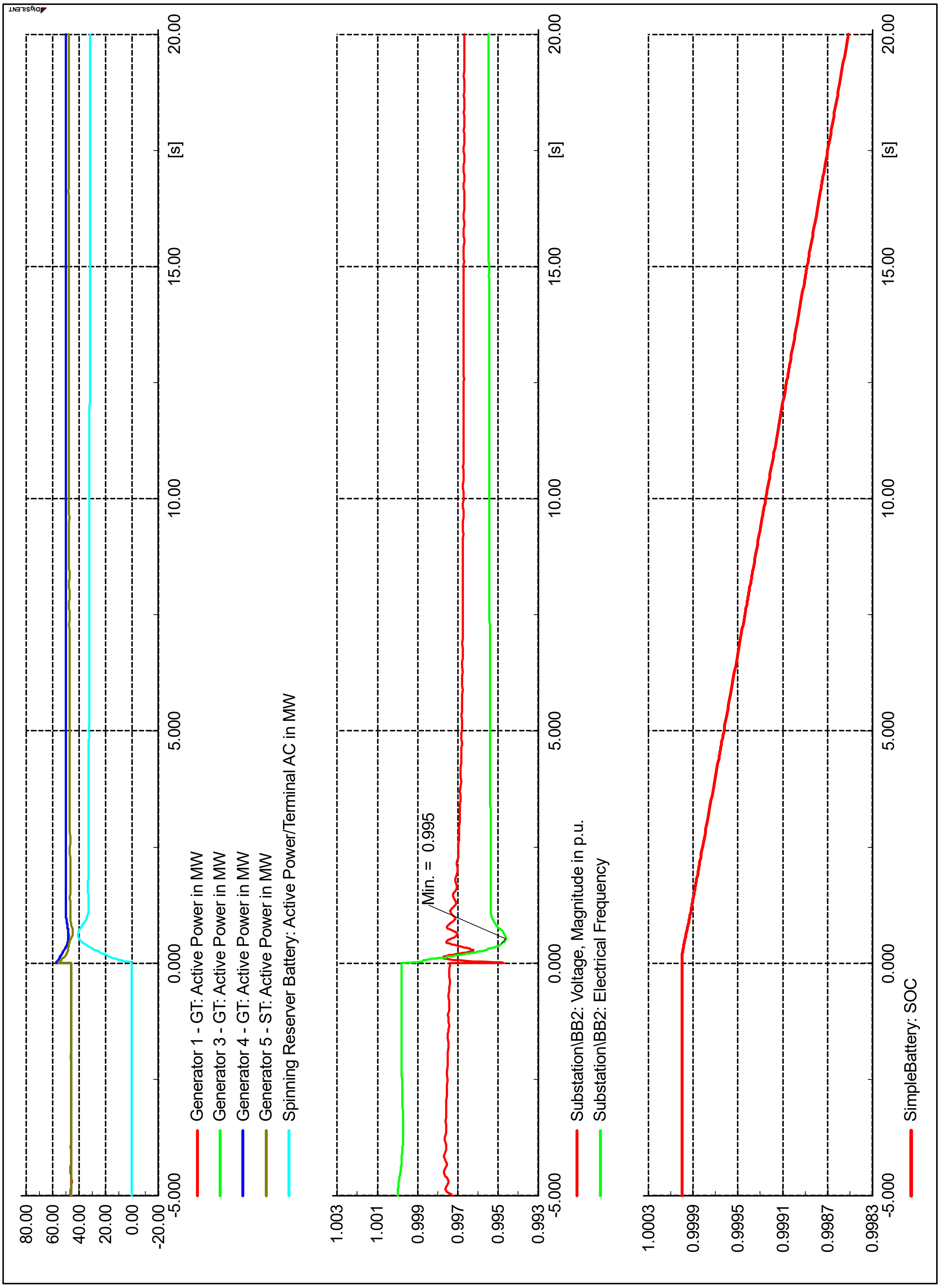

Figure 5.4: Reaction of the Lithium ion battery to the loss of the inverter. A clear increase in power can be observed after which the frequency stabilises. The battery charge starts to decrease in the bottom part of the figure.

5.3 Short circuit

With a generator less in the system the amount of short circuit current available is reduced, a battery is unable to provide more than 1.1 pu current for longer periods of time [21]. This means that the total system short circuit level is reduced. As is the case in the report generated by the Powerfactory software. See Appendix A.6. The total short circuit current has a peak of 18.18 kA which is still more than enough for the protection devices to react.

5.4 Conclusion

The battery is able to provide the spinning reserve once a generating set is out of order. This (main function) is fulfilled better by the battery since it responds faster than the generator does. In the load rejection scenario the functionality is reduced once the battery is full. The system exceeds the 2 % frequency variation. There is no solution within the current frame to solve this issue. The short circuit is still 18x more than in nominal conditions, protection should be capable to distinguishes these conditions.

Thus the battery is a suitable replacement for the spinning reserve.

6

Control design for replacing a gas turbine with solar PV and a VRF battery

The reduction of fuel use for the generation of power is beneficial in three ways, firstly there is no more emission of CO_2, secondly no tax has to be paid on the CO_2 and lastly the fuel gas can be sold. Since the gas powered power plant size is reduced the maintenance is also reduced. The solar PV and VRF battery replacing this turbine is earned back within 13.1 years as mentioned in Chapter 2.

In order to answer the main question the sub-question: *"What is the operational impact of integrating these inverter based generation into the LNG plant model?"* will be answered. In this chapter the infrastructure for the solar PV and VRF battery are explained and the controls for the inverter are designed.

Additional requirements for Solar PV and VRF Batteries
Solar PV is much more variable in its power output than gas turbines [3]. This leads to additional requirements for the solar PV and the VRF batteries:

1. The maximum amount of solar energy should be used at all times.
2. Excess energy (>50 MW) should be used to charge the battery.
3. When the solar output is below 50 MW, the battery will not charge nor discharge during the day.

Required behaviour during disturbances
The lithium ion battery should be able to react to several scenarios. For the defined case studies the reaction of the inverter can be seen in Figure 6.1.

6.1 Inverter based plant model overview

The financial analysis indicated that the replacement of a gas turbine with Solar PV might be a viable business case. The use of solar PV requires that a storage medium is required for the night period. Both of these parts are modelled as one component in the Powerfactory software. The internal design of this element can be seen in Figure 6.2. This model is an adaptation of the "Island and Gen" Tutorial provided with the Powerfactory software [29].

6.1.1 Solar Photovoltaics

Converting solar energy into electric energy is commonly done using solar PV panels. These solar panels should operate at the Maximum Power Point (MPP). Making sure that the voltage of each panel is at its MPP is done using a converter. To reduce the number of inverters the solar panels are connected into strings. These strings produce power at a MPP voltage of 1500 V. At this point the string is capable of converting the most solar energy into electric energy [14]. Thus fulfilling the first requirement set in this chapter.

Each of these strings is connected to at DC-DC converter to regulate the voltage and achieve maximum power output. The DC-DC converters are connected to a DC busbar where the night time storage is located. See Figure 6.2.

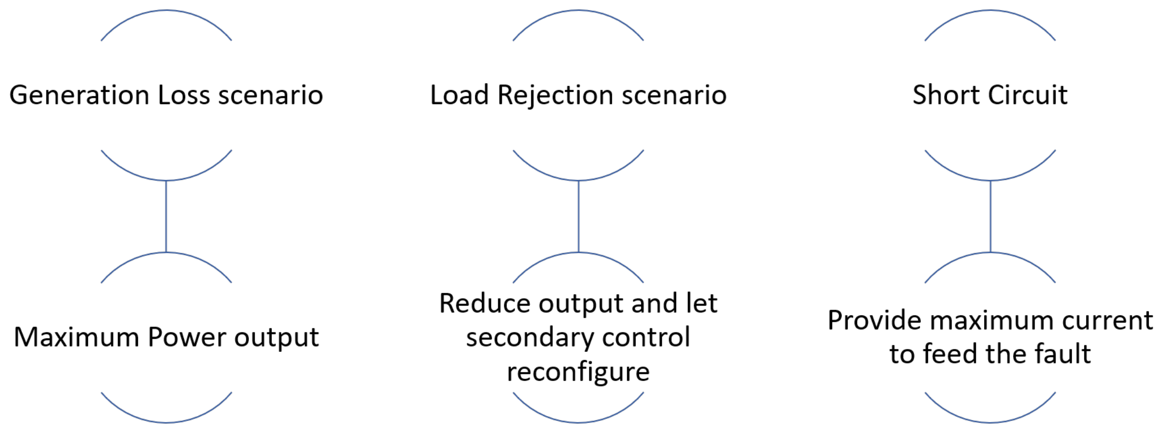

Figure 6.1: Required reaction of the inverter.

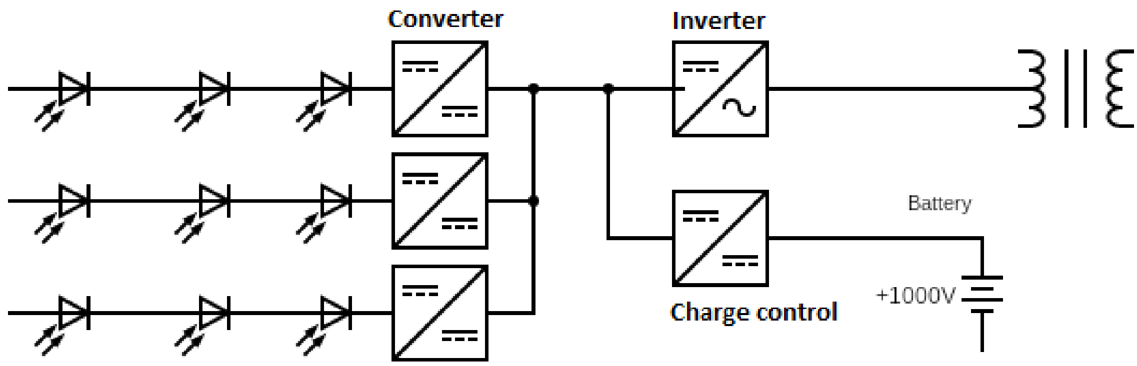

Figure 6.2: Design of the PV and battery medium voltage - DC infrastructure.

6.1.2 Vanadium Redox Flow battery

The night time battery should be at least 614.16 MWh (50 MW · 12 hrs + 14.16 MWh winter night time storage. See Chapter 2.5.2). This battery should be able to charge and discharge for the ROI time (13+ years) without degradation. The only feasible storage method for the sites location is vanadium redox flow battery. The redox reaction producing the electrons can be found in Equation 6.1 and Equation 6.2.

$$V^{+}(III) + e^{-} \Longleftrightarrow V(II) \tag{6.1}$$

$$V(IV) \Longleftrightarrow V^{+}(V) + e^{-} \tag{6.2}$$

The night time storage is directly connected to the DC bar of the system. This reduces the number of conversions. The DC charge controller connects the individual cell to the DC bar. This enables the system to (dis)charge at variable rates enabling flexibility to changing conditions(Clouds, shade, etc). Thus fulfilling the second requirement stated in the beginning of this Chapter.

6.2 Inverter control

The inverter should be able to comply with the Shell DEP as mentioned in Chapter 3 and the additional requirements in Chapter 6. To model the whole system as good as possible it is divided into several parts. These can be seen in Figure 6.3.

6.2.1 Solar energy conversion modelling

To translate changing conditions in temperature and irradiance to the electric energy, the PV panels are modelled with these parameters. These variables combined with the actual DC bus voltage are fed to the solar PV

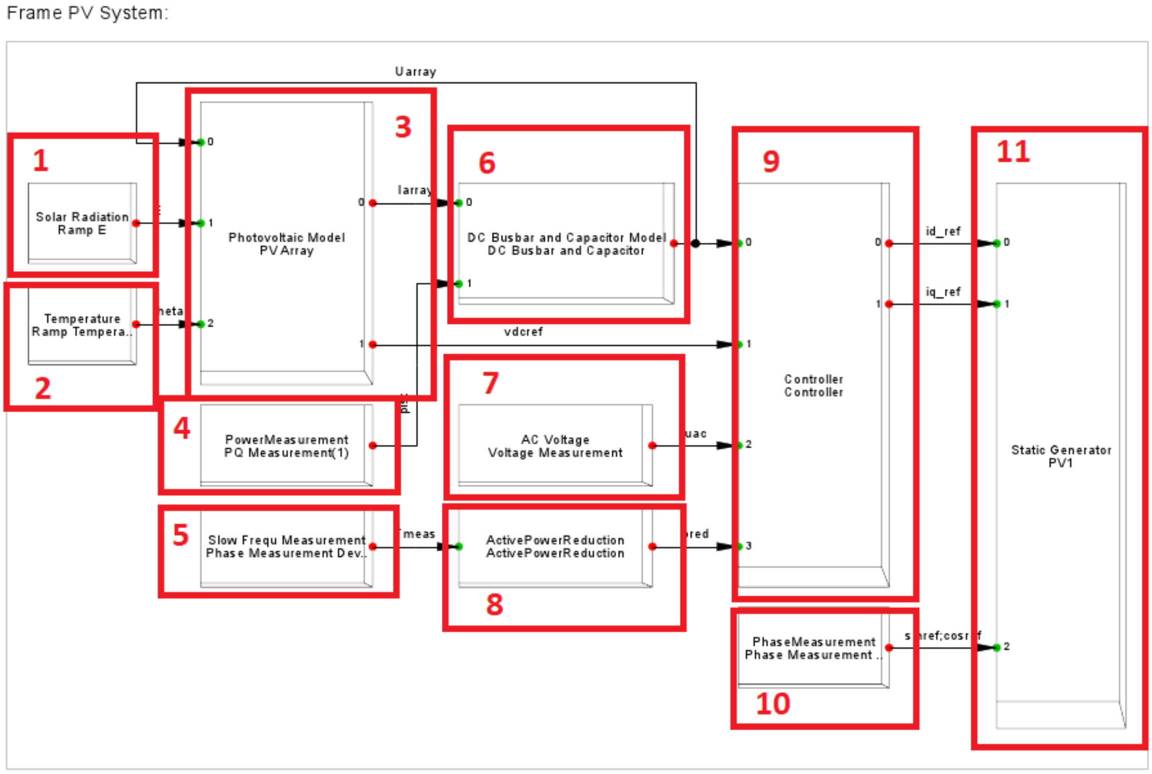

Figure 6.3: Internal control of the PV control, elements indicated in 6.1.

Table 6.1: Table indicating the elements of the 6.3.

#	Item	Element	Function
1	Solar Radiation	ElmDsl	Input for Solar data
2	Temperature	ElmDsl	Input for Temperature
3	Photovoltaic Model	ElmDsl	Model implementation for a single panel, multiplied by the designed plant
4	Power measurement	StaPQmea*	Measurement of the output power
5	Slow Frequency Measurement	ElmPhi*	Frequency measurement
6	DC Busbar and Capacitor Model	ElmDsl	DC busbar model
7	AC Voltage	StaVmea	Measurement of the grid voltage
8	Active Power Reduction	ElmDsl	Frequency based active reduction of the active power output
9	Controller	ElmDsl	Controller housing
10	Phase Measurement	ElmPhi*	Phase measurement for synchronisation
11	Static Generator	ElmGenstat	Inverter

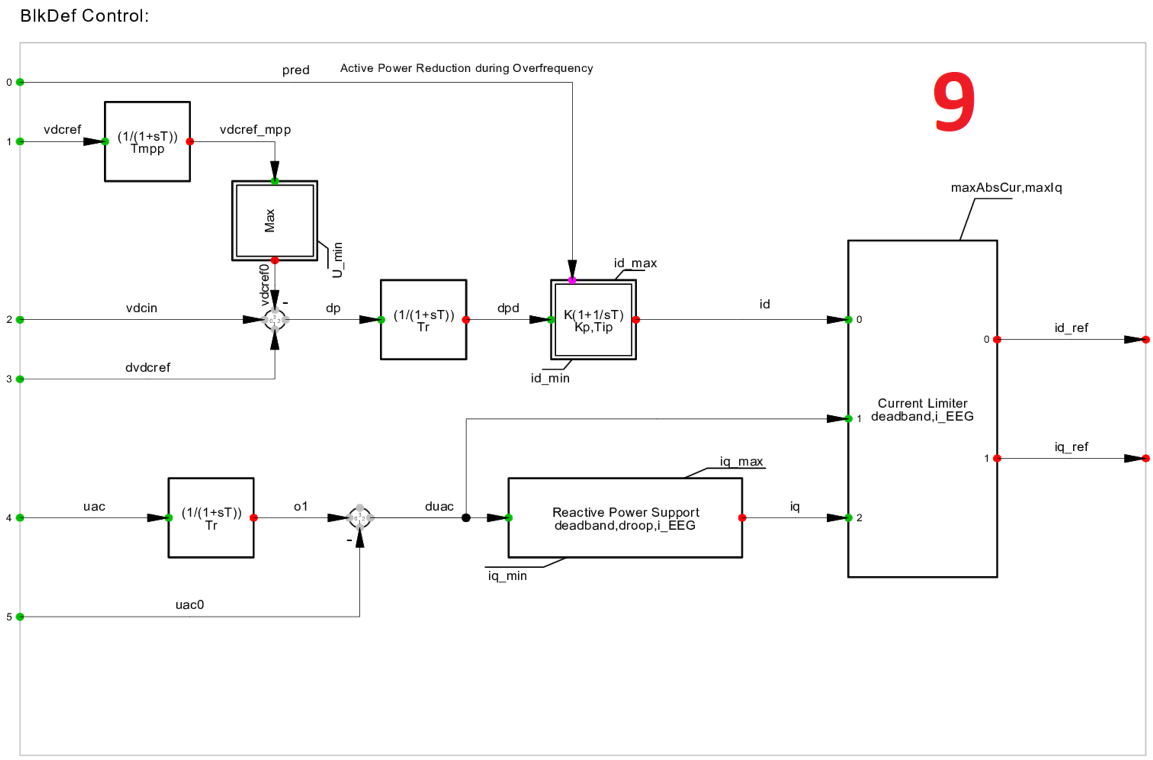

Figure 6.4: Inside look of the Controller of the PV.

panel model (element 3 in Figure 6.3).

Solar panel model
The model is based on the SunPower P17 355 Com panel. SunPower is a supplier of many large utility scale PV parks. Their panels are reliable (20+ year warranty) and efficient (16.2 %) [37]. Furthermore their price follows the trend given in [15].

Multiple of these panels are connected in series to generate the 1500 V on the DC busbar. The voltage on this busbar will change based on the amount of power being inverted by the inverter [6].

6.2.2 Controller

The MPP voltage is delayed and subtracted from the current DC busbar voltage. The DC busbar voltage is directly related to the active power output of the inverter since the busbar voltage is reduced when there is an active power flow. The number is then delayed and fed to a PI controller. This controller is influenced by the active power reduction parameter which is calculated based on the current frequency. If the frequency is exceeds by >200 mHz the active output of the inverter is reduced. This limit is introduced in order not maximise the usage of solar energy. If no reduction is required the number is fed to the inverter. See Figure 6.4.

Reactive power
The inverter is also capable of delivering reactive power to change the voltage in the system. Based on the difference in AC voltage and the reference, the reactive power is calculated. This is then fed to the inverter.

Both the active and reactive required currents are sent to the inverter, which based on the voltage angle starts firing the switches, to produce these currents.

7

Case studies and result for replacing a gas turbine with solar PV and a VRF battery

Remaining in stable conditions while large variations (load rejection, short circuit and generation loss) are occurring in the system is very important for a LNG plant. The process requires constant cooling. In order to study the impact of replacing large synchronous gas fired, CO_2 emitting turbines with solar PV the following case studies are conducted. This is done to answer the sub question: *"What is the operational impact of integrating these inverter based generation into the LNG plant model?"*.

Structure

This is done by performing the (same) three test, Load rejection, generation loss and short circuit. Each of these test will be conducted separately and combined using Matlab. The individual results can be seen in the appendices.

Change in single line diagram

With an increasing number of Solar PV the ROI is decreased. Thus the stability is verified for increasing number of PV. This change can be observed in Figure 7.1.

7.1 Load rejection scenario

The controls of the solar PV enable the output of the inverter to ramp down the production once the threshold is exceeded.

Behaviour

During the load rejection of the first compressor the PV ramps down its output, this results in a reduced frequency change. As can be seen in Figure 7.2. During the second compressor disconnecting the frequency change is increased per solar PV. Since the output power of the solar PV is already reduced the reaction is delay until the frequency surpasses the previous peak frequency peak. This delay causes a new higher peak. The reduced inertia will result in a steeper frequency change (a higher rate-of-change-of-frequency (ROCOF)). During the cascading loss of two compressors the PV ramps down output of the inverter. The control to enable this is explained in Chapter 6.2.2. The individual PV reactions to the different scenarios can be seen in appendices A.9,A.10,A.11 and A.12. The frequencies are plotted in Figure 7.2. In Figure 7.2 this reaction can be seen for increasing numbers of PV plants constructed.

7.2 Generation loss scenario

During the generation loss scenario the PV system is not able to produce any extra power as it is already operating at the maximum of the inverter. This results in a larger frequency dip with each generator replaced by an inverter. As can be seen in Figure 7.3.

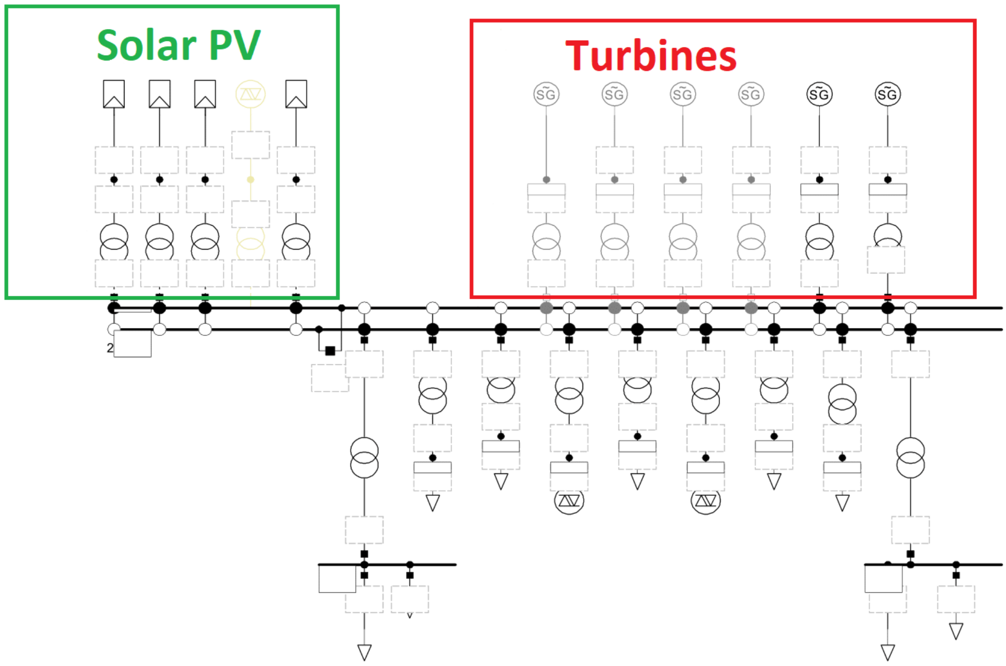

Figure 7.1: On the left, the solar PV VRF battery combination, on the right the gas turbine.

7.3 Short circuit

In Figure 6.1 the goal of the inverter system is shown during a short circuit, the inverter should feed the fault with maximum power. The short circuit current provided by the inverter the maximum is 0.59 kA. The maximum current of the gas turbine is 3.62 kA. This large difference will result in a slower reaction of conventional protection devices. These protection devices follow the curve visible in 7.4. Since the maximum current output of the inverter is 1 pu conventional trip curves will not work. It is not within scope of this research to find solutions for this issue. The exact figures of the short circuit contribution can be found in appendixes A.7.

7.4 All PV generation

Replacing the fifth generator by an inverter leads to overproduction by the PV if the inverter is used to it maximum capacity. Since the 5 inverter can supply more than enough energy to run the system the sixth generator can also be disconnected. Thus having no inertia in the system anymore. The control in this scenario start to oscillate in several ways. This leads to a situation where the system is not stable.

This is the result of grid feeding inverters. This issue can be resolved by using grid forming inverters. These inverters use different hard and software to be able to generate the power at the right frequency. This is not in the scope of this project and thus is not analysed. Thus no simulations can be preformed.

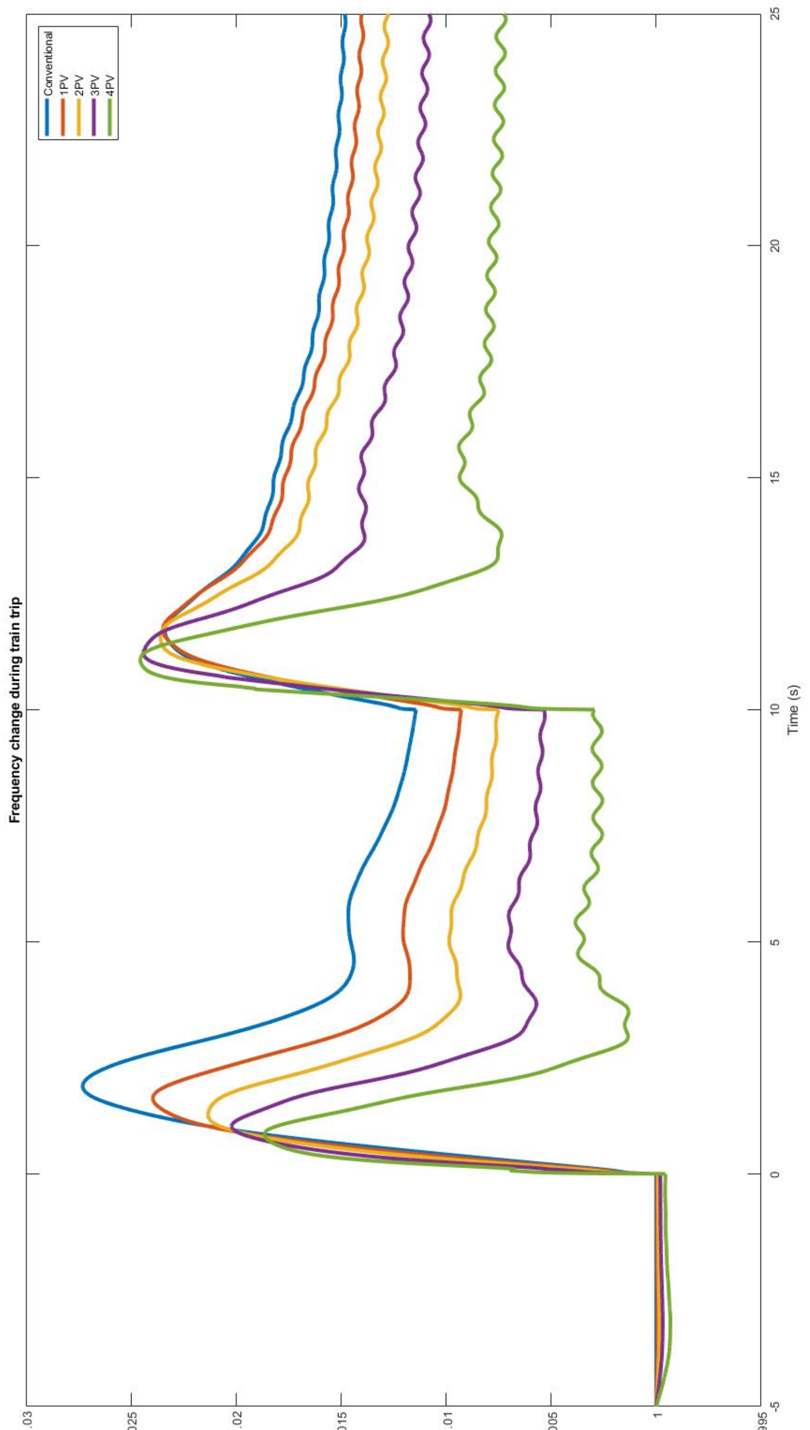

Figure 7.2: Frequency reaction of increasing number of solar PV implemented in the system. Thus less inertia in the system, resulting in a larger frequency change.

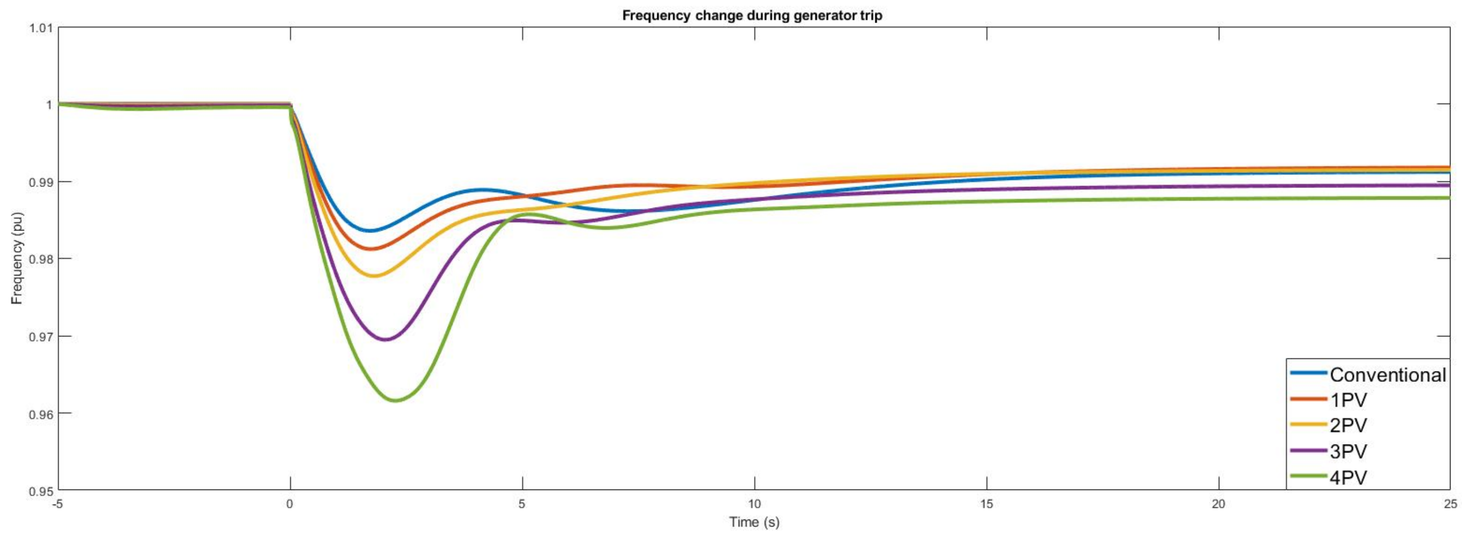

Figure 7.3: Increased frequency change due to less spinning reserve in the system.

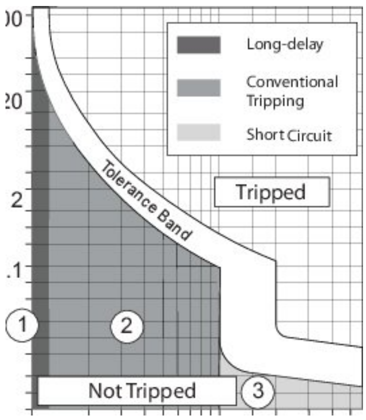

Figure 7.4: Typical trip curve. (Source: [11])

8

Conclusion and recommendations

To reduce cost and CO_2 in a large industrial plant various options are possible. For the LNG plant several solutions are available to reduce the cost and CO_2 emissions of the power generation. But all of these have a impact on the cost and performance of the LNG plant. This research focused on two implementations of inverter based generation for a large industrial plant. The main research question was: *"What are the implications of replacing gas turbine driven synchronous generators with a combination of solar PV and batteries on dynamic performance and cost within a islanded LNG plant with a load of* 230 MW*?"*.

8.1 Sub questions

To answer the main question 3 sub questions where devised. These where:

- What are the cost drivers within conventional power generation of a islanded LNG plant?
- Which inverter based generation can be used to reduce the emissions and/or costs of the power generation for a islanded LNG plant?
- What is the operational impact of integrating these inverter based generation into the LNG plant model?

8.1.1 What are the cost drivers within conventional power generation of a islanded LNG plant?

A main cost drivers within a conventional power plant is the construction cost. The cost decreases very rapidly with an increase in power plant size. The cost for the conventional 300 MW power plant is 264 M$. The second large cost is the operational expenditure. This amounts to 15 M$/year/turbine, almost equally divided between fuel, CO_2 tax and maintenance.

8.1.2 Which inverter based generation can be used to reduce the emissions and/or costs of the power generation for a islanded LNG plant?

To answer this question two variations where explored:

Reduce the capital expenditure

By reducing the power plant to 250 MW will decrease the capital expenditure. But can lead to unwanted scenarios if a turbine trips. To mitigate these risks a lithium ion battery can be added. The capital expenditure of the power plant including the battery is 280 M$ (16 M$ extra). The maintenance is reduced by 0.94 M$. Leading to a return of investment period of 16.6 years.

Reduce CO_2 by replacing gas turbines with solar PV and VRF batteries

Reducing the amount of CO_2 produced during the liquefaction process is a key goal for Shell. This can be accomplished by replacing the gas turbines with solar PV and a VRF battery. This increases the CapEx with 222 M$ but decreases the OpEx with 14 M$. The ROI is 13 years for the first turbine, The ROI will be lower with every turbine replaced.

There are 520043 tilting panels required to provide enough energy for both winter and summer time with energy generated during the day to charge the night time battery. The battery should be a VRF battery since this is the only technology available that is able to handle this many loading cycles (20 years, 365 days).

8.1.3 What is the operational impact of integrating these inverter based generation into the LNG plant model?

The third sub questions was answered in order to understand the impact on the sites reliability. For this research two models where adapted.

Lithium ion battery replacing the spinning reserve

The battery is able to react faster to a trip of one of the generators. The result is less frequency variation and thus less chance of damaging the equipment. In the load rejection scenario the battery is unable to respond since it is already fully charged. It is not financially viable to keep the battery in a less charged state. In the short circuit the total current is reduced since one turbine is removed. This is not an issue since this the total current is still large enough to distinguish between fault and normal operation.

Replacing gas turbines with solar PV and VRF battery

Using the energy generated by the solar PV to its maximum enables us to reduce the amount of gas used and reduce the emissions of the CO_2. This means that the inverter is used at its maximum capacity (50 MW). During the generation loss scenario the inverter is unable to provide more energy. Thus the frequency change is large with every turbine replaced.
In the load rejection scenario the PV ramps down after the frequency exceeds the 200 mHz threshold. The second compressor disconnecting leads to an increased frequency with the maximum the same for every configuration. This is due to the fact that the PV output power is already reduced and thus cannot adjust.
The inverter can only provide 1 pu current during a short circuit. The protection devices cannot distinguishes between normal operations and short circuit conditions.

8.1.4 Main research question

With these three research question answered the main question can be answered. The main question was: *"What are the implications of replacing gas turbine driven synchronous generators with a combination of solar PV and batteries on dynamic performance and cost within a islanded LNG plant with a load of* 230 MW *?".*

The answer is, The lithium ion battery for replacing the spinning reserve has a positive effect on the maintenance and has a return of investment within 16.6 years. The operational scenarios showed mixed results. For the lithium ion battery the result was an improved reaction in the generation loss scenario. Because the ramp rate of the battery is much larger than the generator it is replacing. The control is able to detect a variation in frequency and starts to provide active power. In both the load rejection and the short circuit the contribution of the inverter is limited. The battery is unable to be absorb the excess energy since the battery is already full in the load rejection scenario. In the short circuit study case the maximum output current of the inverter is 20x lower than that of the generator it is replacing.

The second implementation is to replace the generator with a combination of solar PV and VRF batteries. This increase the capital expenditure by 82 %. The operational expenditure is greatly reduced and the output of CO_2 is reduced by 21 %. For the solar PV and the VRF battery the load rejection study case shows improved reaction. The reaction is faster than that of the turbine it is replacing since the extra energy can be converted instantly this results in less frequency deviation. In the generation loss study case and the short circuit the reaction of the inverter is limited. In the generation loss scenario the inverter is providing maximum output power to decrease the gas consumption of the remaining turbines and is unable to provide more. The inverter is also limited in the short circuit current during the short circuit study case. This results in 1 pu current.

8.1.5 Contributions

This research has shown that for large industrial islanded sites the use of a lithium ion battery is beneficial to the reduction of operational expenditure. The battery ensures there is enough capacity to replace the largest generating unit during a trip.

The second contribution is an improved insight in the financial viability of the use of solar PV for powering a large industrial site in a high solar potential country. The investment is earned back within 13 years while not emitting CO_2.

Model adjustment
A model for the lithium ion battery has been adjusted. Then several studies where conducted. These showed a improved performance for case a generator trips. For the solar PV a control model for the ramping down behaviour was created and several tests have been conducted. The stability was improved in the load rejection scenario by the PV ramping down.

8.2 Recommendation

This research has shown that the use of inverter based generation seems economically viable. The lithium ion battery replacing the spinning reserve is a direct measure that can be taken to reduce the operational expenditure and reduce the change in frequency during a generation loss scenario.

For the implementation of solar PV and a VRF battery the financial side looks very promising. A short analysis is conducted but more in depth simulations are needed to verify the impact on the process during changing conditions both financially and technically.

8.3 Suggestion for future work

This research answered several questions but also opened new questions. These are categorised based on the the different partners:

8.3.1 Shell

For Shell there are several interesting opportunities to improve the system. These are:

- **DC operations**
  Two big compressors are fed via a VSD. This VSD does not require AC power. Solar PV produces DC energy, thus if the VSD can run on this DC energy the amount of conversions is reduced. Thus improving efficiency.
- **Process optimisation day only production**
  If the system can be designed such that production is only conducted during the day the amount of solar PV can be reduced. This would create a totally different financial analysis. No GT and no VRF battery are needed and the output of the plant will be reduced.
- **Investigate the use in other facilities**
  Both financial calculations are made for the site in Tanzania. Since this is a solar rich country the yield of the panels is very high. The impact of implementing the same techniques in other facilities can be explored in future work.

8.3.2 TU Delft

From a scientific perspective this research opens new questions on the need for controls in a islanded industrial grid. The main suggestions are:

- **Low inertia protection**
  With the increase of inverter based generation in all power generation the amount of inertia will reduce. This will lead to less short circuit current being available. Conventional protection thus will not work anymore. It is suggested that the TU Delft researches how to detect short circuits within islanded systems.
- **Grid forming inverter control**
  In order to reduce the emissions of the generation to zero the system will need to have grid forming inverters. The implementation of these controls must be further developed to understand the impact in a industrial islanded grid.

A

Appendices - Additional figures

A.1 Solar PV potential map

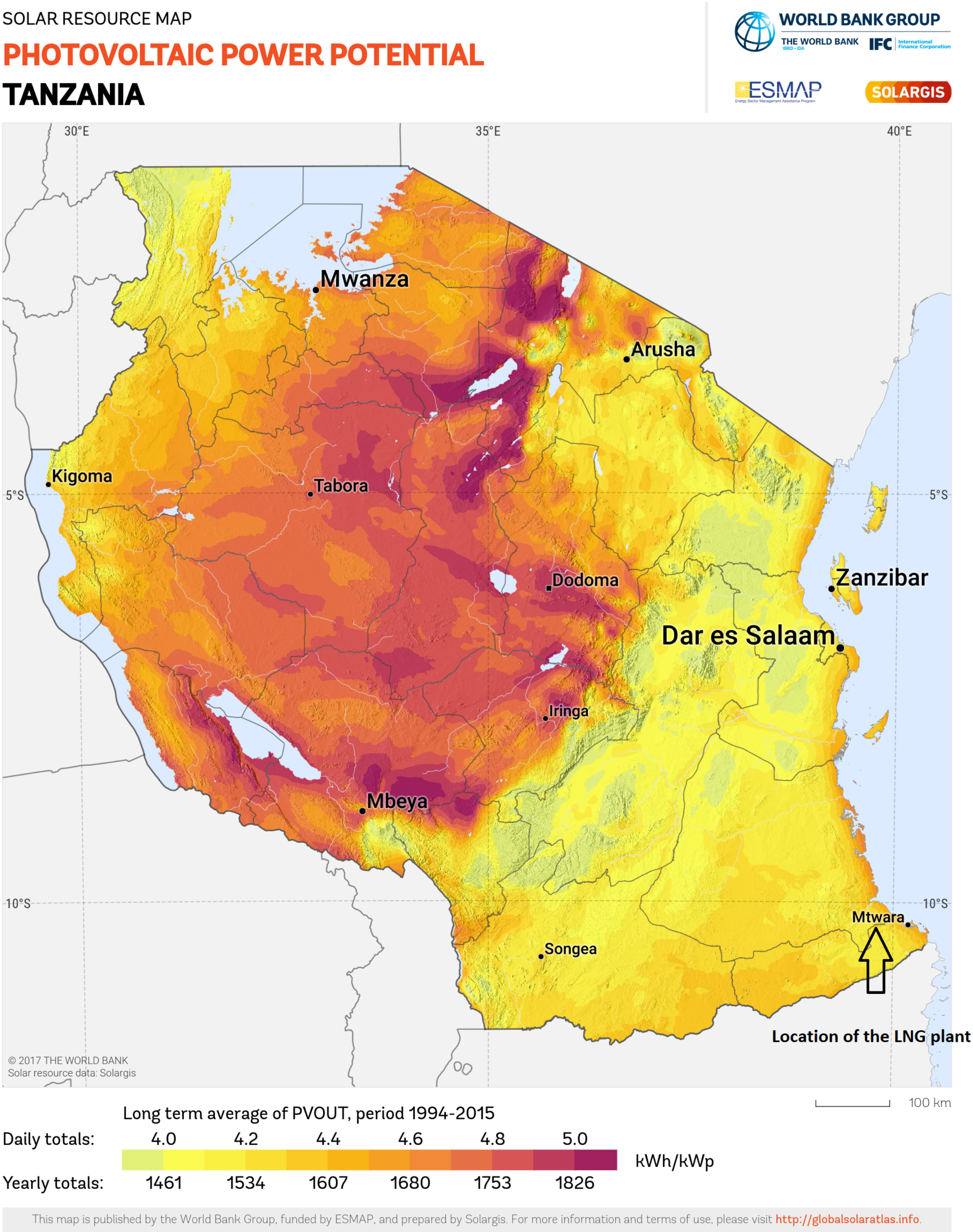

Figure A.1: Solar irradiance potential for Solar PV with the Mtwara site at 4.3kWh/kWp.

A.2 Daylight curve

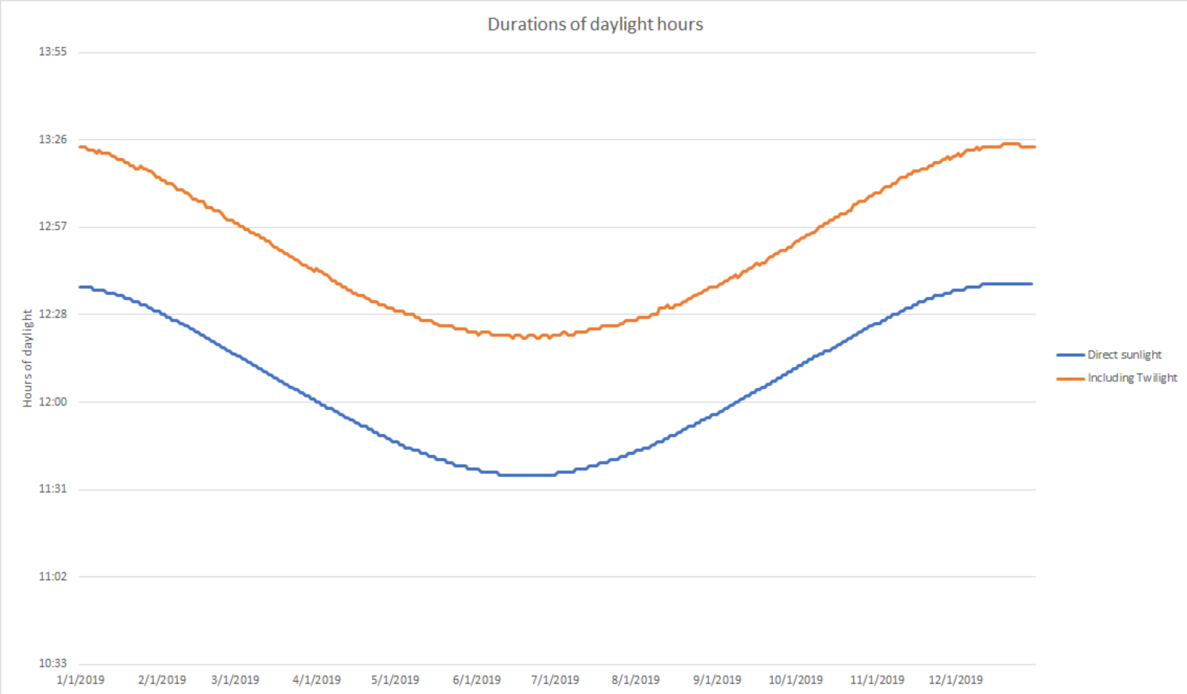

Figure A.2: Hours of direct daylight with the shortest day having 11:43 of direct sunlight.

A.3 GGOV1

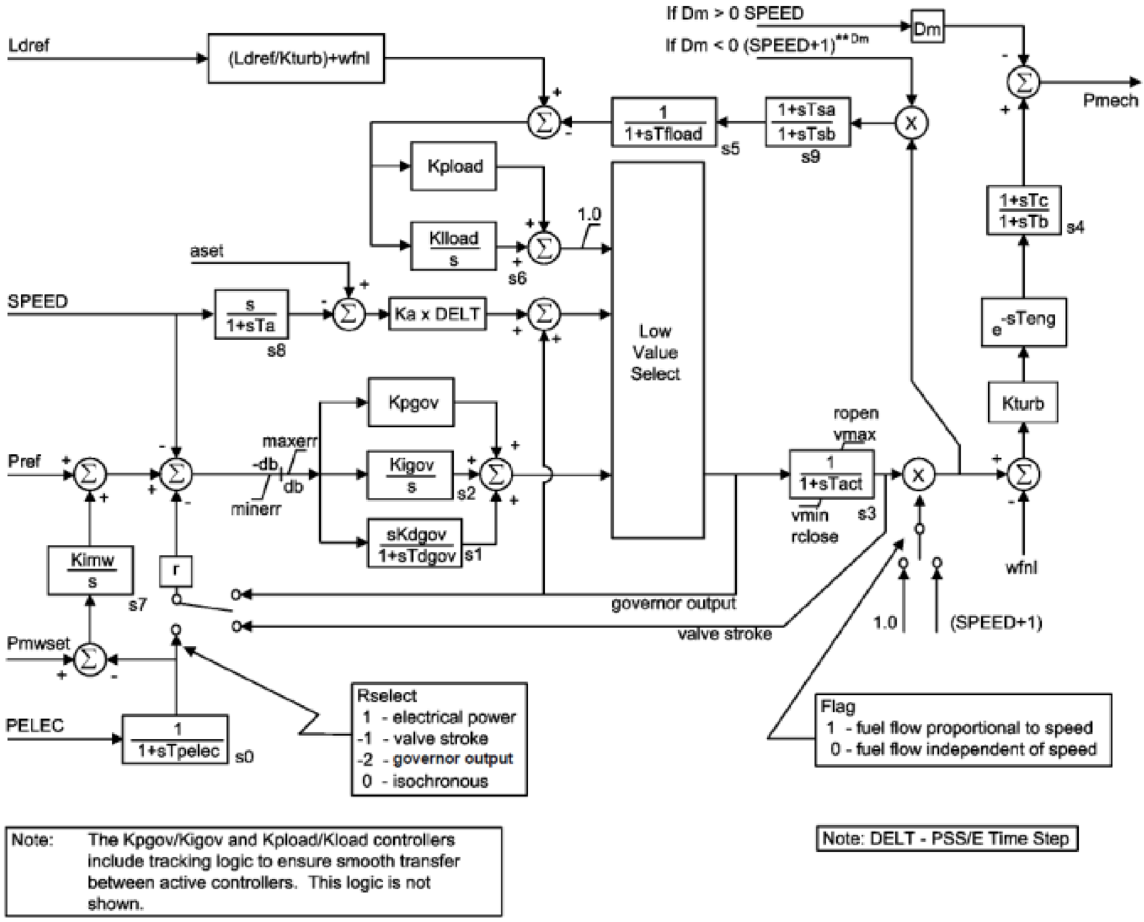

Figure A.3: Schematic implementation of the GGOV1 Governor for the Gas turbines.

A.4 IEEET1

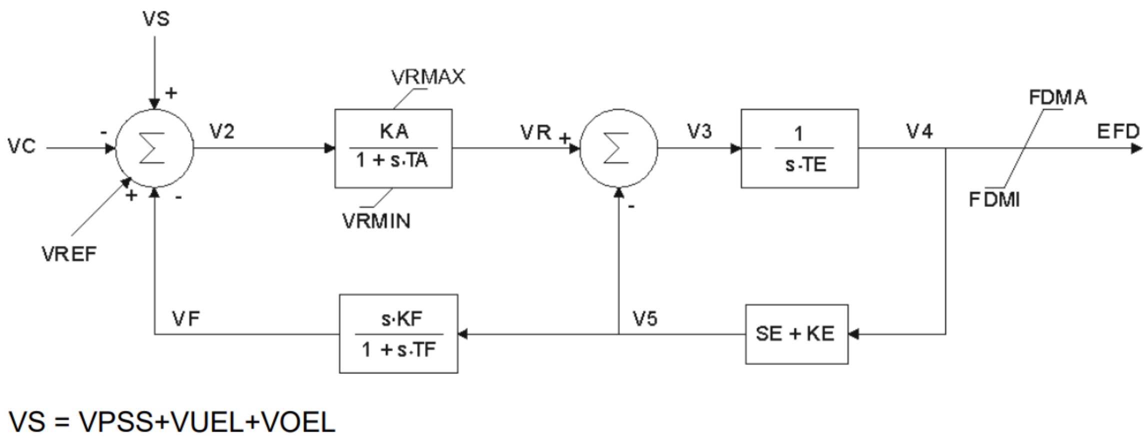

Figure A.4: Schematic implementation of the IEEET1 AVR for the Gas turbines.

A.5 Short circuit report conventional

	DIgSILENT PowerFactory 2019	Project:
		Date: 9/20/2019

Fault Locations with Feeders
Short-Circuit Calculation / Method : complete / Max. Short-Circuit Currents

Short-Circuit Duration
Break Time 0.10 s
Fault Clearing Time (Ith) 1.00 s

Short-Circuit Event Number	Object	Fault Resistance [Ohm]	Fault Reactance [Ohm]	Fault Type	Phases
1	.\Substation\BB2	0.000	0.000	3-Phase Short-Circuit	

Grid: Grid System Stage: Grid Annex: / 1

	rtd.V. [kV]	Voltage [kV]	Voltage [deg]	c-Factor	Sk" [MVA]	Ik" [kA]	Ik" [deg]	Ik' [kA]	Ik' [deg]	ip [kA]	Ib [kA]	ib [kA]	Ith [kA]
Substation													
BB2	132.00	0.00	0.00	1.00	1920.75 MVA	8.40 kA	-83.6	0.00	0.0	23.63 kA	0.69	11.53	7.48
CB0	BB1				0.00 MVA	0.00 kA	0.0	0.00	0.0	0.00 kA			
Gen 1 Trans	Terminal(1				338.63 MVA	1.48 kA	95.9	1.18	97.6	4.17 kA			
Gen 2 Trans	Terminal(9				283.33 MVA	1.24 kA	97.7	0.98	99.6	3.49 kA			
Gen 3 Trans	Terminal(5				338.55 MVA	1.48 kA	95.9	1.18	97.6	4.16 kA			
Gen 4 Trans	Terminal(6				338.55 MVA	1.48 kA	95.9	1.18	97.6	4.16 kA			
Gen 5 Trans	Terminal(7				283.33 MVA	1.24 kA	97.7	0.98	99.6	3.49 kA			
Gen 6 Trans	Terminal(8				338.55 MVA	1.48 kA	95.9	1.18	97.6	4.16 kA			

Figure A.5: Short circuit on the 132KV busbar, with 6 generators current peak (Ip) = 23.36.

A.6 Short circuit report lithium ion

Short-circuit calculation started...
Short-circuit calculated at Terminal Substation\BB1
Short-circuit calculated at Terminal Substation\BB2
Short-circuit calculated at Terminal Grid\Bus 4
Short-circuit calculated at Terminal Grid\Compressor String 1
Short-circuit calculated at Terminal Grid\Compressor String 2
Cannot compute a short-circuit at a DC line 'Grid\DC-Terminal'.
Short-circuit calculation successfully executed!

		DIgSILENT PowerFactory 2019	Project: Date: 9/28/2019

Fault Locations with Feeders
Short-Circuit Calculation / Method : complete   3-Phase Short-Circuit / Max. Short-Circuit Currents

Short-Circuit Duration		Fault Impedance	
Break Time	0.10 s	Resistance, Rf	0.00 Ohm
Fault Clearing Time (Ith)	1.00 s	Reactance, Xf	0.00 Ohm

Grid: Grid   System Stage: Grid   Annex: / 1

		rtd.V. [kV]	Voltage [kV]	Voltage [deg]	c-Factor	Sk" [MVA]	Ik" [kA]	Ik" [deg]	Ik' [kA]	Ik' [deg]	ip [kA]	Ib [kA]	ib [kA]	Ith [kA]
Substation														
BB1		132.00	0.00	0.00	1.00	1484.30 MVA	6.49 kA	-80.6	5.30	-78.8	18.18 kA	5.40	15.54	7.93
CB0	BB2					1484.30 MVA	6.49 kA	99.4	5.30	101.2	18.18 kA			
2-Winding Trans	Terminal(1					0.00 MVA	0.00 kA	0.0	0.00	0.0	0.00 kA			
2-Winding Trans	Terminal(1					0.00 MVA	0.00 kA	0.0	0.00	0.0	0.00 kA			
2-Winding Trans	Terminal(1					0.00 MVA	0.00 kA	0.0	0.00	0.0	0.00 kA			
2-Winding Trans	Compressor					0.00 MVA	0.00 kA	0.0	0.00	0.0	0.00 kA			
BB2		132.00	0.00	0.00	1.00	1484.30 MVA	6.49 kA	-80.6	5.30	-78.8	18.18 kA	5.40	15.54	7.93
CB0	BB1					0.00 MVA	0.00 kA	0.0	0.00	0.0	0.00 kA			
2-Winding Trans	PV1 Bus(5)					0.00 MVA	0.00 kA	0.0	0.00	0.0	0.00 kA			
2-Winding Trans	Terminal(1					0.00 MVA	0.00 kA	0.0	0.00	0.0	0.00 kA			
2-Winding Trans	Terminal(1					0.00 MVA	0.00 kA	0.0	0.00	0.0	0.00 kA			
2-Winding Trans	Terminal(1					0.00 MVA	0.00 kA	0.0	0.00	0.0	0.00 kA			
2-Winding Trans	Terminal(1					0.00 MVA	0.00 kA	0.0	0.00	0.0	0.00 kA			
2-Winding Trans	Compressor					0.00 MVA	0.00 kA	0.0	0.00	0.0	0.00 kA			
Gen 1 Trans	Terminal(1					321.20 MVA	1.40 kA	99.3	1.15	101.3	3.93 kA			
Gen 2 Trans	Terminal(9					255.40 MVA	1.12 kA	99.7	0.90	101.9	3.13 kA			
Gen 3 Trans	Terminal(5					301.98 MVA	1.32 kA	99.5	1.07	101.8	3.70 kA			
Gen 4 Trans	Terminal(6					301.98 MVA	1.32 kA	99.5	1.07	101.8	3.70 kA			
Gen 5 Trans	Terminal(7					255.40 MVA	1.12 kA	99.7	0.90	101.9	3.13 kA			
Gen 6 Trans	Terminal(8					0.00 MVA	0.00 kA	0.0	0.00	0.0	0.00 kA			
Spinning reserv	Bus 4					48.46 MVA	0.21 kA	95.5	0.21	90.0	0.59 kA			
Bus 4		10.50	0.00	0.00	1.00	782.68 MVA	43.04 kA	-84.9	38.60	-83.6	120.41 kA	38.96	109.56	51.88
Spinning Reserv	DC-Termina					47.65 MVA	2.62 kA	-84.3	2.62	-90.0	7.33 kA			
Spinning reserv	Substation					735.04 MVA	40.42 kA	95.1	35.99	96.9	113.08 kA			

Figure A.6: Short circuit on the 132KV busbar, with 5 generators and the lithium ion battery current peak (Ip) = 19.32kA, which is less than the conventional case of 23kA. The battery only provides 0.22kA of short circuit current.

A.7 Programming for the Controls

Table A.1: PQ Control.

Tr = 's';'Filter time constant, active path'	0.01
Trq = 's';'Filter time constant, reactive path'	0.1
Kp = 'pu';'Proporional gain - id-PI-controller'	2.
Tip ='s';'Integrator time constant -id-PI-contr.'	0.2
Kq='pu';'Proporional gain for AC-voltg. support'	0.
AC Deadband='pu';'deadband for proportional gain'	1.
Tiq='s';'Integrator time constant -iq-I-contrl.'	0.002
id_{min}	-1.
iq_{min}	-1.
id_{max}	1.
iq_{max}	1.

Table A.2: Frequency Control.

db='pu';'deadband for frequ. control'	0.004
droop=;'0.02/0.04 -> full active power within 1Hz/2Hz'	0.004

Table A.3: Charge Control.

ChargeCur='pu';'min charging current';	0.
maxSOC='pu';'maximal SOC, charging will be stopped';	0.
minSOC='pu';'minimal SOC, discharging will be stopped';	1.
maxAbsCur	1

Table A.4: Battery model.

CellsParallel)='int';'Amount of parallel cells';	65
CellsInRow='int';'Amount of cells in row';	60
RiCell='ohm';'Intern Resistance per cell';	0.001
CellCapacity='Ah';'Capacity per cell';	80
u_{min}='V';'Voltage of empty cell';	12
u_{max}='V';'Voltage of full cell';	13.85
Unom='kV';'Nominal Voltage of Source';	0.9
SOC0='int';'State of Charge at Initialisation';	1

A.8 Short circuit reports PV

		DIgSILENT PowerFactory 2019	Project: Date: 10/10/2019

Fault Locations with Feeders
Short-Circuit Calculation / Method : VDE 0102 Part 0 / DIN EN 60909-0 3-Phase Short-Circuit / Max. Short-Circuit Currents

Asynchronous Motors Always Considered Decaying Aperiodic Component (idc) Using Method B	Grid Identification Automatic Conductor Temperature User Defined No	Short-Circuit Duration Break Time 0.10 s Fault Clearing Time (Ith) 1.00 s Voltage factor c Standard defined table

Grid: Grid System Stage: Grid Annex: / 1

	rtd.V. [kV]	Voltage [kV]	[deg]	c-Factor	Sk" [MVA]	Ik" [kA]	[deg]	ip [kA]	Ib [kA]	Sb [MVA]	Ik [kA]	Ith [kA]
Substation												
BB2	132.00	0.00	0.00	1.10	1718.60 MVA	7.52 kA	-89.50	19.43 kA	5.59	1278.06	3.07	5.58
CB0	BB1				0.00 MVA	0.00 kA	0.00	0.00 kA				
Gen 1 Trans	Terminal(1				320.00 MVA	1.40 kA	90.05	3.62 kA				
Gen 2 Trans	Terminal(9				354.76 MVA	1.55 kA	90.74	4.02 kA				
Gen 3 Trans	Terminal(5				320.00 MVA	1.40 kA	90.05	3.62 kA				
Gen 4 Trans	Terminal(6				320.00 MVA	1.40 kA	90.05	3.62 kA				
Gen 5 Trans	Terminal(7				354.76 MVA	1.55 kA	90.74	4.02 kA				
PV Trans 1	PV1(1)				49.31 MVA	0.22 kA	95.63	0.53 kA				

Figure A.7: Short circuit report 1 PV implemented.

		DIgSILENT PowerFactory 2019	Project: Date: 10/10/2019

Fault Locations with Feeders
Short-Circuit Calculation / Method : VDE 0102 Part 0 / DIN EN 60909-0 3-Phase Short-Circuit / Max. Short-Circuit Currents

Asynchronous Motors Always Considered Decaying Aperiodic Component (idc) Using Method B	Grid Identification Automatic Conductor Temperature User Defined No	Short-Circuit Duration Break Time 0.10 s Fault Clearing Time (Ith) 1.00 s Voltage factor c Standard defined table

Grid: Grid System Stage: Grid Annex: / 1

	rtd.V. [kV]	Voltage [kV]	[deg]	c-Factor	Sk" [MVA]	Ik" [kA]	[deg]	ip [kA]	Ib [kA]	Sb [MVA]	Ik [kA]	Ith [kA]
Substation												
BB2	132.00	0.00	0.00	1.10	1412.96 MVA	6.18 kA	-89.38	15.95 kA	4.71	1077.75	2.88	4.83
CB0	BB1				0.00 MVA	0.00 kA	0.00	0.00 kA				
Gen 1 Trans	Terminal(1				320.00 MVA	1.40 kA	90.05	3.62 kA				
Gen 2 Trans	Terminal(9				354.76 MVA	1.55 kA	90.74	4.02 kA				
Gen 3 Trans	Terminal(5				320.00 MVA	1.40 kA	90.05	3.62 kA				
Gen 4 Trans	Terminal(6				320.00 MVA	1.40 kA	90.05	3.62 kA				
PV Trans 1	PV1(1)				49.31 MVA	0.22 kA	95.63	0.53 kA				
PV Trans 2	PV2(1)				49.31 MVA	0.22 kA	95.63	0.53 kA				

Figure A.8: Short circuit report 2 PV implemented.

		DIgSILENT PowerFactory 2019	Project: Date: 10/10/2019

Fault Locations with Feeders
Short-Circuit Calculation / Method : VDE 0102 Part 0 / DIN EN 60909-0 3-Phase Short-Circuit / Max. Short-Circuit Currents

Asynchronous Motors Always Considered Decaying Aperiodic Component (idc) Using Method B	Grid Identification Automatic Conductor Temperature User Defined No	Short-Circuit Duration Break Time 0.10 s Fault Clearing Time (Ith) 1.00 s Voltage factor c Standard defined table

Grid: Grid System Stage: Grid | Annex: / 1

	rtd.V. [kV]	Voltage [kV]	[deg]	c-Factor	Sk" [MVA]	Ik" [kA]	[deg]	ip [kA]	Ib [kA]	Sb [MVA]	Ik [kA]	Ith [kA]
Substation												
BB2	132.00	0.00	0.00	1.10	1142.13 MVA	5.00 kA	-89.01	12.86 kA	3.87	883.90	2.41	3.91
CB0	BB1				0.00 MVA	0.00 kA	0.00	0.00 kA				
Gen 1 Trans	Terminal(1				320.00 MVA	1.40 kA	90.05	3.62 kA				
Gen 2 Trans	Terminal(9				354.76 MVA	1.55 kA	90.74	4.02 kA				
Gen 3 Trans	Terminal(5				320.00 MVA	1.40 kA	90.05	3.62 kA				
PV Trans 1	PV1(1)				49.31 MVA	0.22 kA	95.63	0.53 kA				
PV Trans 2	PV2(1)				49.31 MVA	0.22 kA	95.63	0.53 kA				
PV Trans 3	PV3(1)				49.31 MVA	0.22 kA	95.63	0.53 kA				

Figure A.9: Short circuit report 3 PV implemented.

		DIgSILENT PowerFactory 2019	Project: Date: 10/10/2019

Fault Locations with Feeders
Short-Circuit Calculation / Method : VDE 0102 Part 0 / DIN EN 60909-0 3-Phase Short-Circuit / Max. Short-Circuit Currents

Asynchronous Motors Always Considered Decaying Aperiodic Component (idc) Using Method B	Grid Identification Automatic Conductor Temperature User Defined No	Short-Circuit Duration Break Time 0.10 s Fault Clearing Time (Ith) 1.00 s Voltage factor c Standard defined table

Grid: Grid System Stage: Grid | Annex: / 1

	rtd.V. [kV]	Voltage [kV]	[deg]	c-Factor	Sk" [MVA]	Ik" [kA]	[deg]	ip [kA]	Ib [kA]	Sb [MVA]	Ik [kA]	Ith [kA]
Substation												
BB2	132.00	0.00	0.00	1.10	871.37 MVA	3.81 kA	-88.40	9.77 kA	3.02	690.04	1.95	2.99
CB0	BB1				0.00 MVA	0.00 kA	0.00	0.00 kA				
Gen 1 Trans	Terminal(1				320.00 MVA	1.40 kA	90.05	3.62 kA				
Gen 2 Trans	Terminal(9				354.76 MVA	1.55 kA	90.74	4.02 kA				
PV Trans 1	PV1(1)				49.31 MVA	0.22 kA	95.63	0.53 kA				
PV Trans 2	PV2(1)				49.31 MVA	0.22 kA	95.63	0.53 kA				
PV Trans 3	PV3(1)				49.31 MVA	0.22 kA	95.63	0.53 kA				
PV Trans 4	PV4(1)				49.31 MVA	0.22 kA	95.63	0.53 kA				

Figure A.10: Short circuit report 4 PV implemented.

A.9 String trip report 1 PV implemented

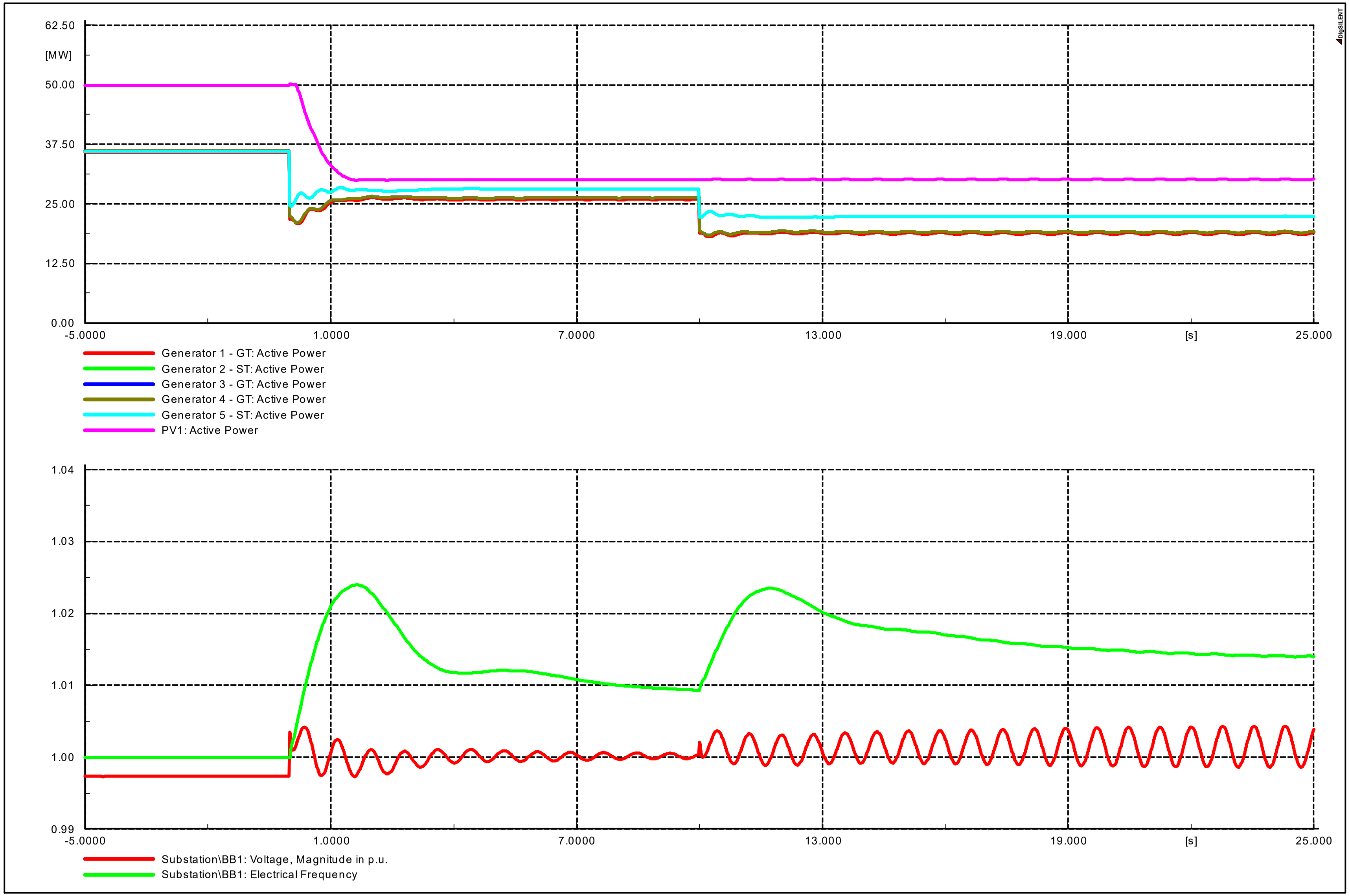

Figure A.11: String trip with 5 turbines and 1 solar PV park

A.10 String trip report 2 PV implemented

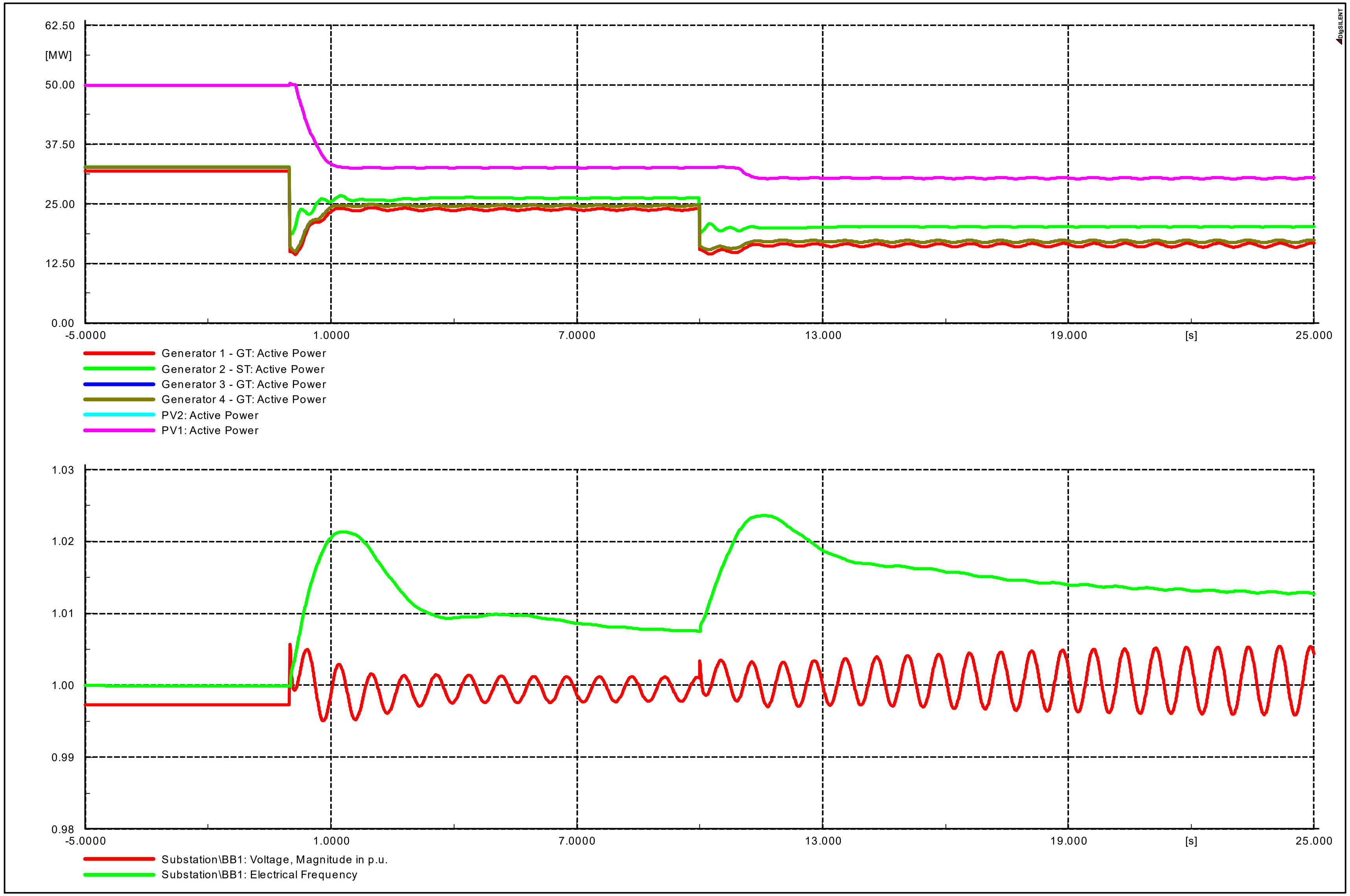

Figure A.12: String trip with 4 turbines and 2 solar PV park

A.11 String trip report 3 PV implemented

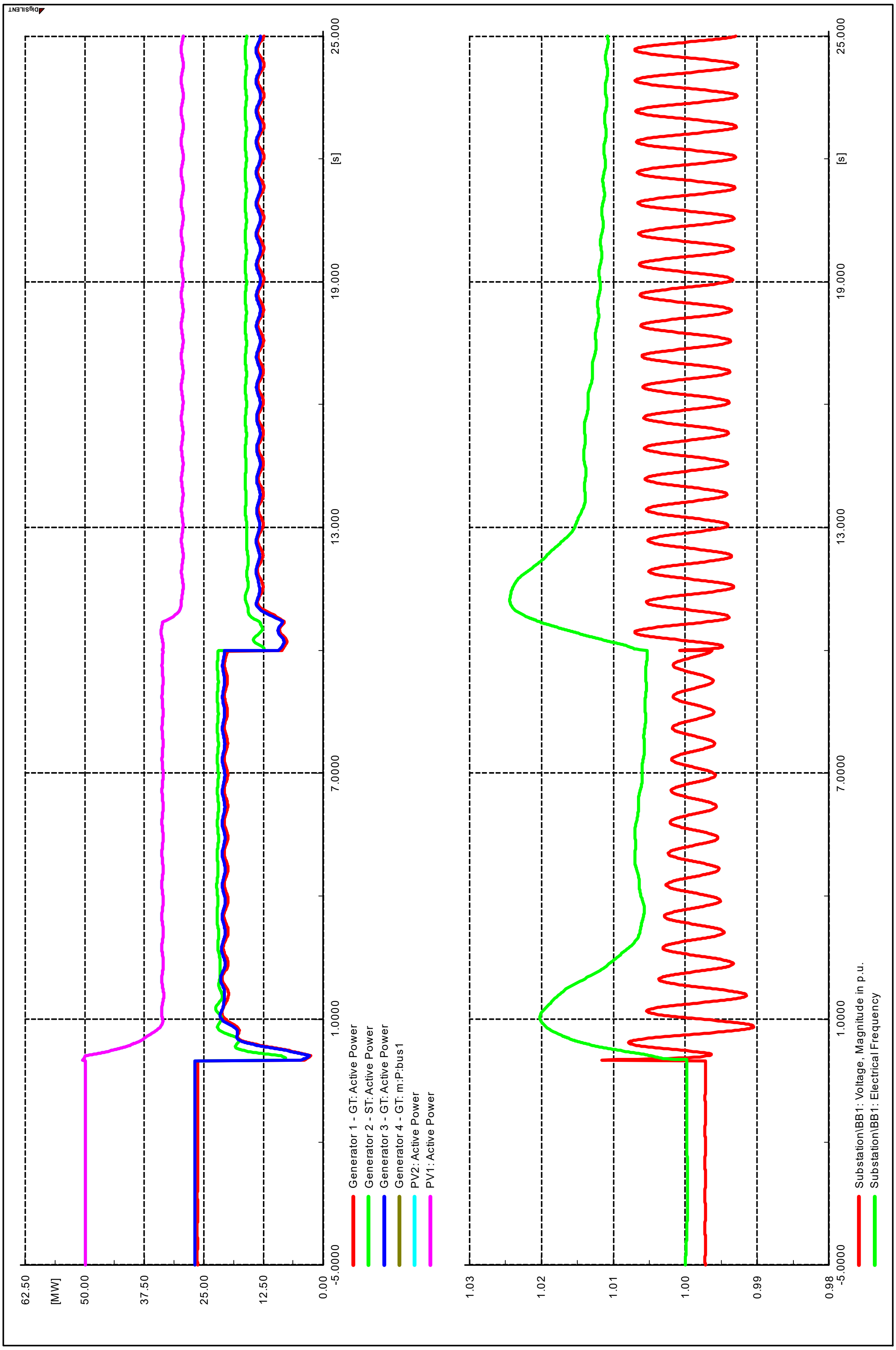

Figure A.13: String trip with 3 turbines and 3 solar PV park

A.12 String trip report 4 PV implemented

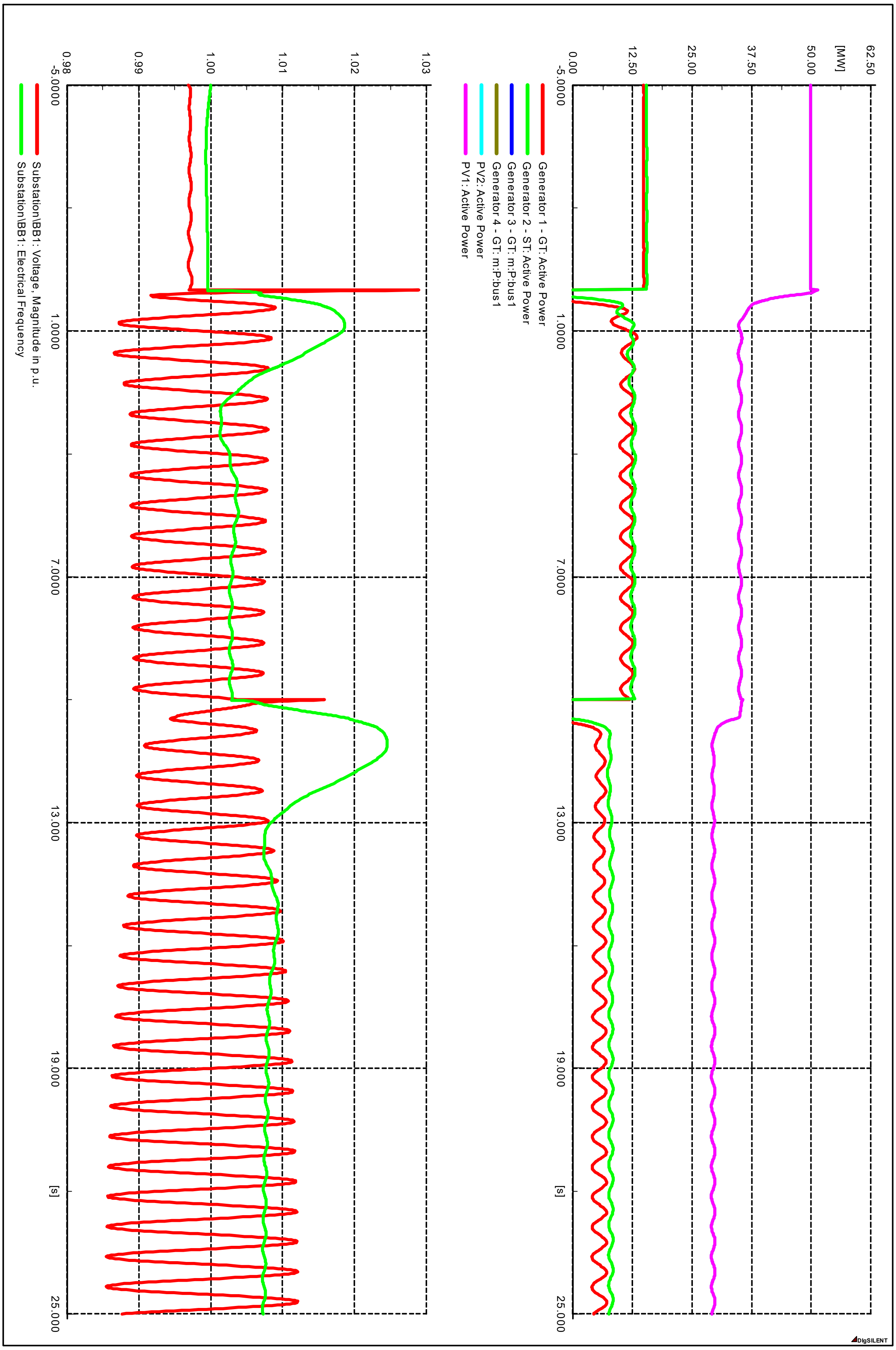

Figure A.14: String trip with 2 turbines and 4 solar PV park

A.13 Generation trip report 1 PV implemented

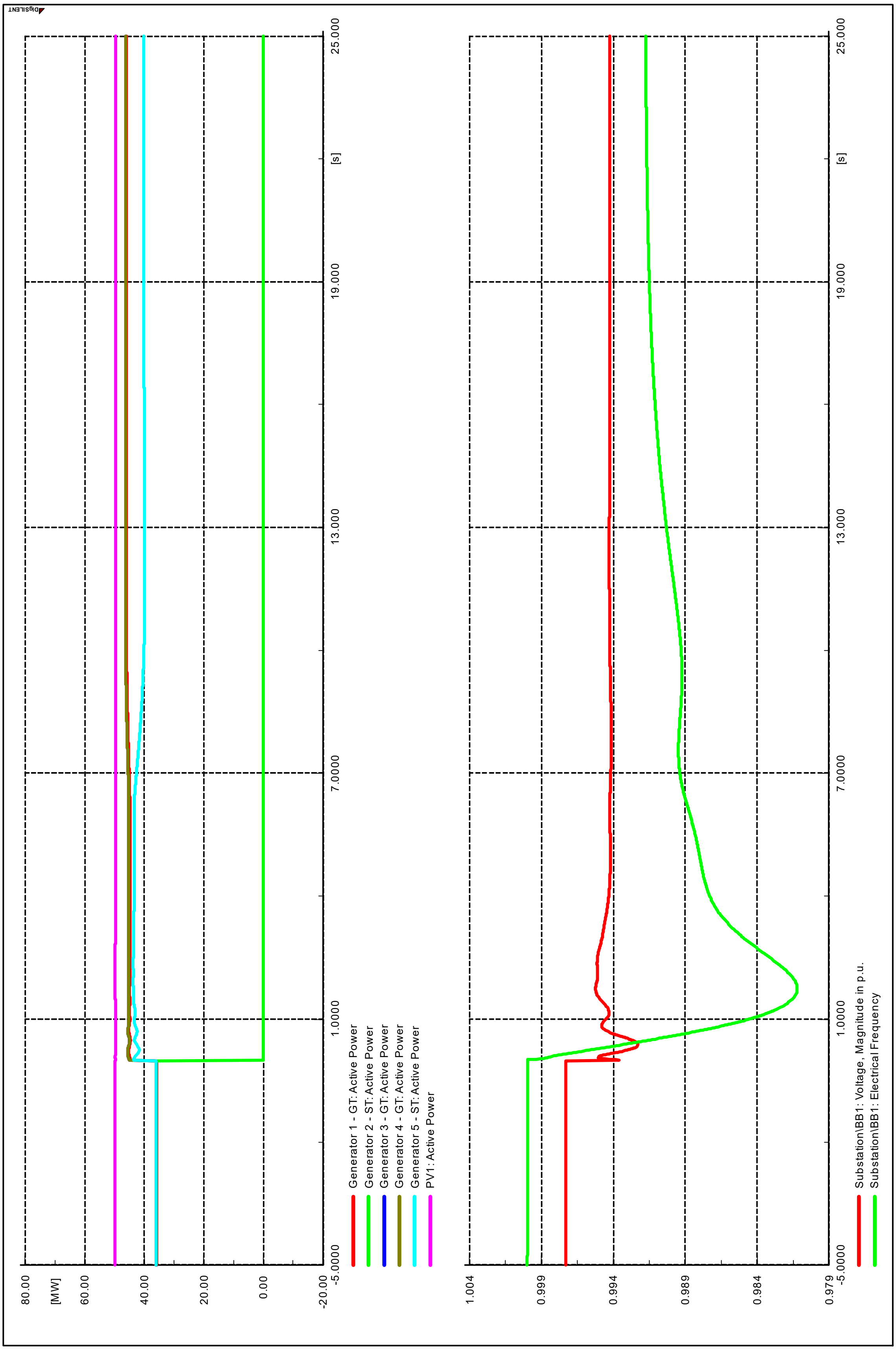

Figure A.15: Caption

A.14 Generation trip report 2 PV implemented

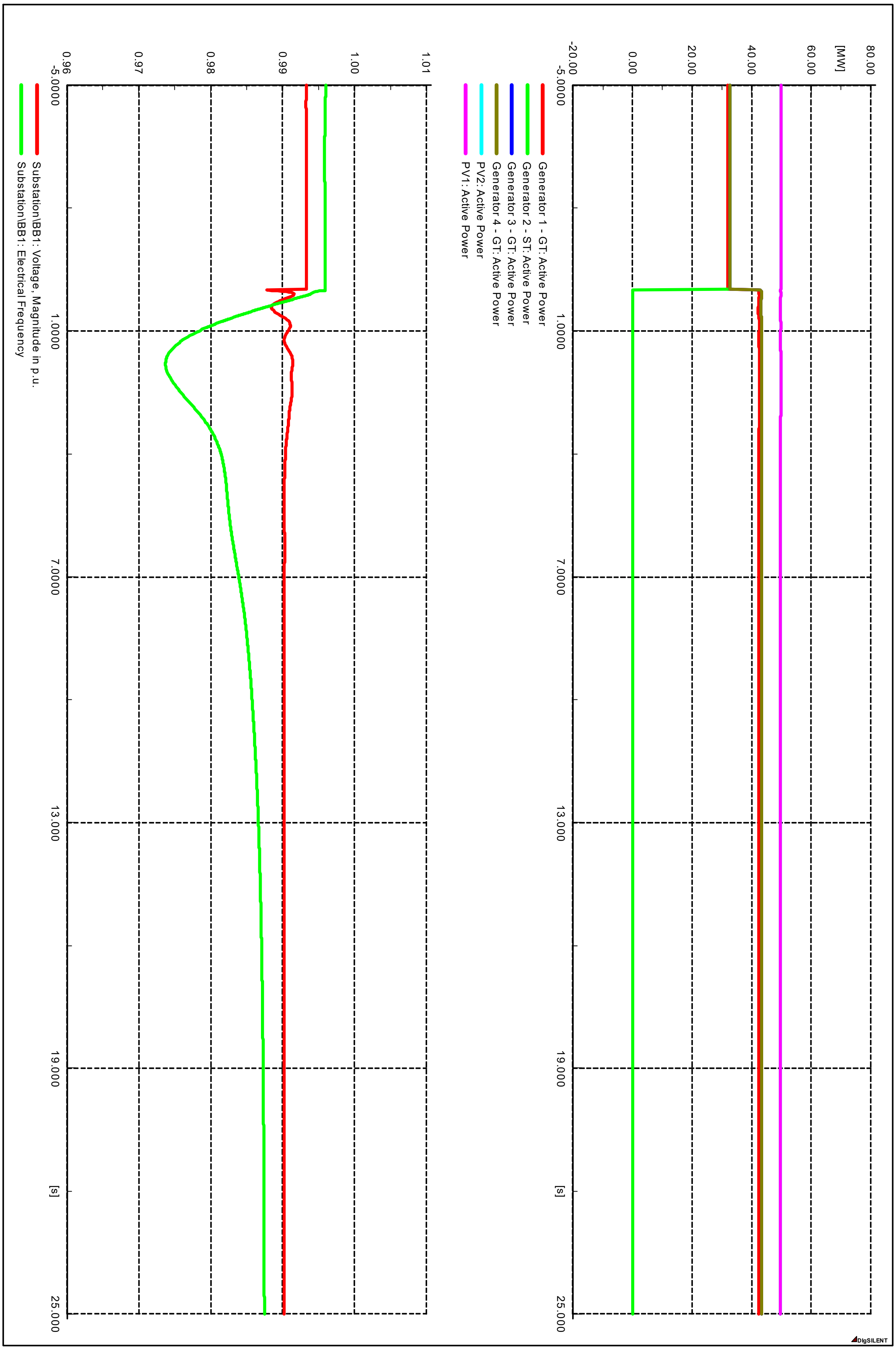

Figure A.16: Caption

A.15 Generation trip report 3 PV implemented

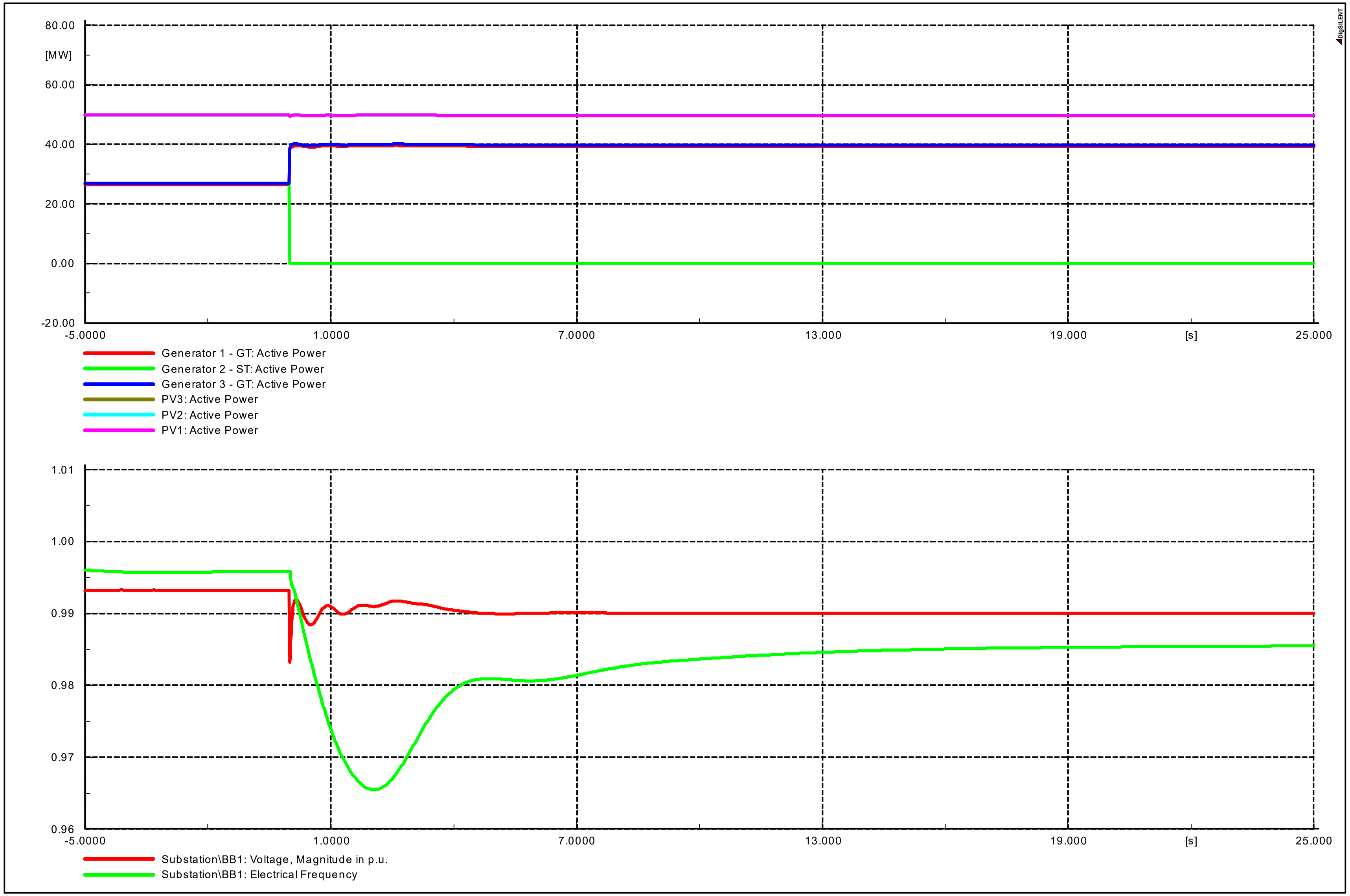

Figure A.17: Caption

A.16 Generation trip report 4 PV implemented

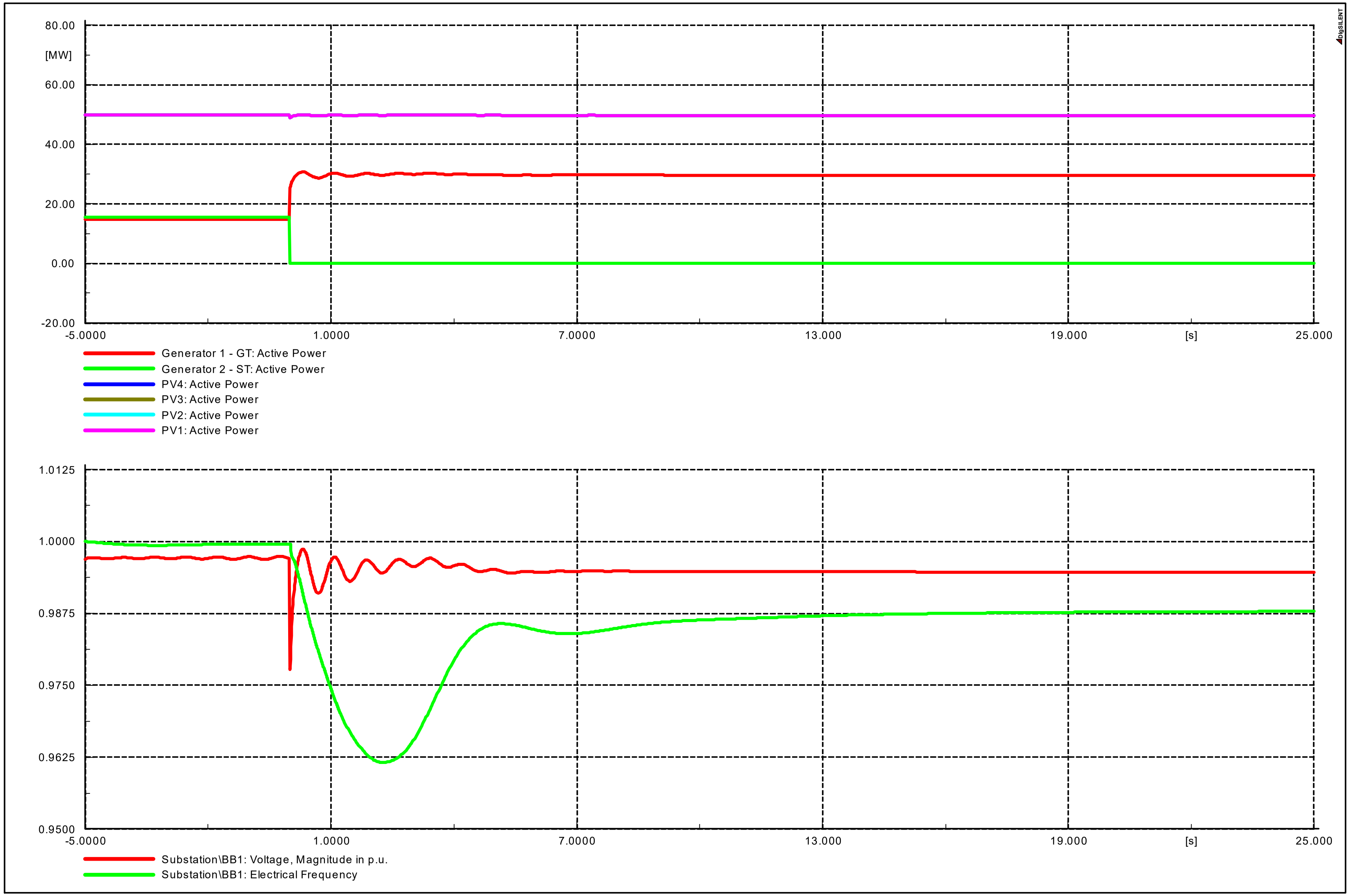

Figure A.18: Caption

B

Appendices - Battery technology analysis

B.1 Battery technology analysis

B.1.1 Role of batteries within grids

Large scale batteries are becoming more common within electrical grids. There are several roles which these batteries can full fill. Firstly is the stabilisation role.

Stabilisation Maintaining a constant frequency is key to keep the system running. The battery at the Horndale Windfarm[1] has 70 MWh allocated to this very role. During short loss of load the battery can absorb energy and during the loss of a generation unit the battery can take over while others spin up.

Price regulation The Horndale Windfarm has 30 MWh capacity to deliver energy when the prices are high, the battery is charged during low prices. These prices are set on the market with by the utility companies. This mode of operations earned Neoen(owner of the Horndale battery) $50M$\$ during it first year of operations.

B.1.2 Tanzanian use

In Tanzania the battery (and the whole plant) will not be connected to the national grid. Thus price regulation is not an option since both consumption and generation is owned by Shell. The stabilisation is necessary to maintain the frequency within the grid. To absorb load the battery should not be full, the impact of this will be analysed in the financial report

B.2 Li-ion

Lithium-ion (Li-ion) batteries are the most found batteries at this moment. The batteries are found in powerbanks, laptops, ups's and grid supporting form. The reason they are used very often is their light weight and high power density. These characteristics combined with the relative low cost makes them very attractive for a fast amount of use cases.First the basic working of the Li-ion battery is explained then the different lithium batteries will be explored.

B.2.1 Working of Li-ion

All lithium batteries have the same principle working. In figure B.1 the battery layout can be seen. During charging the voltage is applied and the electrons are force to the anode. When they accumulate here the positively charged lithium-ions are attracted back to the anode side. Through the electrolyte. The electrolyte is a membrane which only lets lithium-ions pass. When all the lithium-ions are near the anode the battery is charged.

Discharging During the discharging the electrons flow through load and are recombined with the lithium ions at the cathode. When all lithium ions are recombined with the electrons the battery is completely discharged.

[1] https://hornsdalewindfarm.com.au/

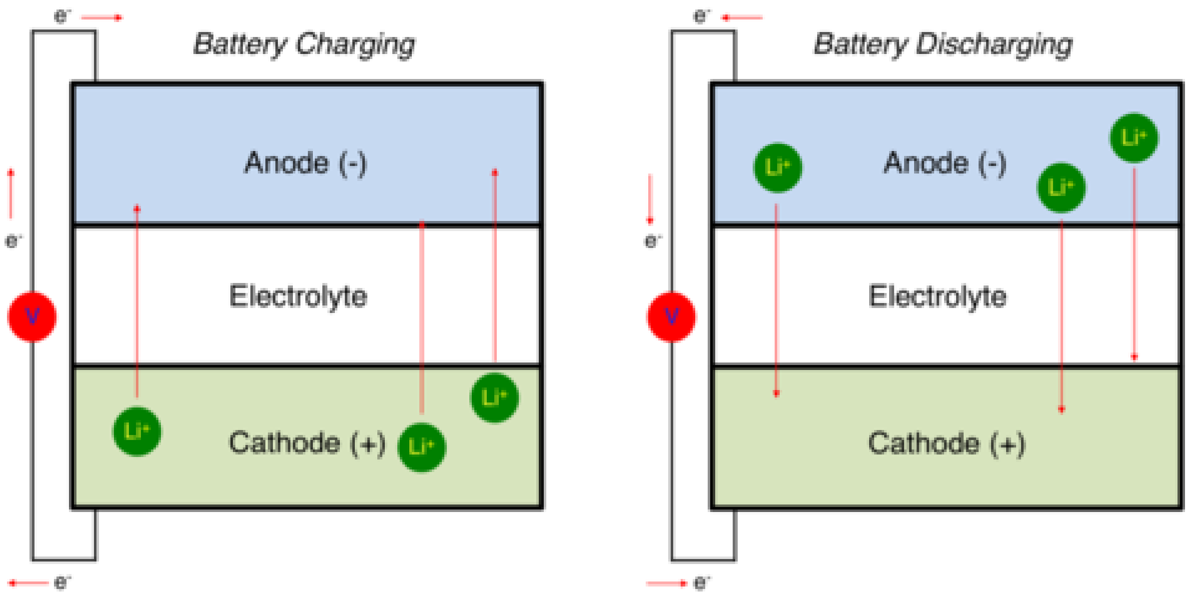

Figure B.1: Physical explanation of a battery

Degradation of electrolyte When lithium ions flow in the electrolyte they can attach to the structure. These atoms become crystallised within the electrolyte. During normal operations these crystals protect the device from short circuiting (by repelling electrons and thus forcing them through the load. But once these crystals become to large they stop the flow of lithium ions and thus will halt operations of the battery. The cycle durability is between 400-1200 and is directly related to the Depth of Discharge (see figure B.2).

B.2.2 (Semi) Fluid Li-ion

Fluid Li-ion batteries are mass produced at this moment. They are very cheap to make and have a long lifespan. There are several safety concerns and in the past years they have lead to some accidents. It is possible to mitigate most of the risk with a good battery management system, but determining the life cycle, state and internal damages will always remain based on calculation as it is not possible to open a battery.

Fluid Li-ion implementations in 2019 The technology used at Hornsdale windfarm is an off the shelf system built by Tesla. This project is the first large scale application of Tesla Powerpacks. These powerpacks can be made out of old Tesla car li-ion batteries fitted with a DC-DC converter[2]. The configuration requires 1 DC-AC inverter with every 8 powerpacks. A set of 8 powerpacks can deliver 700KVA. More info regarding these can be found at `https://www.tesla.com/nl_NL/powerpack`.

Fluid, Wh = +, Cycle = 0, W/s = ++, Feasible = ✓ Liquid electrolytes are common in batteries. LiPF6, LiBF4 and LiClO4 are all salts which are dissolved in an organic solvent. LiPF6 is the used in most of the situation. LiPF6 has some problems, the ionic conduction sensitivity to hydrolysis and thermal stability are poor. But all LiPF6 is the most balanced of the previous named salts.

In the solutions the power and energy density is related to the amount of salts dissolved. Making them score high on the energy requirement. The downside of these batteries is the accumulation on cathode and anode. The creation of these crystals leads to decreased efficiency and thus lifetime. Making them score low on the life cycle rating. LiPF6 is capable of providing discharging is 40 times its Ah rating. Scoring very high in the ramprate requirement

Gel, Wh = ++, Cycle = +, W/s = ++, Feasible = ✓ Most batteries are LiPo (lithium Polymer), these are filled with an electrolyte gel. This gel is what contains the electrons. Common electrolytes are poly(ethylene oxide)

[2] `https://www.tesla.com/nl_NL/blog/teslas-closed-loop-battery-recycling-program`

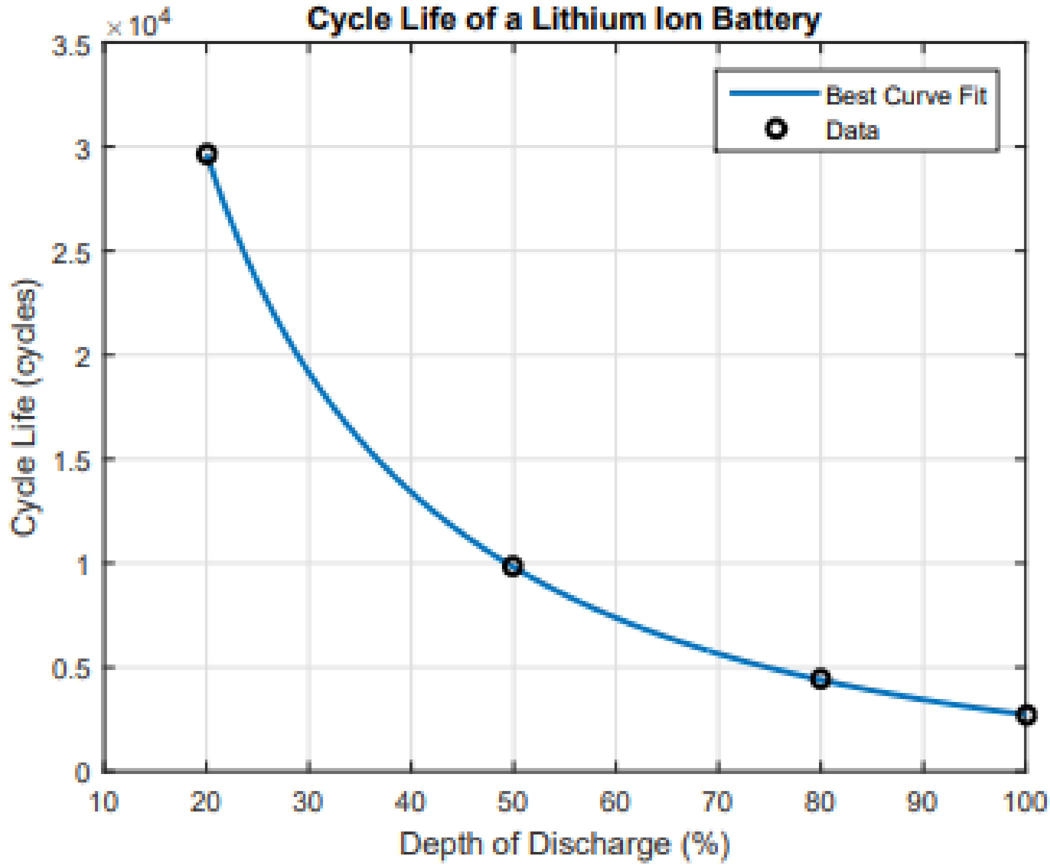

Figure B.2: Impact of Discharge Depth on lithium ion [25]

(PEO), poly(acrylonitrile) (PAN), poly(methyl methacrylate) (PMMA) or poly(vinylidene fluoride) (PVdF)[3]. These batteries suffer less from the forming of crystals. So scoring better on the lifecycle criterion

B.2.3 Solid Li-ion

Combining lithium with ceramic or polymers can create a battery with a solid crystal structure, enabling the battery to have a energy density 70% higher compared to conventional Li-ion batteries. [33]. While according to [4] these batteries are able to last 23000 cycles. They are currently used in several small devices such as pacemakers, RFID and wearable devices. There are several companies trying to produce these batteries on a larger scale, non have been successful so far. This is due to the high probability of forming dendrites, these pathways between cathode and anode will lead to permanent damage. If the forming of these dendrites can be reduced/cancelled than solid Li-ion can be very promising. Solid Li-ion scores very high in all categories. But the technology has to mature further.

Lithium Oxide, Wh = 0, Cycle = -, W/s = +++, Feasible = X Metal-air electrolytes are a new technique on the market. The theoretical capacity of 40MJ/kg is high compared to conventional (Fluid) batteries. In the lab results of 2000Wh/kg are recorded, this is 3.3 times higher than conventional batteries. These figures come from very small testing size. According to [1].

Lithium sulfur, Wh = +, Cycle = —, W/s = ++, Feasible = ✓ lithium Sulfur batteries are in rapid development, with a energy density of 2567wh/Kg. They promise a high energy density while being made out of a common and inexpensive material. The downside of using Sulfur is the degradation of the cathode is much higher than in other solid Li-ion batteries[12]. Thus reducing the lifetime.

B.3 Redox Flow Batteries

Wh = +++, Cycle = +++, W/s = –, Feasible = ✓

Redox Flow Batteries (RFB) are based on a different chemical reaction to produce energy. The system is based on the redox reaction taking place between two fluids. These fluids are stored in 2 tank. The system is shown in figure B.3. The flow can be controlled via valves and pumps. The amount of fluid being pumped controls the amount of Energy. Power is produced at the terminals of the battery while energy is stored in the chemical reaction. The sizing of the terminals determines the amount of power the battery is able to produce. This enables the system to be more flexible in its scaling. The Redox reaction has no negative reaction on the cathode and anode. This enables the battery to be totally discharged without any repercussions. This makes the life cycle stat very high, while having unlimited energy. The only downside of this technology is the ramprate, this is not very high because of the valves and pumps needed to operate.

B.4 CAES

Wh = +++, Cycle = +++, W/s = +++, Feasible = x Compressed air energy storage (CAES) is the process of converting energy in pressured air. When the energy is needed the air is released while flowing over a generator. The technique is used in a variety of use cases and sizes.

On small scale the pressure is kept within a cylinder and released when needed. This system is seen on ships where the (diesel) engine needs to speed up. Instead of installing a starter motor, the pressurised air is blown in the cylinder of the engine, starting the engine. The amount of energy that can be stored is limited by the tank size.

The second (and large scale) storage medium is a cavern in the ground. When a oil/gas field is depleted it can be used as a large air tank. The air can be released when needed and generate electricity via a generator. The whole charging and discharging is 24-45% efficient. But can store fast amounts of energy.

B.5 Hydro

Wh = +++, Cycle = +++, W/s = 0, Feasible = x Pumped hydro storage is a storage mechanism that transfers gravitational energy into electric energy and vice versa. During daytime water is pumped to an elevation and when the power is needed the water flows back through a turbine and creates the energy.

[3] https://en.wikipedia.org/wiki/lithium_polymer_battery

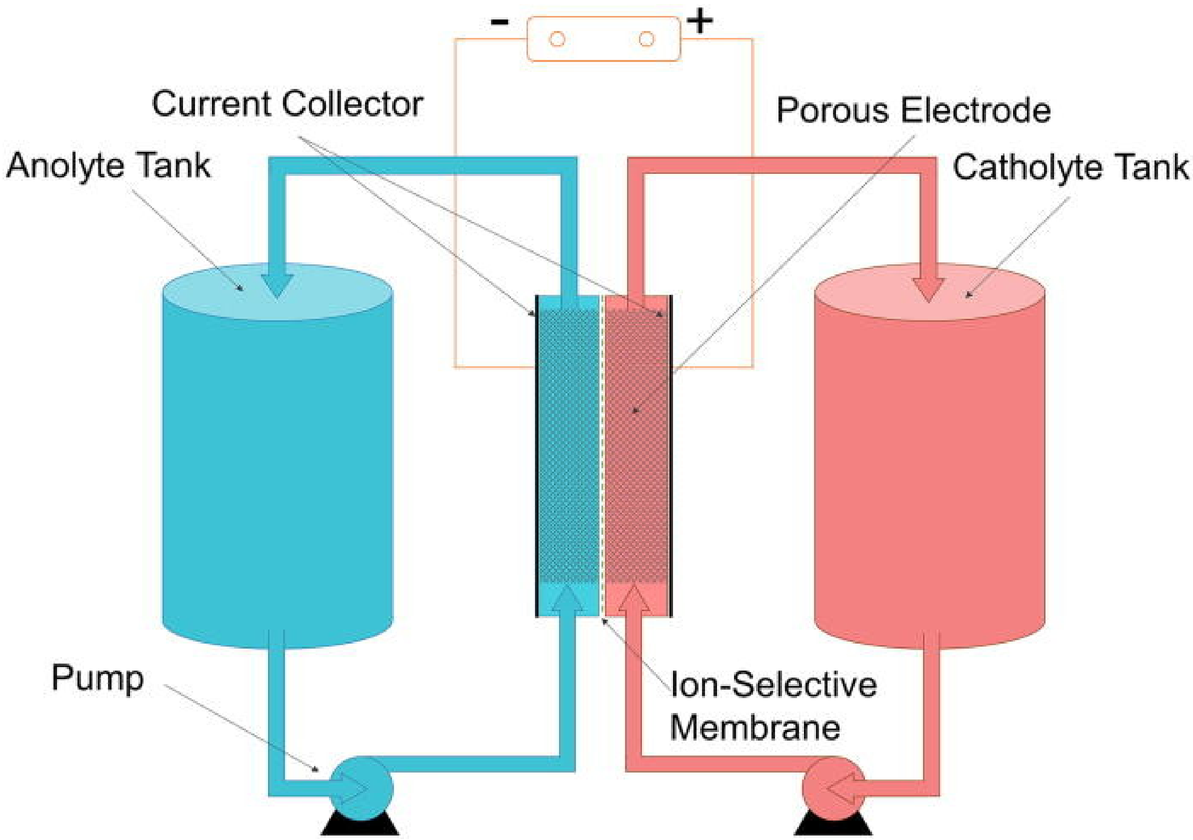

Figure B.3: Redox Flow Battery, source: https://commons.wikimedia.org/w/index.php?curid=59002803

For this technique to be implemented a (natural) height difference needs to in place. This is not the case in the area chosen for this project. Thus failing to meet the feasibility requirement.

		Wh	Cycle	W/s	Feasibility
Fluid Li-ion					
	LiPF6	+	+	++	Yes
	LiPo	++	+	++	Yes
Solid Li-ion					
	lithium Oxide	0	-	+++	No
	lithium Sulfur	+	—	++	Yes
Redox Flow Battery					
	VRFB	+++	+++	–	Yes
CAES					
	Cavern	+++	+++	++	No
	Tank	–	+++	+++	Yes
Hydro		+++	+++	0	No

Bibliography

[1] K. M. Abraham* and Z. Jiang. K. m. abraham* and z. jiang. *J. Electrochem. Soc., Vol. 143, No. 1,*, 143:6, 01 1996. doi: http://jes.ecsdl.org/content/143/1/1.

[2] O. Asowata, J. Swart, and C. Pienaar. Correlating the power conversion of a pv panel to the solar irradiance obtained from meteonorm. In *2013 IEEE International Conference on Industrial Technology (ICIT)*, pages 684–689, Feb 2013. doi: 10.1109/ICIT.2013.6505754.

[3] R. Bhat, M. Begovic, I. Kim, and J. Crittenden. Effects of pv on conventional generation. In *2014 47th Hawaii International Conference on System Sciences*, pages 2380–2387, Jan 2014. doi: 10.1109/HICSS.2014.299.

[4] Maria Braga, Chandrasekar Subramaniyam, Andrew Murchison, and John B. Goodenough. Non-traditional, safe, high-voltage rechargeable cells of long cycle life. *Journal of the American Chemical Society*, 140, 04 2018. doi: 10.1021/jacs.8b02322.

[5] Paul Breeze. The cost of power generation. `http://lab.fs.uni-lj.si/kes/erasmus/The%20Cost%20of%20Power%20Generation.pdf`, 2010.

[6] Alan Callegaro, Jing Guo, Michael Eull, Benjamin Danen, Jason Gibson, Matthias Preindl, Berker Bilgin, and Ali Emadi. Bus bar design for high-power inverters. *IEEE Transactions on Power Electronics*, PP:1–1, 04 2017. doi: 10.1109/TPEL.2017.2691668.

[7] North American Electric Reliability Corporation. Modeling notification gas turbine governor modeling initial distribution: August 2017. `https://www.nerc.com/comm/PC/NERCModelingNotifications/Gas_Turbine_Governor_Modeling.pdf`, 2017.

[8] K. Dietl and K. Link. Start up optimization of combined cycle power plants: Controller development and real plant test results. In *2018 5th International Conference on Control, Decision and Information Technologies (CoDIT)*, pages 599–604, April 2018. doi: 10.1109/CoDIT.2018.8394850.

[9] Renew Economy. Tesla big battery outsmarts lumbering coal units after loy yang trips. `https://bit.ly/2Ua5o8U/`, 2017. Accessed: 2019-31-8.

[10] M. E. Farrag, A. Haggag, R. B. Parambu, and C. Zhou. Optimum charging rate for a lithium-ion battery using comsol livelink for matlab model. In *2017 Nineteenth International Middle East Power Systems Conference (MEPCON)*, pages 677–682, Dec 2017. doi: 10.1109/MEPCON.2017.8301254.

[11] Xing Fu, Xiaorui Wang, and Charles Lefurgy. How much power oversubscription is safe and allowed in data centers. In *How much power oversubscription is safe and allowed in data centers*, pages 21–30, 01 2011. doi: 10.1145/1998582.1998589.

[12] Y. Gorlin M.U.M. Patel A. Freiberg Q. He M. Piana M. Tromp H.A. Gasteiger. Understanding the charging mechanism of lithium-sulfur batteries using spatially resolved operando x-ray absorption spectroscopy, 01 2016.

[13] E. Ela Gevorgian, Vahan and Y. Zhang. Investigating the impact of wind generation participation in interconnection frequency response. IEEE transactions on Sustainable Energy, vol. 6.3, pp. 1004-1012,2015, 2015.

[14] E. Gkoutioudi, P. Bakas, and A. Marinopoulos. Comparison of pv systems with maximum dc voltage 1000v and 1500v. In *2013 IEEE 39th Photovoltaic Specialists Conference (PVSC)*, pages 2873–2878, June 2013. doi: 10.1109/PVSC.2013.6745070.

[15] Mario; Eichhammer Wolfgang; Sensfuß Frank; Pudlik Martin; Pfluger Benjamin; Resch Gustav; Olmos Luis; Ramos Andrés; Rivier Michel; Kost Christoph; Senkpiel Charlotte; Peter Frank; Veum Karina; Slobbe Johann; Joode Jeroen de Held, Anne; Ragwitz. Estimating energy system costs of sectoral res and ee targets in the context of energy and climate targets for 2030: Report, 2015.

[16] IRENA. Irena (2017), electricity storage and renewables: Costs and markets to 2030, international renewable energy agency, abu dhabi. `https://www.irena.org/-/media/Files/IRENA/Agency/Publication/2017/Oct/IRENA_Electricity_Storage_Costs_2017.pdf`, 2017. Accessed: 2019-31-8.

[17] Mark Jacobson and Vijaysinh Jadhav. World estimates of pv optimal tilt angles and ratios of sunlight incident upon tilted and tracked pv panels relative to horizontal panels. *Solar Energy*, 169:55–66, 07 2018. doi: 10.1016/j.solener.2018.04.030.

[18] Samuel C. Johnson, Dimitri J. Papageorgiou, Dharik S. Mallapragada, Thomas A. Deetjen, Joshua D. Rhodes, and Michael E. Webber. Evaluating rotational inertia as a component of grid reliability with high penetrations of variable renewable energy. *Energy*, 180:258 – 271, 2019. ISSN 0360-5442. doi: https://doi.org/10.1016/j.energy.2019.04.216. URL `http://www.sciencedirect.com/science/article/pii/S0360544219308564`.

[19] S. Kamala, B. D. Reddy, B. Sen, S. K. Panda, and G. Amaratunga. Improvement of power quality and reliability in the distribution system of petrochemical plants using active power filters. In *2018 IEEE International Conference on Industrial Technology (ICIT)*, pages 419–424, Feb 2018. doi: 10.1109/ICIT.2018.8352214.

[20] S. Karki, M. D. Mann, and H. Salehfar. Substitution and price effects of carbon tax on co2 emissions reduction from distributed energy sources. In *2006 Power Systems Conference: Advanced Metering, Protection, Control, Communication, and Distributed Resources*, pages 236–243, March 2006. doi: 10.1109/PSAMP.2006.285394.

[21] J. Keller and B. Kroposki. Understanding fault characteristics of inverter-based distributed energy resources. `http://research.iaun.ac.ir/pd/bahador.fani/pdfs/UploadFile_9423.pdf`, 2010.

[22] P. Kundur. Power system stability and control. New York, McGraw-hill,, 1944.

[23] Ju Liu, Dongjun Yang, Wei Yao, Rengcun Fang, Hongsheng Zhao, and Bo Wang. Pv-based virtual synchronous generator with variable inertia to enhance power system transient stability utilizing the energy storage system. *Protection and Control of Modern Power Systems*, 2, 12 2017. doi: 10.1186/s41601-017-0070-0.

[24] Pukar Mahat, Z. Chen, and Birgitte Bak-Jensen. Control strategies for gas turbine generators for grid connected and islanding operations. In *Control strategies for gas turbine generators for grid connected and islanding operations*, pages 1 – 8, 05 2010. doi: 10.1109/TDC.2010.5484471.

[25] Kevin Mallon, Francis Assadian, and Bo Fu. Analysis of on-board photovoltaics for a battery electric bus and their impact on battery lifespan. *Energies*, 10:943, 07 2017. doi: 10.3390/en10070943.

[26] NETL. National energy technology laboratory (netl). 2010. cost and performance baseline for fossil energy plants, 2010.

[27] M. E. Nimvari, A. Hadidi, A. Jafarian, and N. Garjasi. Analysis of triple combined cycle with mhd generator as a topping cycle. In *The 3rd Conference on Thermal Power Plants*, pages 1–5, Oct 2011.

[28] PowerFactory. Digsilent powerfactory application example battery energy storing systems bess. `https://www.digsilent.de/en/faq-reader-powerfactory/do-you-have-an-application-example-for-a-battery-energy-storage-system-bess.html`, 2018. Accessed: 2019-31-8.

[29] PowerFactory. Digsilent powerfactory application example a pv system and a diesel engine. `https://www.digsilent.de/en/faq-reader-powerfactory/do-you-have-an-example-for-a-co-generation-of-a-pv-system-and-a-diesel-engine.html`, 2018. Accessed: 2019-31-8.

[30] PowerFactory. Digsilent powerfactorytechnical reference documentation overview. Internal document within the powerfactory software, 2019. Accessed: 2019-12-10.

[31] RenewEconomy. Revealed: True cost of tesla big battery, and its government contract. https://bit.ly/2xJT150, 2018. Accessed: 2019-31-8.

[32] D.C. Yeragi J.W.W. Trapman G. Stockinger R. Brandt A. Gujar J.M. van Amelsvoort S. Pilla, U. Triplicane Dwarakanathan. 0.15 t co2/t lng, 2016.

[33] J. Schnell, T. Günther, T. Knoche, C. Vieider, L. Köhler, A. Just, M. Keller, S. Passerini, and G. Reinhart. All-solid-state lithium-ion and lithium metal batteries - paving the way to large-scale production. *Journal of Power Sources*, 382:160–175, April 2018. doi: 10.1016/j.jpowsour.2018.02.062.

[34] E. O. Schweitzer and S. E. Zocholl. The universal overcurrent relay. *IEEE Industry Applications Magazine*, 2(3):28–34, May 1996. doi: 10.1109/2943.491383.

[35] Shell. Shell energy report, shell world energy modela view to 2100. https://go.shell.com/2VJKsFo, 2019. Accessed: 2019-31-8.

[36] N.S. Srivatchan and Rangarajan Partha. Control challenges and techniques in islanded micro grid operation. *International Journal of Applied Engineering Research*, 10:30883–30900, 07 2015.

[37] SunPower. Sunpower® sunpowerperformance series p17 datasheet. https://us.sunpower.com/sites/default/files/media-library/data-sheets/ds-sunpower-p17-355-commercial-solar-panels.pdf, 2019. Accessed: 2019-29-9.

[38] Climates to travel. World climate guide. https://www.climatestotravel.com/climate/tanzania, 2019. Accessed: 2019-31-8.

[39] UN. Paris agreement. https://treaties.un.org/Pages/ViewDetails.aspx?src=TREATY&mtdsg_no=XXVII-7-d&chapter=27&lang=_en&clang=_en, 2018.

[40] Black & Veatch. Cost and performance data forpower generationtechnologies, 2017.

[41] GT World. Gtw handbook. https://gasturbineworld.com/shop/annual-handbook/2014-15-handbook-volume-31/, 2014. Accessed: 2019-31-8.

[42] Zhao Dongmei, Zhang Nan, and Liu Yanhua. Micro-grid connected/islanding operation based on wind and pv hybrid power system. In *IEEE PES Innovative Smart Grid Technologies*, pages 1–6, May 2012. doi: 10.1109/ISGT-Asia.2012.6303168.